
# FUEL-AIR INJECTION EFFECTS ON COMBUSTION IN CAVITY-BASED FLAMEHOLDERS IN A SUPERSONIC FLOW

THESIS

William H Allen Jr., Captain, USAF

AFIT/GAE/ENY/05-M02

**DEPARTMENT OF THE AIR FORCE**
**AIR UNIVERSITY**

**AIR FORCE INSTITUTE OF TECHNOLOGY**

**Wright-Patterson Air Force Base, Ohio**

The views expressed in this thesis are those of the author and do not reflect the official policy or position of the United States Air Force, Department of Defense, or the U.S. Government.

AFIT/GAE/ENY/05-M02

# FUEL-AIR INJECTION EFFECTS ON COMBUSTION IN CAVITY-BASED FLAMEHOLDERS IN A SUPERSONIC FLOW

THESIS

Presented to the Faculty

Department of Aeronautics and Astronautics

Graduate School of Engineering and Management

Air Force Institute of Technology

Air University

Air Education and Training Command

In Partial Fulfillment of the Requirements for the

Degree of Master of Science in Aeronautical Engineering

William H. Allen Jr., BSME

Captain, USAF

March 2005

AFIT/GAE/ENY/05-M02

# FUEL-AIR INJECTION EFFECTS ON COMBUSTION IN CAVITY-BASED FLAMEHOLDERS IN A SUPERSONIC FLOW

William H. Allen Jr., BSME

Captain, USAF

Approved:

| | |
|---|---|
| _____ | _____ |
| Dr. Paul I. King (Chairman) | Date |
| _____ | _____ |
| Maj. Richard J. McMullan, PhD, USAF (Member) | Date |
| _____ | _____ |
| Dr. Mark F. Reeder (Member) | Date |

## Abstract

The Air Force Research Lab, Propulsion Directorate, Wright-Patterson Air Force Base, Ohio has studied several designs regarding cavity flameholding for supersonic RAMJET (SCRAMJET) applications. The most recent of these studies have concluded that direct injection of ethylene fuel into the aft cavity ramp produced an efficient, robust flameholder given specific freestream condition and fuel flow rate.

The main goals of this experiment are: 1) study the effect on combustion of direct fuel and air injection in the main flameholding cavity and 2) characterization of the operational limits (i.e., sustained combustion limits) over a variety of fuel and air flow rates. Direct injection of both fuel and air provided additional capability to tune the cavity such that a more stable decentralized flame results. The addition of air injection provided the most improvement over the baseline case (fuel only) near the upstream portion of the cavity close to the cavity step. Direct air injection provided a second source of oxygen to be consumed during the combustion process thereby expanding the operational limits drastically for each selected fuel flow. This experimental investigation was limited by the size of the flow controllers available and by the maximum allowable material temperature given cavity flow parameters. Lean blowout was not observed to be a function of injected air flow.

**Acknowledgments**

I would like to express my sincere appreciation to my faculty advisor, Mr. Paul King, for his guidance and support throughout my tenure here at AFIT as well as during the course of this thesis effort. The insight and experience was certainly appreciated. I would, also, like to thank my sponsor, Mr. Mark Gruber of AFRL/PRAS and Mr. Mark Hsu of Innovative Scientific Solutions Inc. for both the support and latitude provided to me in this endeavor. This was a tremendous opportunity for me to study such an interesting and promising technology.

William H. Allen Jr.

## Table of Contents

Page

## List of Figures

Page

## List of Tables

Page

## List of Symbols

| | |
|---|---|
| $D$ | Cavity Depth |
| $D_d$ | Downstream Step Height |
| $D_u$ | Upstream Step Height |
| FS | Full Scale |
| HBP | High Backpressure |
| $L$ | Cavity Length ($\theta$=90°) |
| $L^*$ | Cavity Length ($\theta$<90°) |
| LBP | Low Backpressure |
| OR | Offset Ratio ($D_u/D_d$) |
| $x$ | Stramwise Position |
| $y$ | Transverse Position |
| $z$ | Spanwise Position |
| $\theta$ | Aft Ramp Angle |
| $\tau$ | Residence Time |

# FUEL-AIR INJECTION EFFECTS ON COMBUSTION IN CAVITY-BASED FLAMEHOLDERS IN A SUPERSONIC FLOW

## I. Introduction

### Background

Traditionally flight in the hypersonic regime has been accomplished using rocket propulsion systems. Such systems, from a historical standpoint, require more fuel and oxidizer in response to a desire to fly farther or faster. One of the primary disadvantages of rocket propulsion at least for atmospheric hypersonic flight is that they must carry all of their oxidizer on board. This in addition to the increased number of components required to store and transport the oxidizer to the combustion chamber contributes significantly to the overall weight and complexity of the vehicle. The increased weight translates simply into larger vehicles or decreased payloads. Supersonic combustion RAMJET (SCRAMJET) engines would negate the need to carry oxidizer on board of the aircraft as all of the oxygen needed for combustion would be garnered from the atmosphere. Another advantage SCRAMJET engines have over rockets is their ability to be throttled. Thrust levels for rockets are based upon design rather than user input.

SCRAMJET technology lends itself to many different aerospace applications both military and civilian. The high vehicle velocity could mean faster travel over long distances for passengers, and the high kinetic energy could also be applied to weapon systems where targets are neutralized using the kinetic energy of the warhead rather than chemical or nuclear energy. Additionally, time critical targets could be more effectively addressed with high Mach number vehicles. Some even believe that SCRAMJET

engines could reduce the cost required to put satellites into orbit by providing as much as 18,000 mph of the required 25,000 mph escape velocity. Joel Sitz a Program Manager at NASA remarked that "It [SCRAMJETS] has the potential of opening up all new industries … probably some we haven't thought about yet."[1] This type of propulsion system is the subject of both past and current research around the globe.[12,13]

Mechanically the SCRAMJET and RAMJET engines, shown in Figures 1 and 2 respectively, are very simple as neither design incorporates moving parts. Air is introduced through an intake duct and compressed due to the forward momentum of the vehicle. It is important to note that without sufficient flight velocity to provide compression no thrust can be generated by these powerplants. One significant difference between the two engine types is that flow aft of the inlet is subsonic in a RAMJET and supersonic in a SCRAMJET. These conditions are still present in the combustion section of the engine. This of course means that combustion in a SCRAMJET must take place in a supersonic flow which is a much more daunting challenge. Combustion is an exothermic chemical process which requires in general fuel, oxidizer, energy and time for the chemical reaction to take place. The last key ingredient is not easy to come by given supersonic flow through the SCRAMJET. The simple relationship between time distance and velocity would tend to suggest increasing the length of the engine to allow a greater time for combustion to take place given the velocity of the flow through the engine. However this would increase the weight of the engine thereby decreasing an aircraft's payload. Furthermore, it has been noted that the thrust to drag ratio of an engine is approximately proportional to the ratio of the combustor's diameter to its length.[2] This

provides additional incentive to keep the combustor length to a minimum. SCRAMJET and RAMJET schematics provided by the online aviation museum.[3]

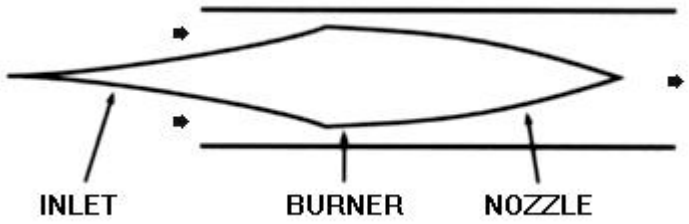


**Figure 1** SCRAMJET engine

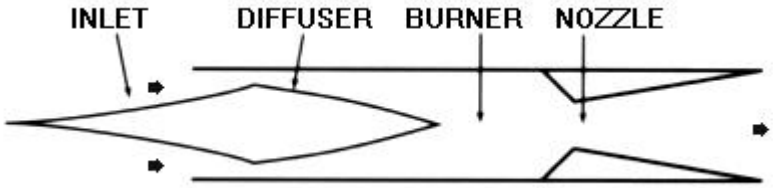


**Figure 2** RAMJET engine

A significant challenge in the generation of SCRAMJET propulsion is completing the combustion process within the engine. Combustion requires that fuel is introduced, mixed with the oxidizer in a sufficient quantity and then provided with energy to start the reaction process. As noted previously, this requires a finite amount of time which, given core velocity through the burner, can be related to distance. Since large distances are not feasible several techniques have been employed both computationally and experimentally to assist the combustion process. First, obstructions and/or fuel injection schemes can be introduced into the supersonic flow causing disruption in the boundary layer and the formation of shockwaves. Previous work has shown this creates a region of high turbulence that can be compared to a region of effective mixing at least on a qualitative

basis. Secondly a cavity can be introduced to the flow creating a subsonic flow region thereby increasing the residence time and creating a region of heated gases to aid in the combustion process.

**Problem Statement**

Previous studies have shown that cavity combustion is most efficient given a single combination of fuel flow rate and freestream conditions. In other words the single controllable parameter, fuel flow rate, must be adjusted or tuned given test or vehicle flight conditions. This study will evaluate the effects of the addition direct air injection, a second controllable parameter. Furthermore, an investigation of the operational limits will be considered.

**Research Focus**

All research was accomplished experimentally using a continuous Mach 2 flow through the test section of a wind tunnel described in chapter 3 of this document. The primary objectives of this study are to evaluate the effects of direct air injection into a cavity based flameholder and to determine its operational limits. Secondary objective are to characterize lean blowout behavior and optimum combustion.

**Methodology**

Advanced diagnostic tools were used to study the combustion process that occurs in typical cavity based flameholders for supersonic combustion applications. Pressure transducers inside the main cavity were used to characterize the shock structure and combustion zone. Additionally, Planar Laser-Induced Fluorescence (PLIF) diagnostics

were used to characterize the flow through the test section. The PLIF diagnostics were specifically configured to collect planar distributions of the OH radical at various axial locations within the cavity under different flow conditions.

# II. Literature Review

## Chapter Overview

Supersonic combustion requires efficient mixing, flameholding and flame stabilization. Several techniques to enhance these properties have been studied. However, detailed information regarding the behavior of these devices namely their optimal shape and fueling strategies, combustion stability and interactions with disturbances in the main air flow is largely unavailable in the existing literature.[4] This chapter provides insight based upon previous research into cavity shape, fueling strategies and overall performance of a cavity based flameholder.

## Relevant Research

Cavity based fuel injection and flameholding offer an obstruction-free flow path in hydrocarbon fueled SCRAMJET engines. Such flame holding cavities can provide the benefit of relatively long residence times and, coupled with a direct cavity fuel injection scheme, can provide robust flame holding with minimal drag penalties in the presence of significant changes in the freestream flow field.

Scramjet engines offer great potential for aviation and space propulsion. However, supersonic combustion remains a challenge due to the high speed core flow and relatively slow chemical reaction rate coupled with a relatively short combustion section. These challenges lend themselves to the introduction of a wall based cavity. The benefit of such a structure is increased residence times and the creation of a hot re-circulating gas. Previous studies categorize cavities as either open or closed. The shear layer of an open cavity spans the entire cavity length whereas the shear layer attaches to

the bottom wall of a closed cavity due to the cavity's increased length. Typically, L/D<10 defines an open cavity while L/D>10 is considered a closed cavity. Figure 3 shows a schematic of both an open (a) and closed cavity (b).

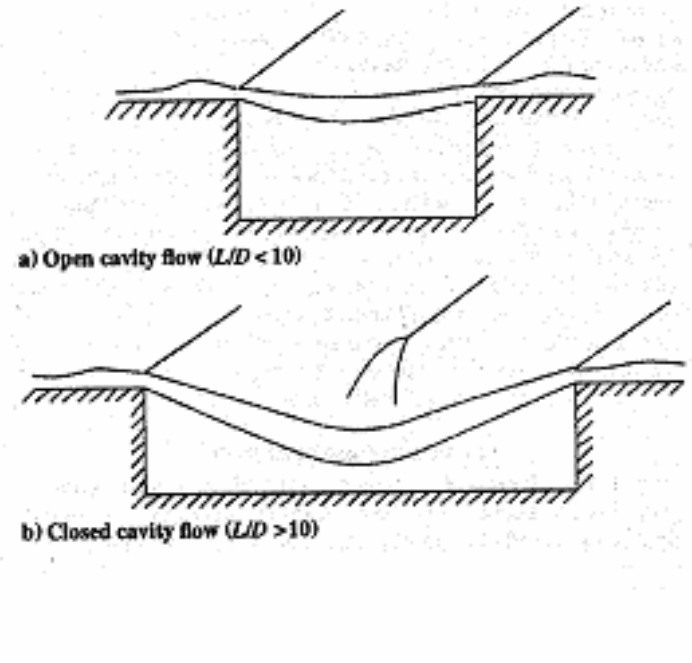


**Figure 3** Cavity flows (Ref 5)

Studies have shown that open cavities impose a smaller drag penalty on a supersonic engine.[4] Therefore, all cavity flows studied were of the open type.

A typical wall cavity based flameholder is shown in Figure 4 below. Previous studies have concluded that variations in geometry affect different aspects of the flow in and around the cavity.

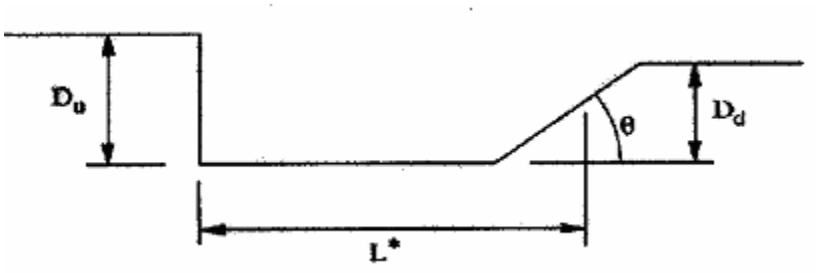


**Figure 4** Cavity geometry (Ref 5)

Note that the cavity length (L*) for a rectangular cavity includes the entire length of the floor and one half of the streamwise (x direction) portion of the aft ramp as expressed mathematically in the following equation.

$$L^* = L + \frac{1}{2} \cdot \frac{D_d}{\tan(\theta)} \qquad (1)$$

Gruber et al. studied the flowfield in and around several different geometric configurations under Mach 3 flow conditions. The study was non-reactive and included both schlieren and shadowgraph photography. Furthermore, a computational fluid dynamics (CFD) routine was executed for various cavity geometries. Residence time ($\tau$) was reduced from CFD data. Starting from a steady state solution the fluid is marked and the simulation is stepped forward in time while the marked fluid is monitored as it exits the cavity. The drag coefficient presented in their study is the drag force normalized by the freestream dynamic pressure and the cavity fore wall area. Some general conclusions from this study are presented below[5]. As the aft wall angle ($\theta$) is reduced from 90° a more stable, two-dimensional flowfield is formed. The separation wave at the forward cavity step changes from compressive to expansive as $\theta$ steps from 90-30-16° as shown in Figure 5. Note that for this setup, compression waves appear darker than expansion waves in schlieren photography due to the increase in density. Additionally, reductions

in the aft ramp angle from 90-30-16° resulted in higher drag coefficients and lower residence times, both of which could be considered detrimental to an effective flameholder. However, the resulting stable flowfield from a decreased aft ramp angle could justify a decrease in residence time and an increase in drag coefficient. "In general, decreasing the aft wall angle should promote both a more acoustically stable cavity flow (and subsequent stable burning) and improved entrainment because the shear layer impinges deeper into the cavity."[5] This trend has been verified in reactive studies. After several injection sites were studied for a fixed cavity geometry, a wider range of sustained flames was established using cavity ramp injection.[4]

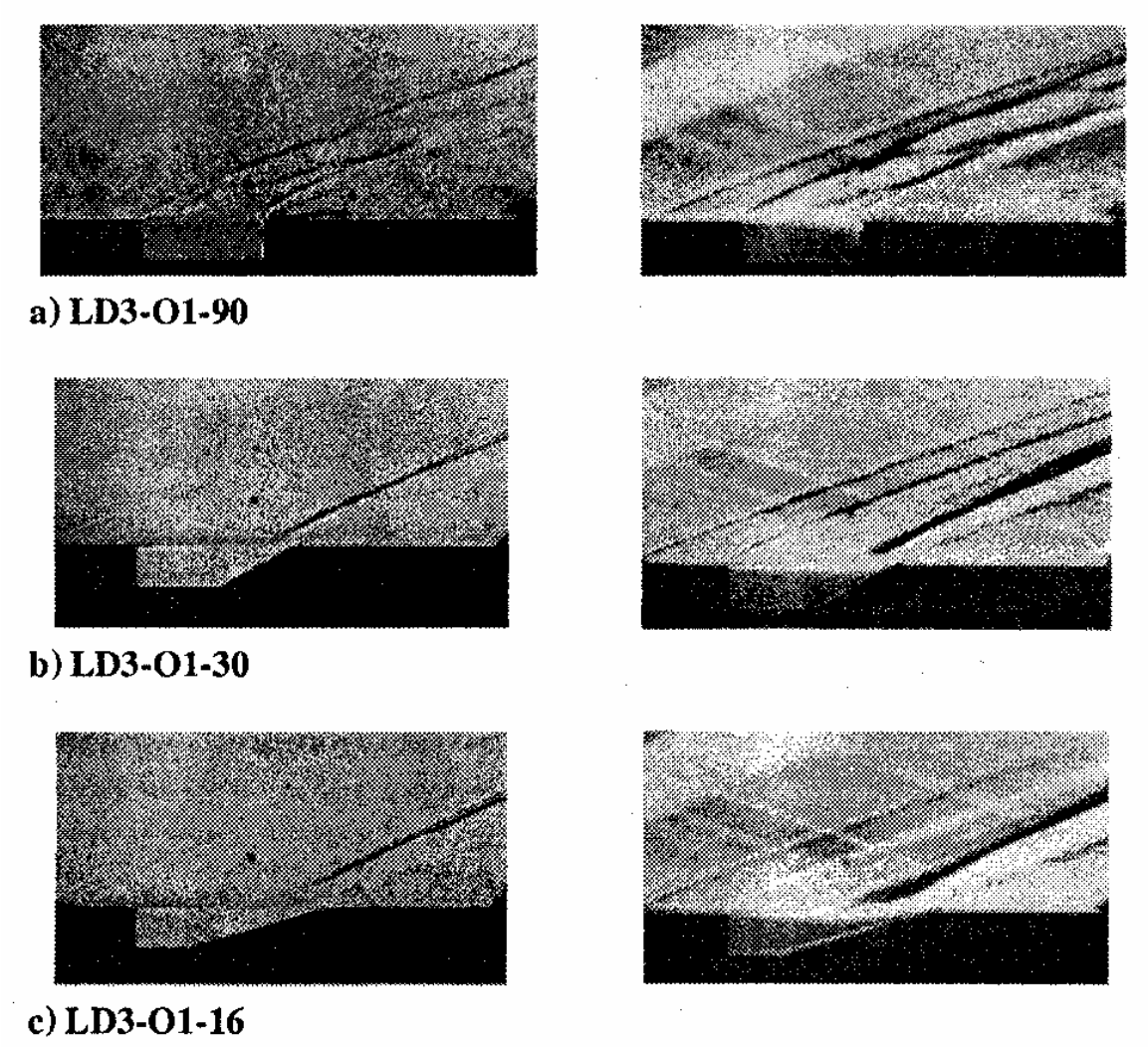


**Figure 5** Aft ramp angle effects (Ref 5)

Changes to the offset ratio cause drastic changes to the flowfield. One of the most notable features is the strong expansion fan at the fore cavity. Increasing the offset ratio seems to influence the vortex structure within the cavity. Note the curved shape of the waves generated by the cavity ($\theta$=90°,OR=1) in Figure 6a.

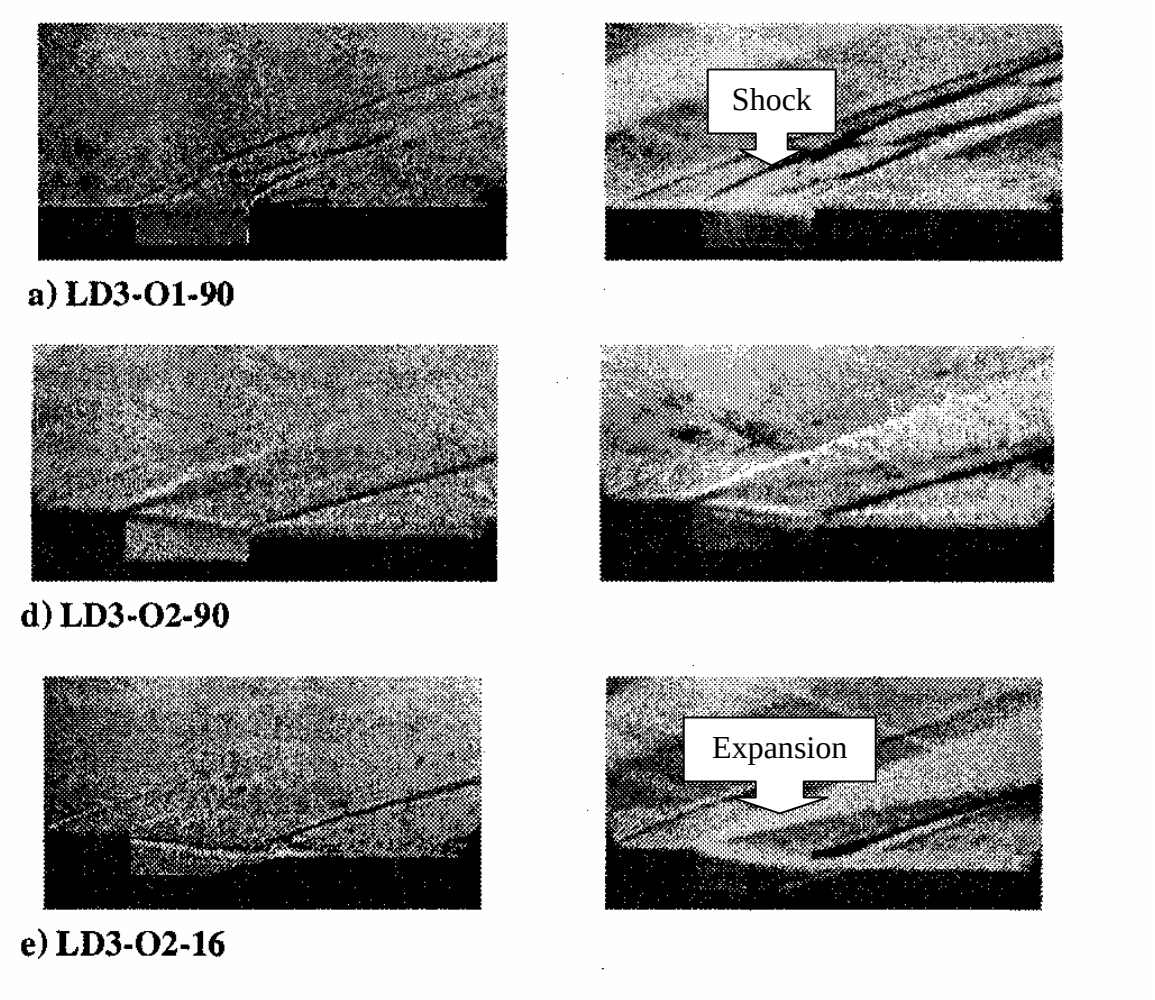


**Figure 6** OR effects (Ref 5)

These waves may be the product of the oscillatory nature of the cavity vortex. When the offset ratio was increased to 2 for the same aft ramp angle curved waves were not generated. Increased length increased the pressure in the recompression region with little influence on the upstream face of the cavity. The increased length also equated to increased form drag and increased free stream entrainment due to the increased shear layer length. Previous low speed combustion studies found optimum flameholding performance coincided with a cavity with its length to depth ratio sized for the minimum aerodynamic drag. Longer cavities produced vortex shedding that resulted in cavity

oscillations and unstable flames and shorter cavities lacked sufficient air entrainment to sustain combustion.[6] As noted before if the cavity length increased such that the cavity was closed (L/D>10) an even greater increase in drag would occur. Cold flow calculations performed by Baurle and Gruber for various geometries show that cavity length determines mass entrainment and cavity depth determines residence time.[5,7]

Cavity geometry impacts the flowfield in and around the cavity. Numerous studies have been accomplished regarding flow over open cavities as it is an often-seen configuration. There are several flow trends that should be noted. First rectangular cavities are usually characterized by a level of unsteadiness. This unsteadiness is observed as oscillations in pressure, density and velocity in and around the cavity. Unsteadiness introduces another complicating element into the cavity flow dynamics and it has been noted that cavity flow can be very three dimensional, especially off centerline. Secondly, the creation of a lobed recirculation zone is commonly noted. Figure 7 shows the pressure contours and stream traces derived from a standard two-dimensional eddy-viscosity-based CFD turbulence model. Notice that two counter rotating lobes are formed for each of the geometries used in the simulation. Decreasing the aft ramp angle appears to decrease the size of the secondary lobe. However, for both L/D and each aft ramp angle studied a primary and secondary vortex was generated. It has been noted in previous subsonic combustor simulations that the sizes of the vortices alternate in time. Cavity flow is further complicated by the three dimensionality of the flow. The simulation results shown in Figure 7 are based on the cavity centerline where the flow tends to be two dimensional in the x-y (streamwise-transverse) plane. However, because

flow is three dimensional additional structures most likely exist in the x-z (streamwise-spanwise) plane. This aerodynamic feature of cavities presents both challenges and benefits to its use as a cavity based flameholder. The region of recirculation will provide additional residence time for combustion to take place. However the dual vortex structure may require more complicated fueling schemes to provide a uniform combustible mixture throughout the cavity.[5]

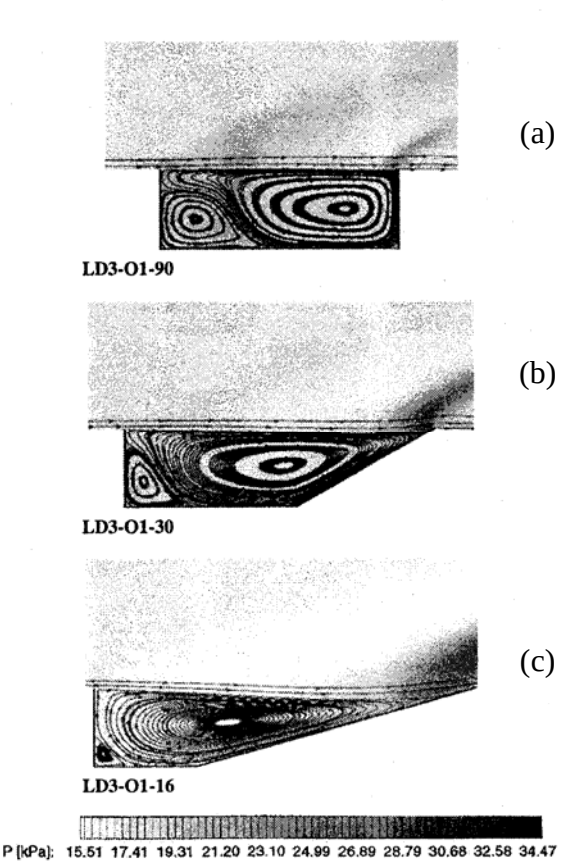


**Figure 7** Stream traces (Ref 5, M=3)

Wright-Patterson AFB propulsion laboratory has performed studies to determine optimal fueling strategies for cavity based "trapped vortex" flameholders. A "trapped vortex" flameholder is obtained when a stationary vortex is established inside the cavity

as shown in Figure 7.[8] Ideally, the cavity will provide a subsonic region more suited for stable combustion and an increase in residence time allowing more complete combustion. Furthermore, the region of hot re-circulating gases could provide a continuous source of ignition. The aforementioned benefits of a cavity based flameholder require that cavity flow, and, in turn, the combustion process is stable. This is a challenge given the wide flight envelope and subsequent burner aerodynamics of a dual-mode engine. A dual-mode engine is one in which flow characteristics through the burner or combustion region could be either subsonic as in the case of a RAMJET or supersonic as in the case of a SCRAMJET. Fueling strategies must be derived to ensure a robust flameholder. First consider the air entrainment rate for both the subsonic (high backpressure) and supersonic (low backpressure) cases. Figure 8 shows a representative shadowgraph images for each case. Notice the shear layer reattachment is on the aft ramp face for the purely supersonic case ( low backpressure) and that it is lifted away (separated) from the cavity in the subsonic/supersonic case (high backpressure).

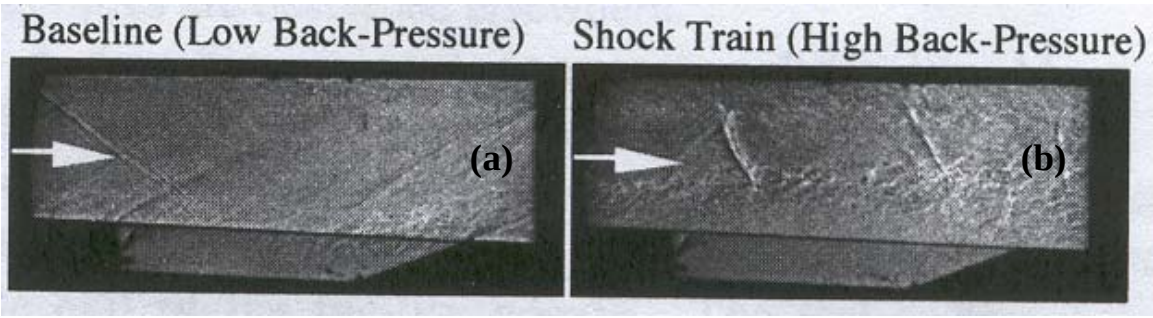


**Figure 8** Cavity flow conditions (Ref 4)

This difference substantially alters the freestream entrainment which could be a mixture of fuel and air, and effectively increases the volume of the cavity in the high backpressure case. It has also been shown that mixing is enhanced within the cavity by the shock train

developed at a high backpressure. Several fuel injection strategies were studied by Gruber et al.[4] for both the high and low backpressure cases. Figure 9 shows the multiple injection ports both inside the cavity (direct injection) and outside of the cavity (passive injection).

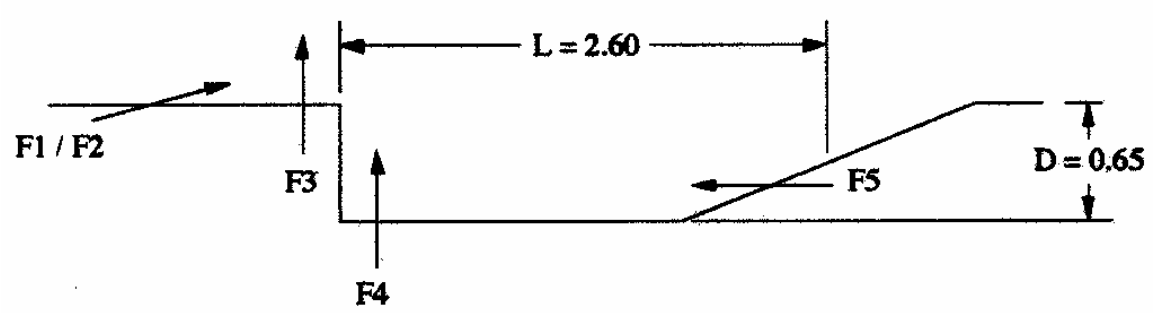


**Figure 9** Fuel injection sites (Ref 4)

Mixing studies involving indirect injection showed higher jet penetration given the high backpressure condition. This equated to a reduced entrainment into the cavity. They also showed that entrainment into the cavity relies largely on diffusion through the shear layer and the interaction between the shear layer and the aft ramp face. Direct injection through F4 and F5 ports were in general better cavity fueling schemes. However, cavity fueling was still dependent on the shear layer interaction with the aft ramp. As noted before the flameholder must be effective during dual-mode operation. Several cavity combustion tests were conducted during the transition from low to high backpressure. The only fueling scheme that produced sustained cavity combustion with the presence of the shock system was F5 (aft ramp injection). The influence of the shock system and shear layer on cavity fueling is minimized by fuel injection from F5. Despite the increased robustness of the flameholder using aft ramp injection fueling schemes, Gruber et al. noticed that some fuel injection pressures resulted in localized combustion regions.

This suggested that the cavity may be too large for efficient mixing and combustion for the conditions tested. A drag penalty is paid for the inclusion of a cavity based flameholder. From this standpoint it is important to ensure that the cavity size is kept to a minimum and therefore efficient use of cavity volume is essential. Figure 10 shows ensemble averaged (EA) and standard deviation (SD) OH-PLIF images at a single streamwise location in the cavity. Fuel flow was set at 40, 60 and 90 standard liters per minute (SLPM) from top to bottom. Notice that at this station, the low fuel flow rate provides the best fuel combustion as evidenced by the increased intensity.

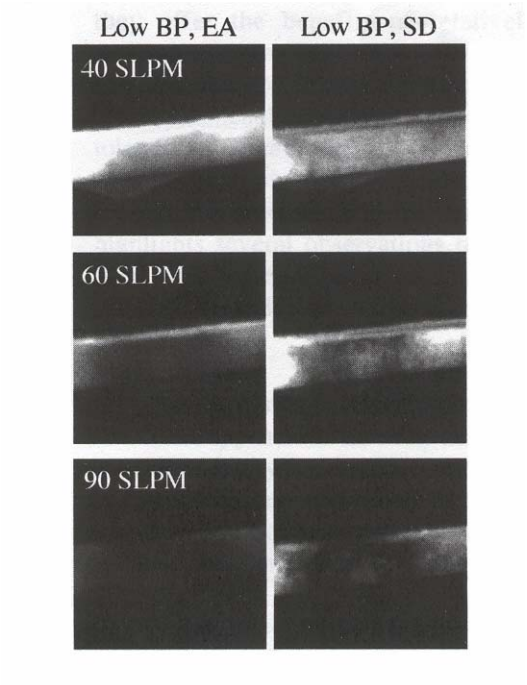


**Figure 10** OH-PLIF fuel distribution (Ref 4)

This indicates that given a fuel-only flow the fuel flow rate must be tuned to obtain maximum utilization of the cavity volume with minimum flame oscillations. Aft ramp fueling strategies appear to offer the best fuel/air distribution within the cavity as well as a wide rage of fuel flow rates over which combustion may be sustained when compared

to other fueling locations studied. The fuel flow rate can be optimized and deviations from this optimal point lead to a flame with increased oscillations and large spatial gradients.[4] Fueling the entire cavity from a single streamwise location can be complicated due to the aerodynamics of the cavity vortices. Fuel must be transported from the injection site forward to the cavity step by means of these structures. Fuel/air ratios further complicate the situation. For efficient use of the cavity volume the fuel/air ratio must be an appropriate mixture throughout the cavity. Figure 11 shows the mass distribution from a non reactive simulation performed along the centerline of a cavity after approximately 3 ms have elapsed.

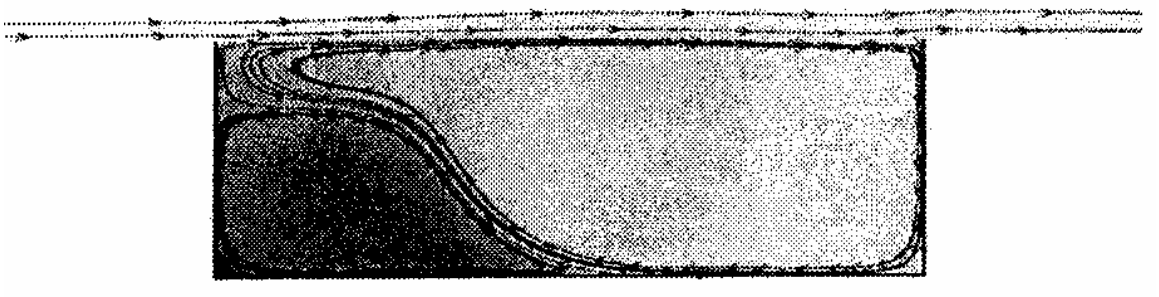

**Figure 11** Mass distribution (Ref 5)

Notice that more mass has been exchanged between the core flow, shear layer and primary lobe than between the secondary and primary lobes. This implies that a single fuel injection site may not be sufficient to fuel the entire cavity uniformly. The residence times and mass exchange rates described above were based on non-reactive flow. Winterfeld compared both isothermal and combusting cavity flameholders and found that compared to isothermal flows, reactive flows exhibited increased residence times and decreased mass exchange rates.[9]

## Summary

Previous studies have concluded that given a properly tuned fuel-only flow into the cavity, minimum flame oscillations and maximum utilization of the cavity volume results. Deviation from this optimal level leads to a flame with increased oscillations and large spatial gradients that decrease the effectiveness of the flame holder.[4] The characterization of cavity-based fueling systems is still largely unavailable. Therefore, the subject of this investigation was to expand the cavity based fueling system such that both fuel and air are directly injected. It is proposed that this method will provide a uniform fuel air distribution within the cavity over a wide range of fuel flow rates and freestream conditions thereby resulting in an efficient, robust flameholder. Additionally, this study included characterization of the operational limits (i.e., sustained combustion limits) over a variety of fuel and air flow rates.

# III. Methodology

## Chapter Overview

The purpose of this chapter is to introduce the test facility, test methods and specific hardware utilized in this study.

## Test Facility

The facility used in this investigation was designed to allow basic studies of supersonic flows using conventional and non-intrusive diagnostic techniques. A continuous supply of clean compressed air is available to provide stagnation conditions

up to 1660°R and 400psia and a total maximum flow rate of 30 lbm/s. Figure 12 is a photograph of this test facility and Figure 13 is a schematic of the test facility.

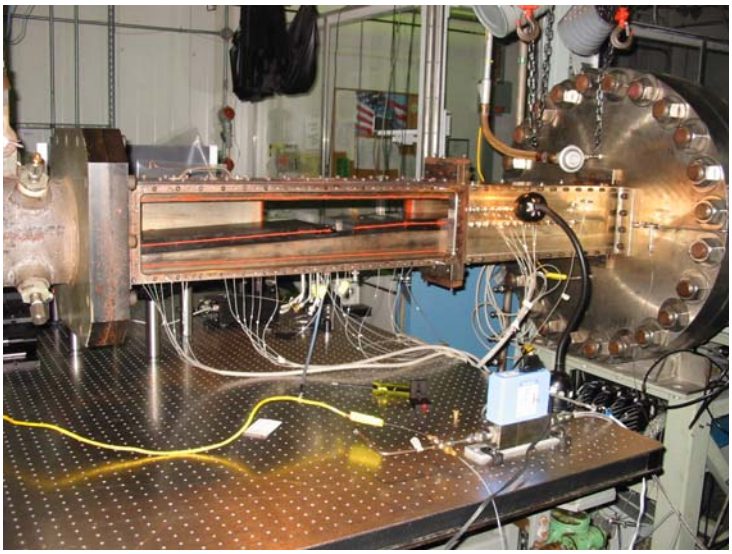

**Figure 12** Test facility photograph

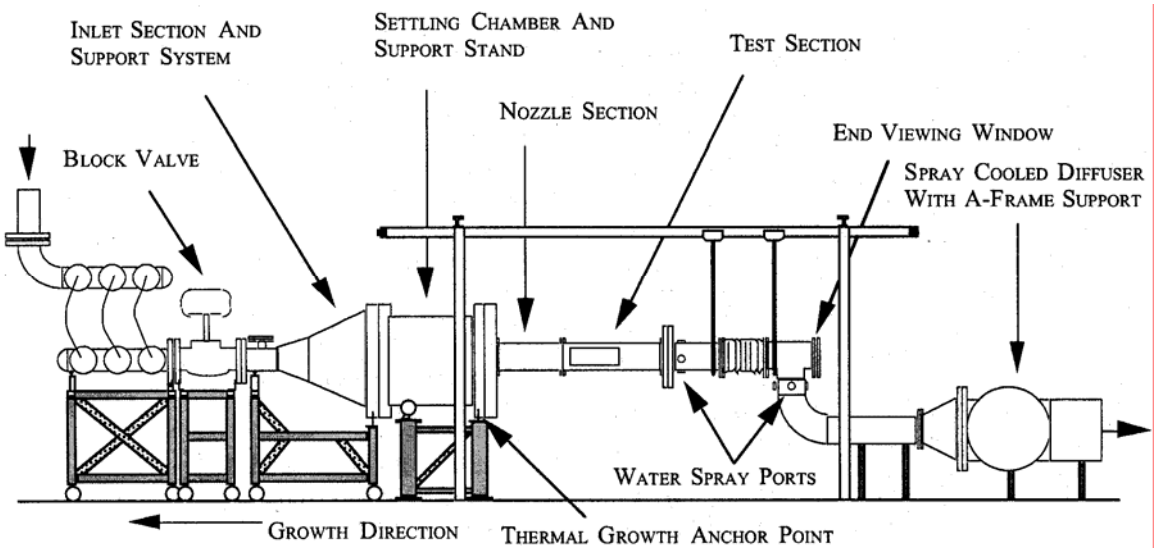


**Figure 13** Test facility schematic (Ref 10)

A two-dimensional converging-diverging Mach 2 nozzle section, configured with an asymmetric nozzle, is used to develop the desired inlet conditions. The test section is

connected directly to the 2-inch high by 6-inch wide exit of the facility nozzle. The test section has a constant-area isolator section (7 inches long), followed by a divergent ramp (2.5 degrees over 29.125 inches in length). Figure 14 is a schematic of the facility flow path. The modular cavity is flush-mounted to the ramp in the divergent section.[10] The

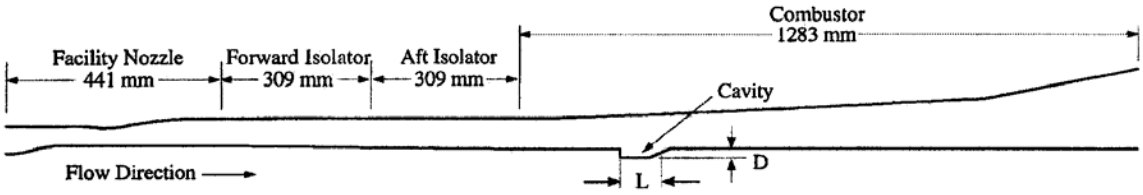


**Figure 14** Flowpath schematic (Ref 6)

cavity, shown in Figures 15 and 16, is recessed from the surface with a 90-degree rearward-facing step, and the trailing edge is configured with a 22.5-degree ramp. The current flameholder configuration has a depth of 0.65 inches and a length of 2.60 inches. Fuel and air injection is accomplished through three sets of injection sites located along the aft ramp. All injectors are directed parallel to the cavity floor.

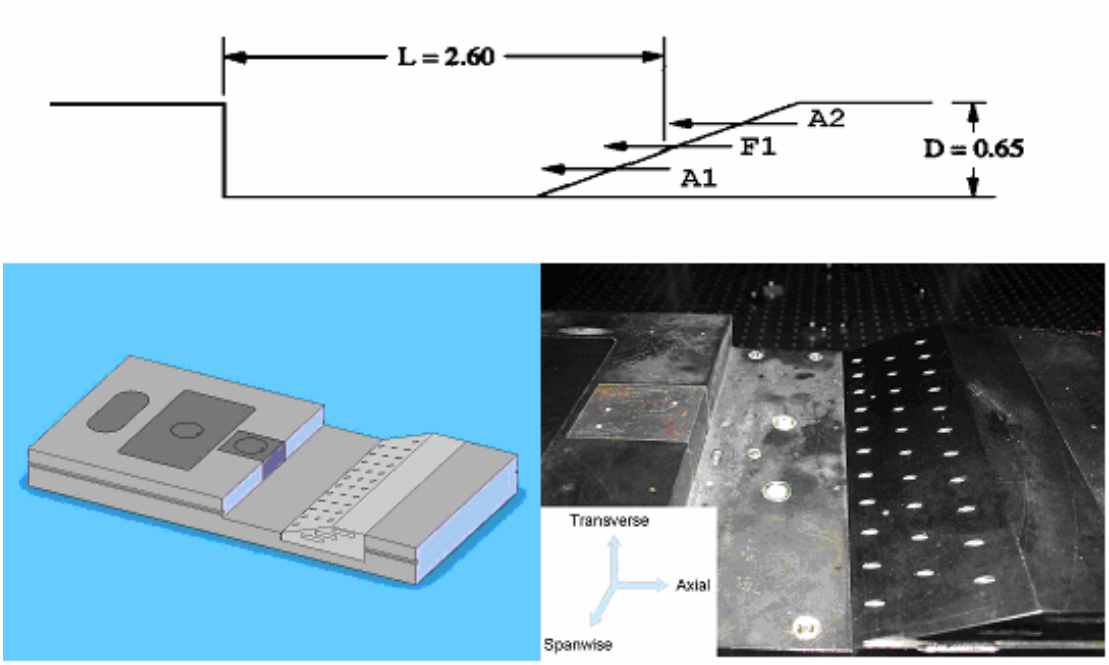


**Figure 15** Cavity geometry

Each spanwise row of injectors is fed from a single manifold and can be configured to inject either air or fuel. The following table provides greater injection site detail.

**Table 1** Spanwise injectors

| Nomenclature | Injection Type | Number of injectors | Injector Diameter (in) | Height above floor (in) |
|---|---|---|---|---|
| Upper Row (A2) | Air | 11 | 0.078 | 0.35 |
| Middle Row (F1) | Fuel | 10 | 0.063 | 0.55 |
| Bottom Row (A1) | Air | 11 | 0.078 | 0.75 |

This fueling scheme allows the fuel oxidizer to be obtained from main two sources: direct injection and free stream entrainment. Free stream entrainment is dependent upon fixed quantities such as cavity geometry and the variable quantity of free stream flow

conditions. This provides the SCRAMJET operator/control module little recourse to optimize the flameholding cavity without considering limiting the flight envelope.

The fuel and air injection system was automated and interfaced with a computer based controller and data collection system. The injection pressure was regulated with a dome loader and controlled remotely with an air-actuated isolation valve. A pressure transducer and thermocouple were used to measure the pressure and temperature of the injectant. All data was recorded in a computer for future analysis. The mass flow rate of gas was measured using a bank of Tylan mass flow controllers. These mass flow controllers are manufactured to output air given their full scale rating which is measured in Standard Liters Per Minute (SLPM). Because one of these controllers was configured to measure the flow rate of ethylene as opposed to air, a correction factor of 0.6 was applied in accordance with the Tylan mass flow controller users manual. The ethylene fuel was introduced into the cavity using a 200 SLPM full scale mass flow controller and the air was metered by a 500 SLPM mass flow controller. As noted before, full scale flow rates are based on air as the fluid. The full scale flow rate for the ethylene controller was calculated to be 120 SLPM. Three fuel flow rates of 38.4, 60 and 90 SLPM (32%, 50% and 75%) were selected for this study. Likewise several different air flows were introduced through A1 and A2 injection sites. Table 2 below shows the calculated equivalence ratio based on the injectant for various air and fuel flow rates.

**Table 2** Introduced equivalence ratio

| | | Fuel Flow Percentage | | | |
|---|---|---|---|---|---|
| | | 32% | 50% | 75% | 90% |
| Air Flow Percentage | 15% | 1.5 | 2.4 | 3.6 | 4.3 |
| | 25% | 0.9 | 1.4 | 2.2 | 2.6 |
| | 30% | 0.8 | 1.2 | 1.8 | 2.2 |
| | 40% | 0.6 | 0.9 | 1.4 | 1.6 |
| | 45% | 0.5 | 0.8 | 1.2 | 1.4 |
| | 50% | 0.5 | 0.7 | 1.1 | 1.3 |
| | 60% | 0.4 | 0.6 | 0.9 | 1.1 |
| | 70% | 0.3 | 0.5 | 0.8 | 0.9 |
| | 75% | 0.3 | 0.5 | 0.7 | 0.9 |
| | 80% | 0.3 | 0.5 | 0.7 | 0.8 |
| | 90% | 0.3 | 0.4 | 0.6 | 0.7 |
| | 100% | 0.2 | 0.4 | 0.5 | 0.6 |
| | | | | | Rich |
| | | | | | Lean |

The equivalence ratio was calculated given the following stochiometric reaction.

$$1C_2H_4 + 3(O_2 + 3.76N_2) \rightarrow 2CO_2 + 2H_2O + 11.28N_2 \qquad (2)$$

Equation 2 expressed generally takes the following form:

$$1C_2H_4 + 3(O_2 + 3.76N_2) \rightarrow \text{Products} \qquad (3)$$

Based on equations 2 and 3 the stochiometric ratio of fuel to air is 1/3 which can be substituted into equation 4 to determine the equivalence ratio ($\theta$) of the injected fuel and air.

$$\theta = \frac{F/A_{actual}}{F/A_{stochiometric}} \qquad (4a)$$

$$\theta = 3F/A_{actual} \qquad (4b)$$

Mixtures that are fuel rich have equivalence ratios greater than one, while lean mixtures can be denoted by equivalence ratios less than one. Stochiometric mixtures have equivalence ratios of unity by definition.

**Hydroxyl Planar Laser-Induced Fluorescence (OH-PLIF) Diagnostic**

PLIF imaging is accomplished by exciting atoms and molecules using a two-dimensional area of laser light. The laser light energy is absorbed by the atoms and molecules which, in turn, can potentially decay back to the ground state. This release of energy is imaged at a right angle to the path of excitation onto a two-dimensional digital camera. As expected, the intensity of the image depends upon the chemical composition and local physical properties of the flow. This study will assume that increased image intensity is a function of increased concentration of OH. In other words, higher signal implies higher concentration.[11]

Instantaneous measurements of the reacting flowfields were obtained using planar laser-induced fluorescence of the hydroxyl radical (OH). As noted previously, this requires the presence of the hydroxyl radical produced during combustion. The laser sheet was formed across the test section using a pair of lenses, a plano-concave and plano-convex cylindrical lens and was approximately 2 inches in height. This sheet was directed across the span of the test section through fused silica windows. A Lumonics Hyperdye dye laser was pumped with the second harmonic of an injection-seeded Spectra Physics Nd:YAG laser (GCR-170). The dye laser was tuned to 587 nm and the output was frequency-doubled using an Inrad Autotraker III. To ensure good overlap of the laser and transition, a portion of the UV beam was split off and directed over a smaller reference flame and then to a fast photodiode. The laser induced fluorescence was focused onto the photocathode of a photomultiplier tube. This signal, along with the photodiode output, was continuously displayed on an oscilloscope, allowing minor

adjustments to be made to the dye laser grating position to minimize the effects of test cell temperature changes. The resulting fluorescence was imaged off-axis to the sheet normal. The transmitting and receiving optical hardware were positioned on a streamwise traversing table allowing remote positioning of the measurement volume at any desired station in the flowfield.[3]

A Princeton Instruments PIMAX CCD camera with a 512x512 pixel array was used to detect the fluorescence. The camera was fitted with a UV lens and Schott glass filters. Note that the LIF images were not corrected for variations in line broadening, electronic quenching, or ground state population.[3]

Traditional pressure and temperature measurements were recorded for each tunnel condition. Pressure measurements were taken using strain gage type transducers located along the centerline of both the top and bottom wall of the test section. Temperature measurements were taken at the cavity rear facing step and at the aft ramp face using Type K thermocouples. The cavity step temperature was determined solely from the single transducer located at the centerline of the test section. Aft ramp temperature could be deduced from a pair of thermocouples offset from the centerline. The readers should reference appendix A for more information on test facilities, equipment and hardware.

**Summary**

The test facility designed and maintained by AFRL provided an excellent resource for the experimental reaction cavity based flameholding studies. Non intrusive techniques namely PLIF and high speed digital emissions video was utilized to provide flow characterization data. These images were reduced primarily through the use of

imaging software (Image J version 1.23jand PDView version 5.0) to determine the mean and standard deviation of a series of chronologically sequential images. Mean images were use to characterize the intensity and concentration of hydroxyl radicals given high speed emissions camera and PLIF diagnostics respectively. Standard deviation results were considered to be a qualitative measure of unsteadiness and therefore flame instability.

# IV. Analysis and Results

## Chapter Overview

The Air Force Research Lab Propulsion Directorate has performed several cavity based flameholding studies. One of the most recent found that direct injection of ethylene fuel into the aft cavity ramp produced an efficient, robust flameholder given specific freestream conditions and fuel flow rates. This chapter discusses the effects of the addition of direct air injection to cavity combustion. Direct injection of both fuel and air provided additional capability to tune the cavity such that a more stable decentralized flame results. The largest improvement over the baseline case (fuel only) was noted near the upstream portion of the cavity close to the cavity step. This injection scheme expanded the operational limits significantly for each selected fuel flow.

**PLIF Diagnostics by Streamwise Station**

The cavity was configured for air injection through the lower injection rows (A1) and for fuel injection through the center row (F1). The test conditions were nominally at Mach 2 with a stagnation pressure and temperature of 80 psia and 580°F with low backpressure (i.e. purely supersonic flow through the test section). Fuel was injected at 35%, 50% and 75% of full flow of the fuel mass controller (120 SLPM). This resulted in fuel flow rates of 38.4, 60 and 90 SLPM respectively. The OH-PLIF diagnostic was configured to acquire planar images at three different streamwise stations as measured from the rear facing step (0.125", 1.5" and 2.5"). Laser planes are shown in Figure 16 below. Freestream flow is indicated by the arrow.

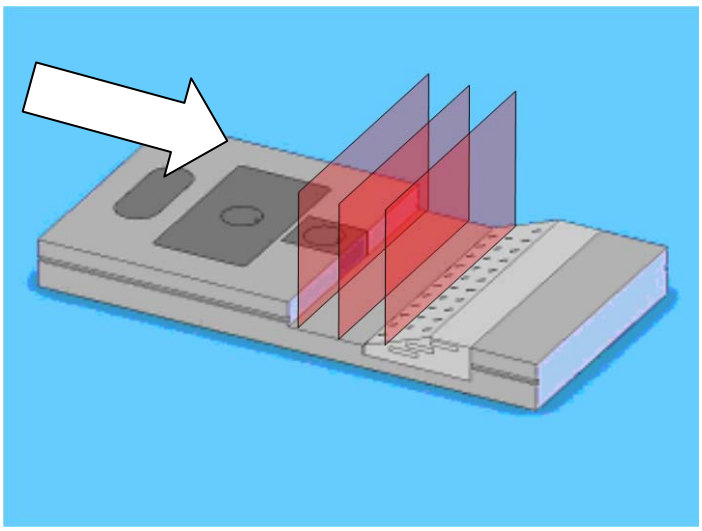

**Figure 16** Laser planes

Station 1 was defined to be located at 0.125 inches from the cavity step and stations 2 and 3 were located at 1.5" and 2.5" from the cavity step, respectively. Baseline cases were run for all fuel flow cases (35%, 50% and 75%) and PLIF images were taken at all

stations. Mean baseline results are shown in Figure 17. Stations 1 through 3 are labeled respectively and unless otherwise noted, all images are presented on the same intensity scale (1800-6000) to allow unbiased comparison. The scale presented above defines pixels with a value of 1800 to be represented by black and pixels with a value of 6000 to be represented as white. Pixels between 1800 and 6000 will be shown in shades of grey. The spanwise centerline of the cavity can be imagined as a vertical line located near the right-hand side of each image.

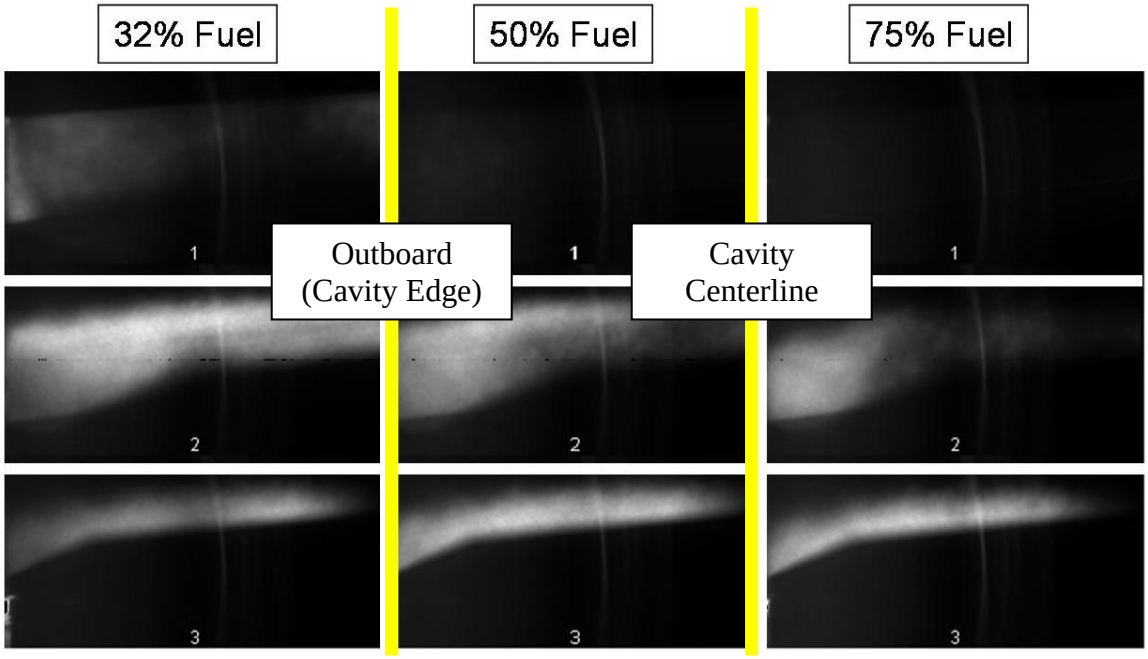


**Figure 17** - Baseline (fuel only)

Given that the images above were acquired at three different streamwise locations throughout the cavity, these images provide information as to where combustion was occurring within the cavity. An efficient cavity should exhibit evidence of combustion reactions, hydroxyl radicals (OH) in this case, throughout its volume. The presence of OH is indicated by increased pixel intensity (white regions) within the photograph. This

study will assume that the presence of OH is proportional to the combustion reaction rate that is taking place at the given section. However, it is important to note that the presence of OH at the measured location could be the result of the production at another location and subsequent diffusion and/or transport to the measured location. This is due to the relatively long life of the hydroxyl radical. Notice that the intensity is highest at stations 1 and 2 given the 32% fuel flow when compared to their respective stations at higher fuel flow rates. This is most notable for station 1 because based on this scale very little intensity is noted at station one for both increases in fuel flow above 32%. Furthermore, the overall intensity at stations 1 and 2 decreases with increases in fuel flow rate. This indicates that as fuel flow increases above 32%, combustion was negatively affected at streamwise stations forward of the aft ramp (stations 1 and 2). Close inspection of station reveal a slight increase in intensity between 32% and 50% fuel loadings and subsequent slight decrease in intensity between the 50% and 75% fuel loadings. Figure 18 shows the mean images taken at station 3 for increasing fuel flow. The images are numbered according to fuel flow rate where image 1 was derived from 32% fuel flow and image 3 was derived from 75% fuel flow. The scale was modified slightly and is bounded between 1800 (black) and 5350 (white).

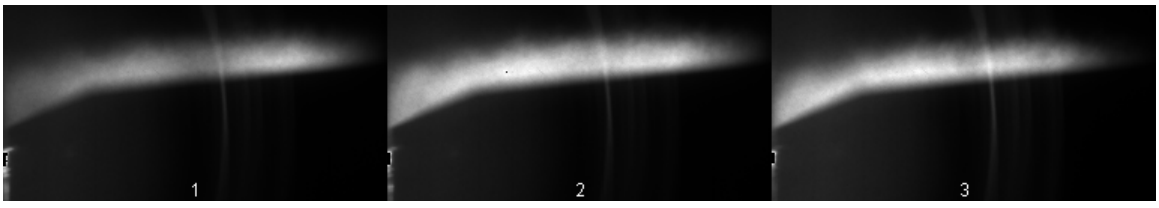


**Figure 18** OH-PLIF diagnostic at station 3

The baseline case exhibits the same trend observed in previous research. Specifically, a cavity that is directly fueled is optimally tuned for a single fuel flow rate. Increases or

decreases from this “optimal” level lead to localized regions of combustion which can be interpreted as inefficient use of the cavity volume. From this standpoint, when fuel was injected at 38.4 SLPM (32%), the cavity was optimally tuned given the fuel only injection schemes studied and shown in Figures 17 and 18 because evidence of combustion was noted at all stations.

Air was directly injected through the bottom injection ports (A1) into the cavity to study its effects on combustion. This was accomplished using a mass flow controller with a full scale capability of 500 SLPM. The same fuel flow rates were utilized for ease of comparison. Figure 19 shows the effects of air injection given a constant fuel flow rate of 32% (58.4 SLPM). Air is injected at 50% (250 SLPM) in addition to the baseline (fuel only) case.

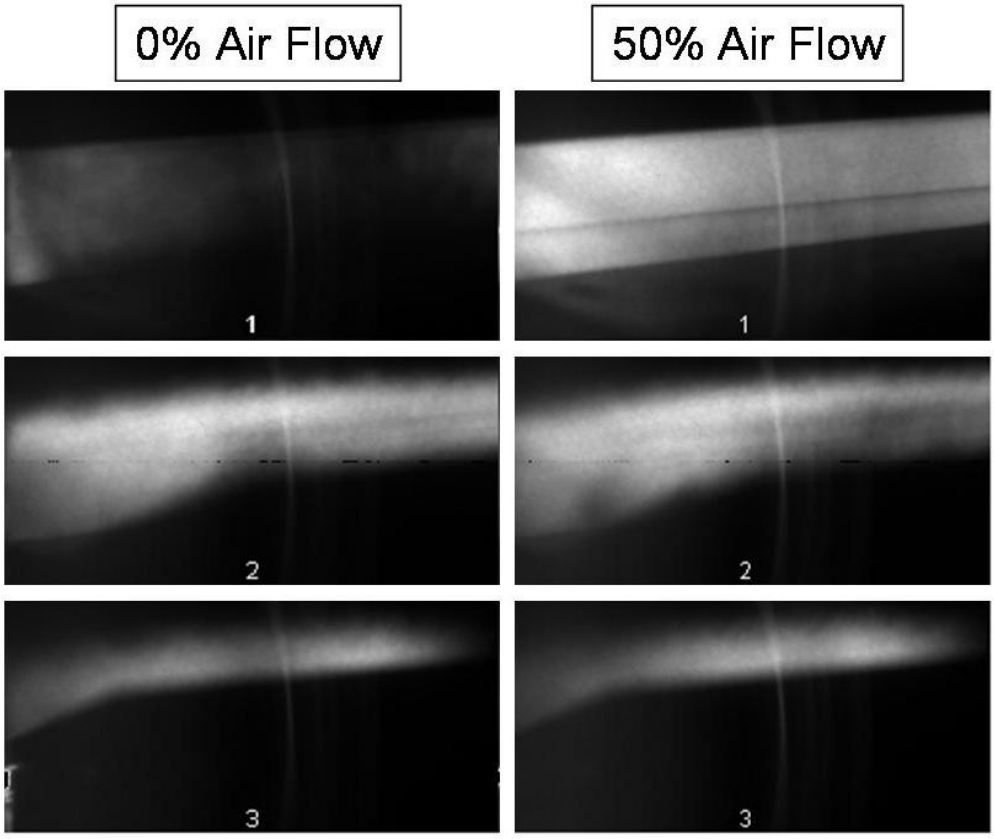


**Figure 19** Increased air flow (32% fuel flow; A1)

Figure 19 shows an improvement in cavity combustion most notably at station 1 whereas very little change is noted at stations 2 and 3. This effect demonstrates that the direct injection of air through the bottom row of injectors can provide another mechanism to optimize the combustion process with the cavity. However as shown above, at this test point, increases in air injection do not necessarily result in improved combustion through the entire cavity because combustion at stations 2 and 3 remain largely unchanged. The most notable increase in combustion was at station 1 near the cavity step.

Fuel was introduced at 50% (60 SLPM) and air was injected at 50% (250 SLPM) and 75% (375 SLPM) in addition to the baseline (fuel only) case through A1. Figure 20 shows the effect of increased air flow given a constant fuel flow rate of 50% (72 SLPM).

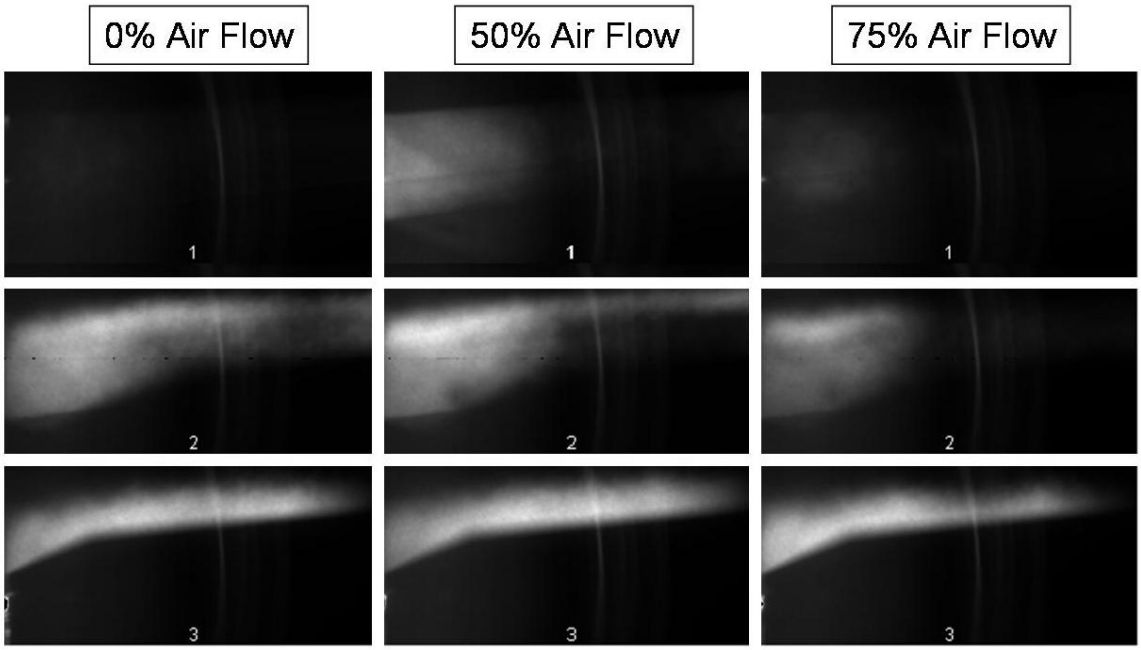


**Figure 20** Increased air flow (50% fuel flow; A1)

The increase in airflow from the baseline case to 50% (250 SLPM) air injection flow rate caused an increase in combustion at station 1. However the continued increase in airflow from 50% to 75% (375 SLPM) resulted in a decrease in combustion at station 1. To better illustrate the changes at station 1 given increases in air injection, station 1 mean images were again computed at a lower intensity level (1800-4500). In other words, the first row of Figure 20 is presented again with a different scale and is shown in Figure 21. Image intensity remained steady for station 2 and 3 given all air loadings applied at this test point.

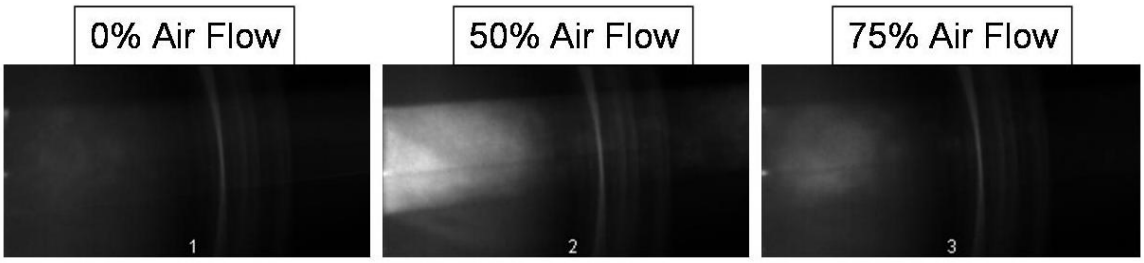


**Figure 21** - Increasing air flow (station 1; 50% fuel flow; A1)

Although there was insufficient resolution given the data to determine the airflow rate that provided the optimum utilization of cavity volume for this fuel loading, when the air flow was at 50%, station 1 exhibited the highest concentration of OH among conditions tested. In the same way that stations 2 and 3 were minimally affected by the introduction of air at 32% fuel loading, combustion at stations 2 and 3 at 50% fuel loading seem to be independent or weak functions of introduced air flow.

Fuel was introduced at 75% (90 SLPM) and air was injected at 85% (425 SLPM) through A1 in addition to the baseline (fuel only) case. Figure 22 shows the effect of increased air flow given a constant fuel flow rate of 75% (90 SLPM).

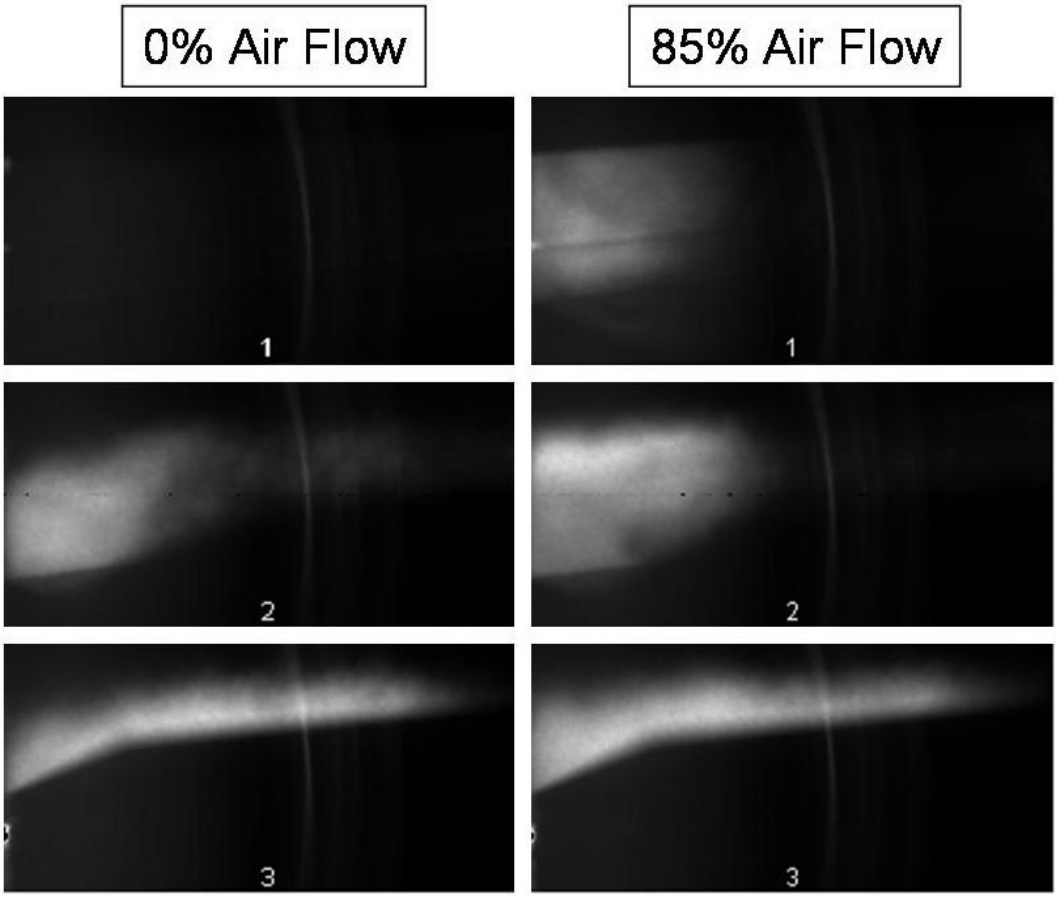


**Figure 22** Increased air flow (75% fuel flow)

The combination of this fuel loading and the introduction of air demonstrated similar trends compared to the 32% and 50% fuel flows. The greatest increase in intensity was evidenced at station 1 although stations 2 and 3 incurred a slight intensity increase given the increased air flow.

This fueling scheme, fuel injection at F1 and air injection at A1, produced an increase in combustion at station 1 in each of the three fuel flow rates. Figures 19 through 22 show that given direct air injection cavity combustion can be optimized for various fuel flow rates. However, as noted before, combustion is not necessarily improved uniformly throughout the cavity. The inconsistency in cavity combustion

throughout the volume is a product of the complexities of mixing, variations in local temperature and pressure and three-dimensional cavity flowfields among a host of other parameters. Figures 7b and 7c show the stream traces of cavities with comparable geometry to the experimental hardware. Notice that two counter-rotating lobed structures are commonly found in such a configuration. This structure complicates the fuel and air transport mechanism especially near the cavity step. As noted before, mass (air, fuel and products of combustion) is transported at different rates between the freestream/cavity shear layer/aft vortex and the forward vortex/aft vortex. Previous aft ramp, direct fuel-only injection studies have concluded that for higher fuel flow rates a fuel rich region is formed near the cavity step.[4] This region, as implied, is not populated by a combustible mixture and therefore contributes to the overall inefficiency of the cavity volume.

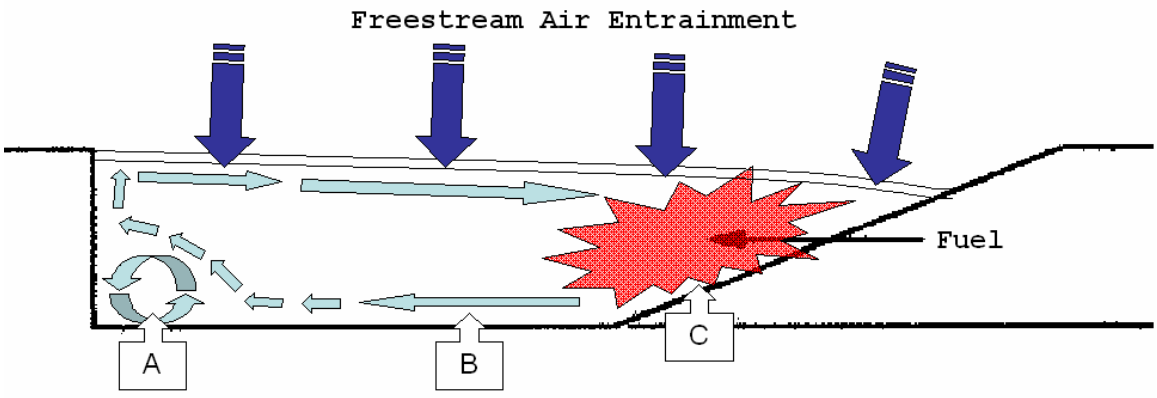


A – Excess fuel is entrained by forward vortex and lacks sufficient oxidizer for combustion
B - Momentum of aft vortex and fuel injectant carry products of combustion and unburned fuel toward the cavity step
C – Combustion region

**Figure 23** Rich cavity combustion (Fuel only injection)

The addition of air injection through A1 served to aid combustion at station 1 when compared to the baseline (fuel only) case. This observation was noted previously and

evidence was presented in figures 19 through 22. As noted in Figure 23, the region sampled at 0.125 inches from the cavity step (station 1) has the potential to become "rich" in the absence of sufficient air injection given the fuel loading. This tendency at station 1 to become rich is offset by the direct air injection. Similar to the positive combination of fuel injectant and cavity vortex, air injected near the bottom cavity floor is complimentary to the local flowfield and improves air transport toward the cavity step. However, this injection scheme merely provides another mechanism to optimize combustion over a range of operating conditions. Increasing air injection without bound does not always equate to improved combustion. As shown in Figure 21 images 2 and 3, increasing the air flow from 50% to 75% at a fuel flow rate of 50% shows a decrease in combustion at station 1

**Operational Limits**

Generally, combustion is known to take place only under specific conditions and the ratio of fuel to air present at any given location must be within a bound determined by the desired reaction. For example, stochiometric combustion of ethylene in air requires 1 part fuel for three parts air as shown in equation 2. The operational limits of a cavity based flameholder are defined to be between lean and rich blowout. Lean blowout occurs when an insufficient amount of fuel is available for the combustion reaction. Likewise, rich blowout occurs when an insufficient amount of air is available. The following section is a characterization of the operational limits of the cavity.

Three test points designed to achieve a rich blowout condition were studied as shown in Table 3. Air was injected at the lower injection port (A1).

**Table 3** Rich blowout test points

| Test Point | Air Flow Rate (SLPM) | Fuel Flow Rate (SLPM) | Backpressure | Blowout |
|---|---|---|---|---|
| 1 | 0 | ≈144 | Low | No |
| 2 | 40 | ≈144 | Low | No |
| 3 | 100 | ≈144 | Low | No |

Rich blowout was not observed at any of the test points listed in Table 3. Therefore, higher fuel flow rates beyond what was available through the 200 SLPM mass flow controller must be utilized to determine the rich operational limits. Notice that all three runs were accomplished in a purely supersonic test section (low backpressure). High backpressure (subsonic/supersonic test section) effectively lifts the cavity shear layer and

significantly increases air entrainment. The reader can reference Figure 8 for representative shadowgraphs for both the low (a) and high (b) backpressure cases. Since rich blowout could not be attained given low backpressure (i.e. relatively low freestream air entrainment), rich blowout was not expected to occur at high backpressure (i.e., relatively high freestream air entrainment). A similar study of the lean blowout characteristics was performed. Air flow rate was fixed using the mass flow controller and the fuel flow rate was decreased slowly until lean blowout occurred. The results for both high and low backpressure are shown below in Figure 24. Each test point was repeated twice.

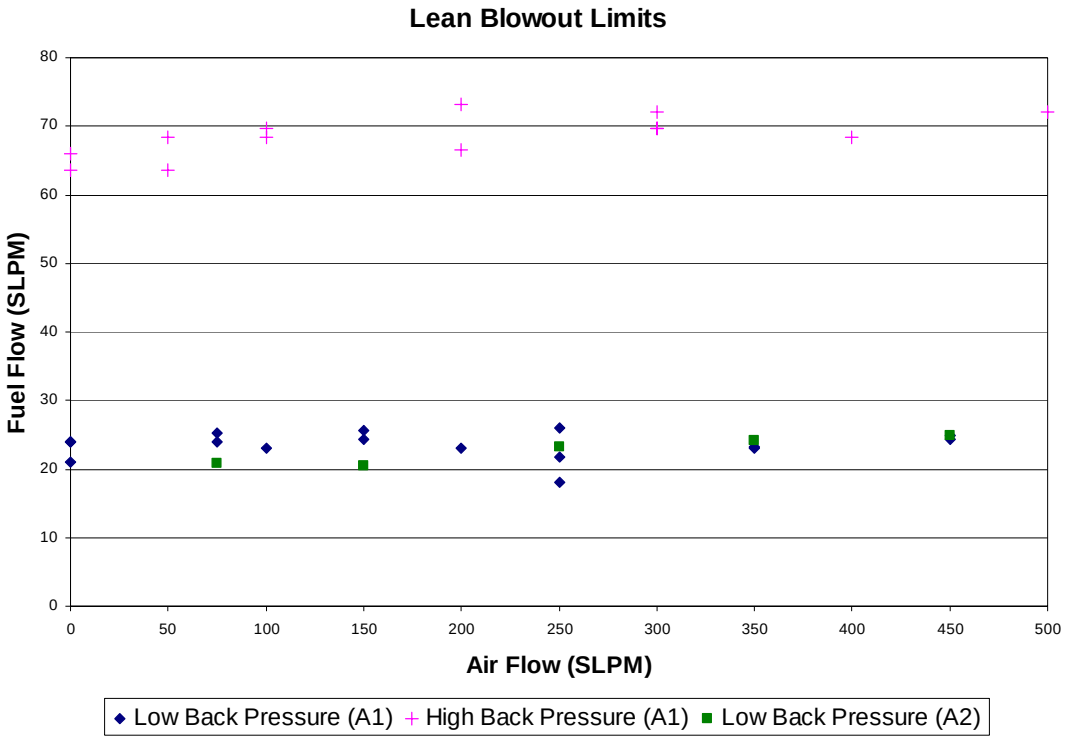


**Figure 24** Lean blowout limits

Lean blowout shows no dependence on air flow rate injected at A1 and very little dependence on air flow injected at A2 for the low backpressure case. Likewise, at the

high backpressure condition, no correlation was observed between air injection at A1 and lean blowout. This trend seems counterintuitive without consideration of representative lean blowout process. As fuel decreases toward lean blowout, frequent oscillations between global and localized combustion regions are evidenced. A high speed emissions camera was positioned normal to the flow to characterize the combustion process. The resulting profile view images were recorded chronologically and then exported into Audio Video Interleave (AVI) format. Figure 25 below is several time slices from the image data acquired during a lean blowout and is presented in tabular form. As time increases images fill rows from left to right and then fill columns from top to bottom. Images were taken at 3,000 frames per second. The time step for Figure 25 is 1.3 milliseconds.

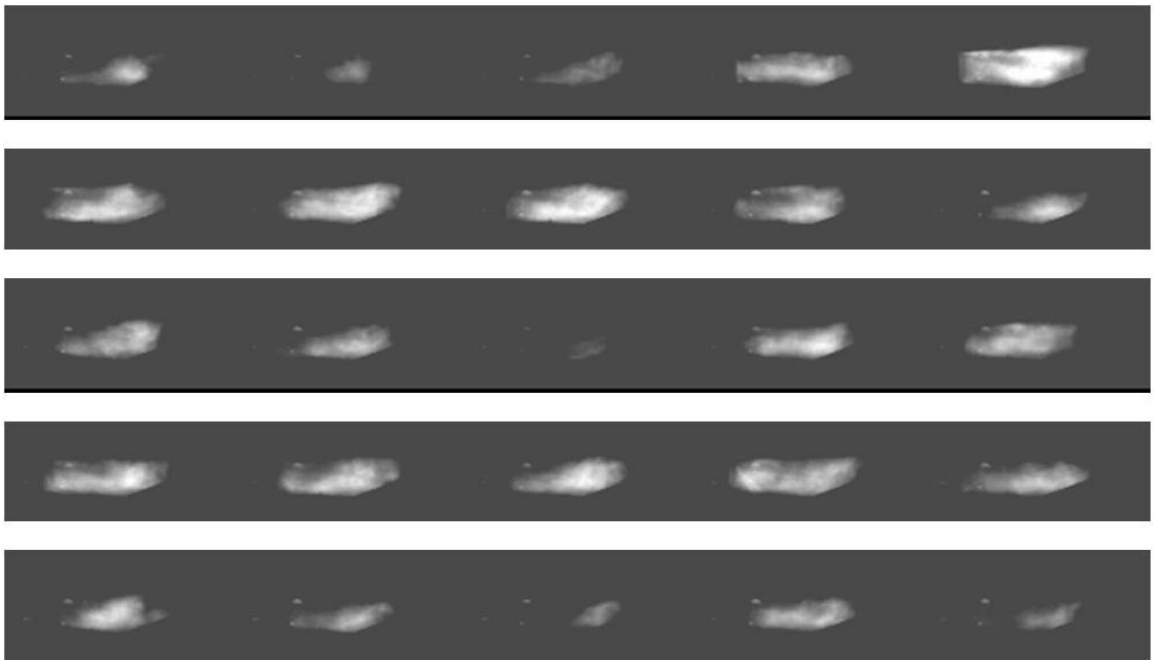

**Figure 25** Representative lean blowout characteristics (Profile View)

The most obvious characteristic of the process shown above is the frequent relocation of zones of combustion. Combustion is shown to take up the entire cavity volume in some images and a small localized region in other images. As shown above, the image located at row 2 column 3 (2,3) shows combustion taking up most of the cavity. However, the image located at (3,3) shows minimal global combustion. The time between these images is 0.005 seconds. Figure 26 is several time slices from the image data acquired during a stable, self-sustaining fueling scheme (F1:50%, A1:50%, A2:0%) and is presented to illustrate the relatively stable combustion away from the lean blowout limits. The time step for Figure 26 is 4 milliseconds.

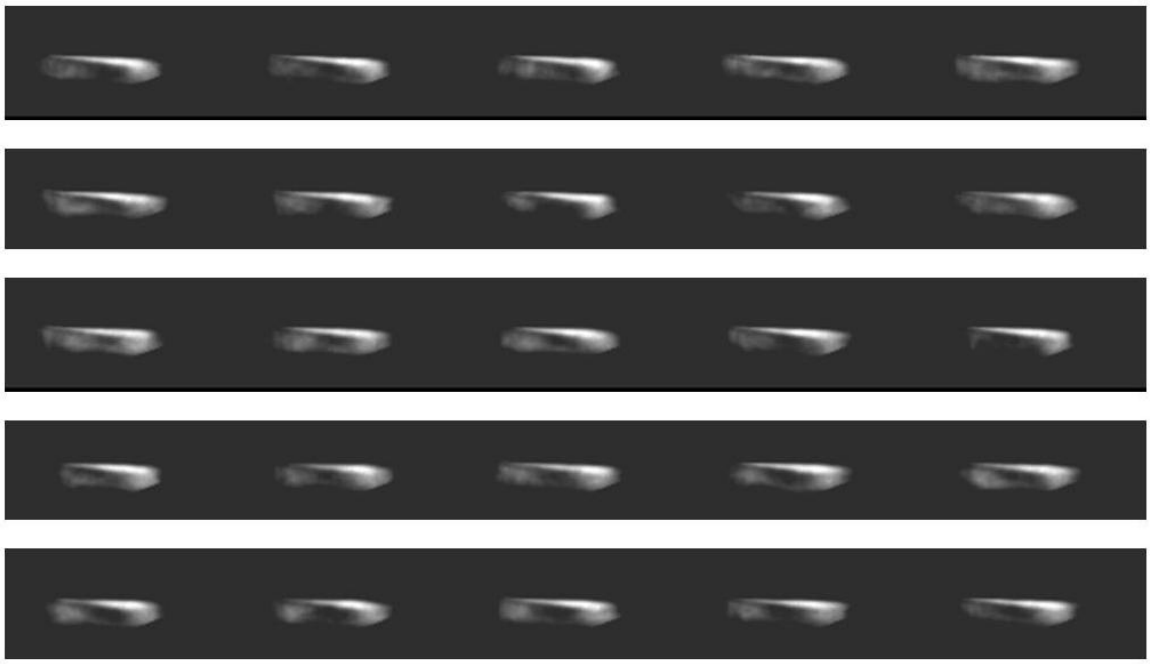

**Figure 26** Combustible mixture (Profile View)

Lean blowout is characterized at low backpressure by the formation of localized structures near the aft cavity ramp. Furthermore, a shear layer flame is not noticed as the cavity approaches lean blowout. This may explain why air injection at A1 and A2 do not

significantly contribute to lean blowout. Figure 27 shows schematically the localized reaction zone as well as locations of the air injection sites A1 and A2.

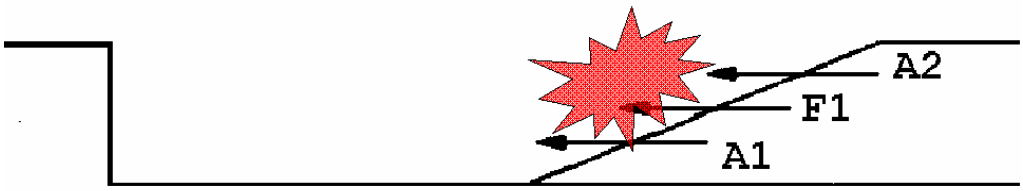


**Figure 27** Lean blowout

Air injection can only be considered beneficial to combustion if sufficient mixing occurs to bring together a combustible mixture of air and fuel. However, given the localized flamefront and the geometric jet offset between both A1 and F1 and A2 and F1, the jets may not interact sufficiently to produce a mixture of proper proportion to positively affect the reaction zone. Air injected through A1 would have to mix with the fuel injected through F1, but the momentum of the injectant and cavity vortex serves to transport the injected air away from the combustion region. This would explain why lean blowout does not appear to be a function of air injection through A1. Heat release in the cavity effectively raises the shear layer, resulting in reattachment higher on the aft cavity wall. As lean blowout was approached, the heat release decreased and the shear layer reattached farther down in the cavity. This phenomenon could locate the upper injection site (A2) too high to contribute to the cavity. The air injectant would be immediately carried downstream without passing through the cavity thereby eliminating its influence on cavity combustion.

**Expanded PLIF Diagnostics at Station 1**

As noted previously, air injection at the A1 site significantly altered combustion near the rear-facing step and air injection at the A2 site did not contribute significantly during the lean blowout characterization. A follow-on investigation was initiated to further characterize the effects of air injection (A1) on combustion near the cavity step. The chosen laser plane was located at 0.25 inches aft of the step, normal to the freestream direction and will be referred to as station 1a. Several sequential images were recorded for each test condition. These images were saved as a single file with an *.spe file extension which was created by Princeton Instruments, Inc. A batch process was then started to find the mean and standard deviation using PDView 5.0 developed by Innovative Scientific Solutions, Inc. The mean is representative of the average combustion location within the laser sheet, while the standard deviation is representative of the change in the combustion region based on the mean. Optimum combustion at an arbitrary location is defined by steady, uniform combustion throughout the area. Therefore, mean images with near constant high intensity and standard deviation images with constant low intensity should be representative of optimum combustion. This process was accomplished for both high backpressure (HBP) and low backpressure (LBP) cases. The HBP condition was established by incrementally closing a downstream valve until the shock train was positioned just forward of the cavity.

The following two figures present the mean and standard deviation of images taken at a fuel flow rate of 35%, LBP and various air injection mass flow rates. The scale for each figure is included and takes the form of (black-white).

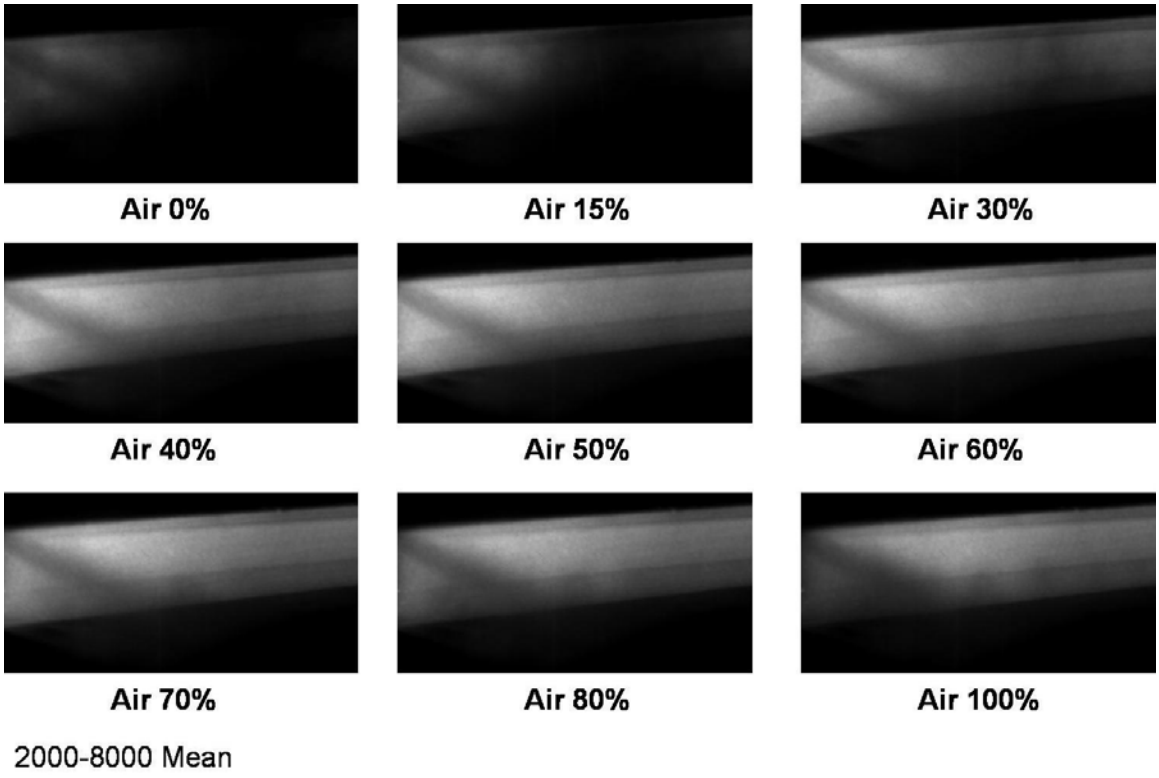


**Figure 28** LBP - 32% fuel flow (Station 1a; A1)

Figure 28 shows a gradual increase in the combustion present at station 1a given increases in air flow. There is very little difference between the mean images acquired at an air flow of 40% through 90%. Figure 29 is the standard deviation of all images collected at this test point.

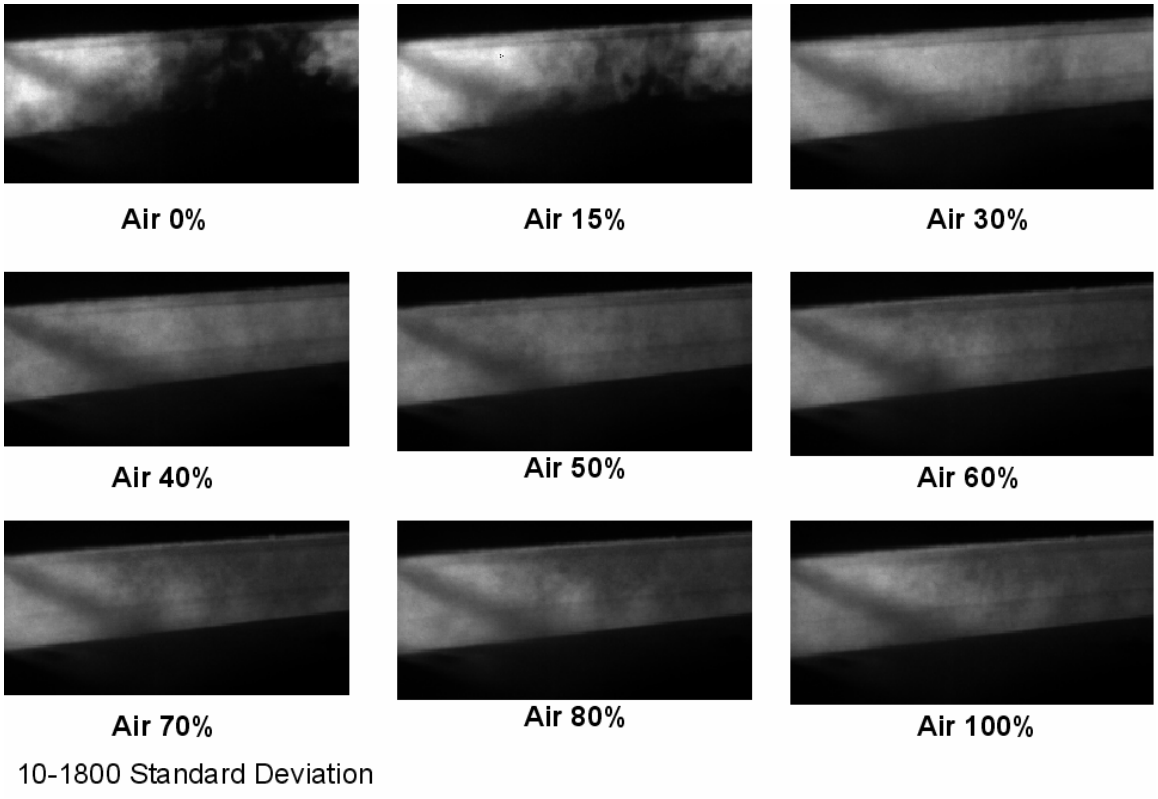


**Figure 29** LBP - 32% fuel flow (Station 1a; A1)

The images from air injection between 30% and 90% are very similar for both the mean and standard deviations. Stable combustion appears to be taking place at station 1a for air injection above 15% as indicated by the mean and standard deviation images. For 32% fuel flow, 50% air flow seems to optimally tune the cavity evidenced by a relatively uniform bright mean and a relatively uniform dim standard deviation. Combustion could not be established in the cavity given the high backpressure test condition and the fuel flow rate of 32%. Notice in Figure 24 that the lean blowout fuel flow rate was nearly constant at approximately 70 SLPM. Therefore, combustion would not be expected below this fuel flow rate.

The images in the following figures were obtained with a constant fuel flow rate of 50%, various air flow rates injected through A1 and low backpressure. Figure 30 is the mean of all images collected at this test condition.

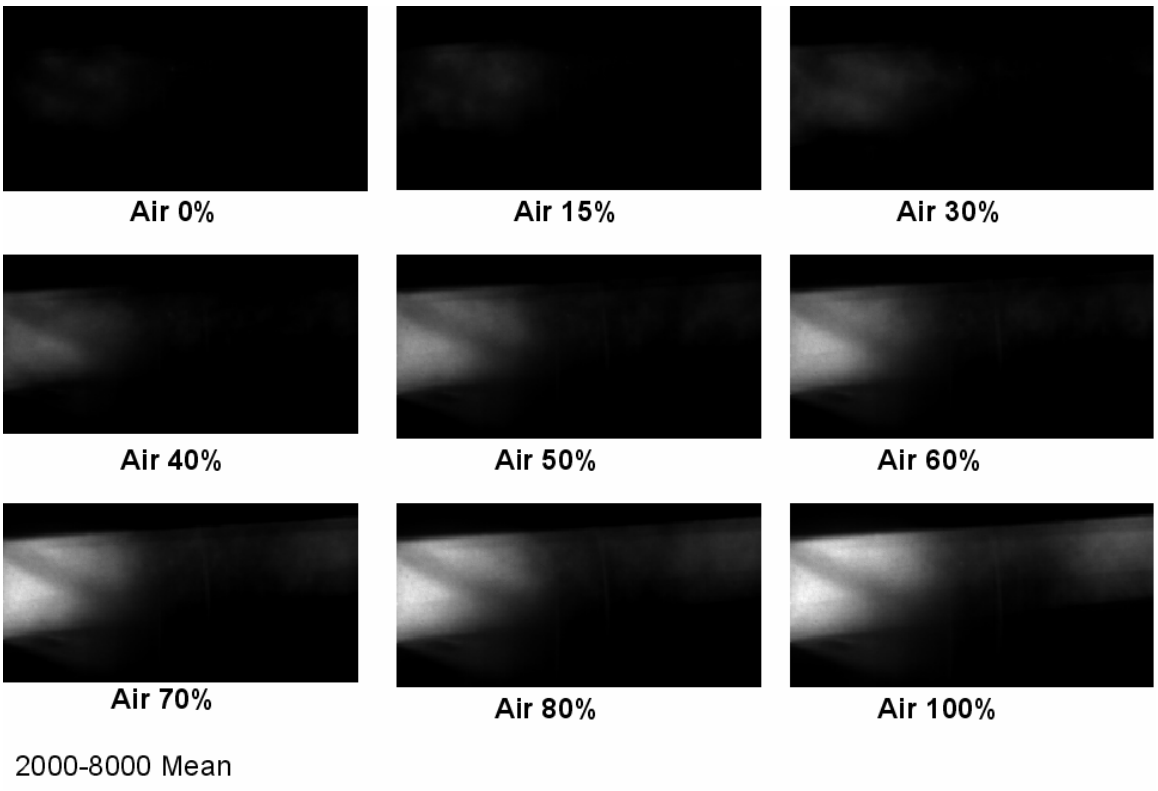


**Figure 30** LBP - 50% fuel flow (Station 1a; A1)

Notice that combustion is very weak between air flow rates of 0% and 30% and that combustion is not yet uniform across the area even at 100% air flow. Because combustion tends to improve with the addition of air, it is believed that there is a relatively rich condition at station 1a given little or no injected air flow. As stated before, if air injection was not a controllable parameter, this fuel flow of 50% would create a rich region near the cavity step resulting in inefficient use of the entire cavity volume. Figure 31 shows the standard deviation images for the 50% fuel flow, various air flows, and low backpressure.

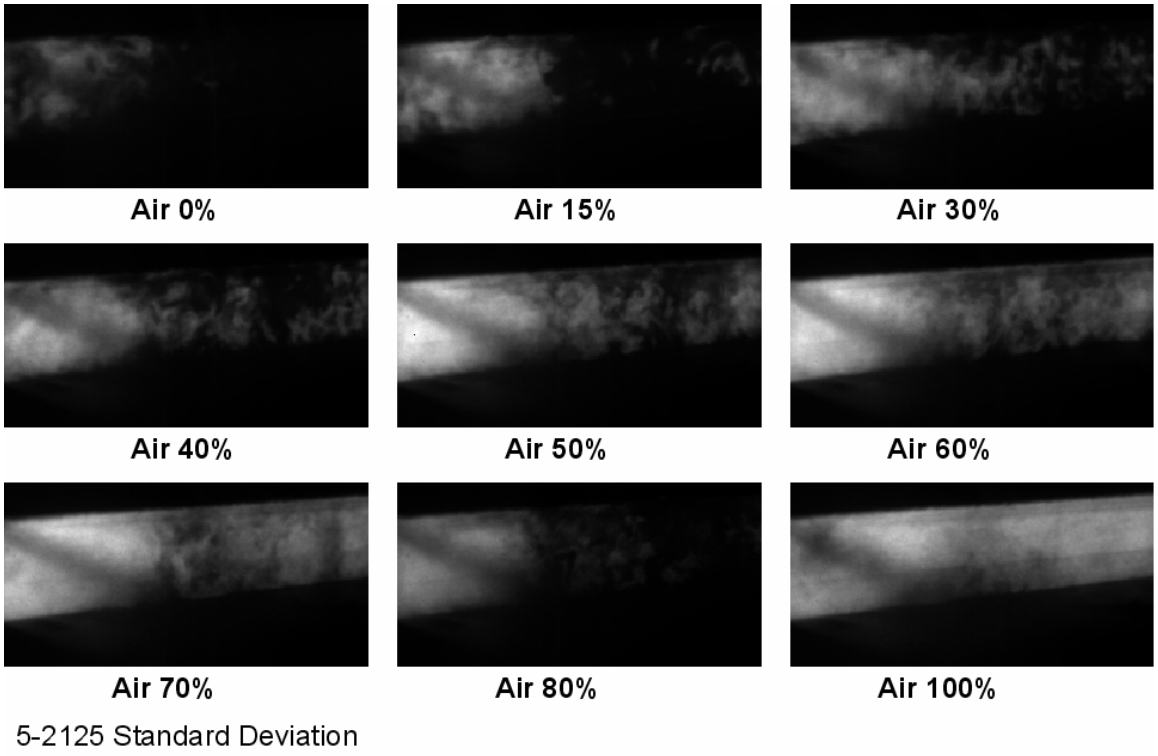


**Figure 31** LBP - 50% fuel flow (Station 1a; A1)

The standard deviation images also show increased combustion given increased air injection. Of the conditions tested, air flow at 100% seems to produce the most suitable combustion at station 1a. Because no decrease in combustion was noted for increases in air flow, the optimal fueling condition may not have been located during this study due to the air mass flow controller maximum flow rate. Combustion could not be established in the cavity given the high backpressure test condition and the fuel flow rate of 50%.

The following images were obtained with a constant fuel flow rate of 75%, various air flow rates injected through A1 and low backpressure. Figure 32 is the mean of all images collected at this test condition.

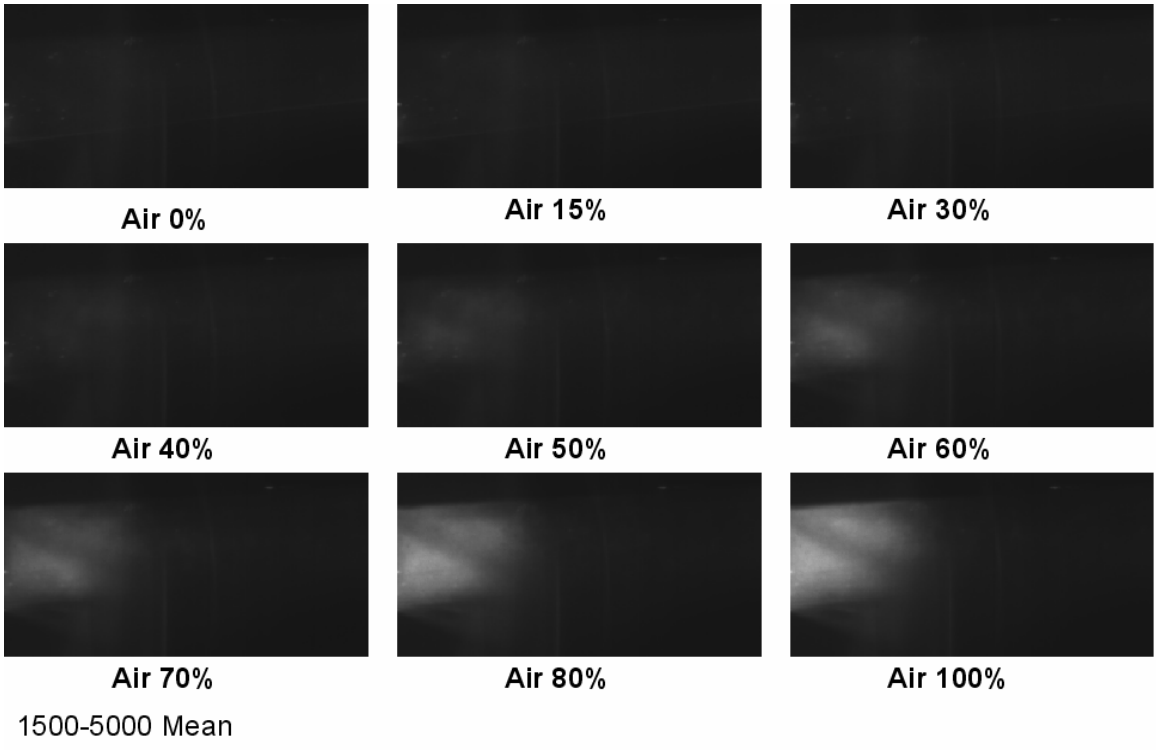


**Figure 32** LBP - 75% fuel flow (Station 1a; A1)

The mean images collected at 75% fuel flow resemble the mean images collected at 50% fuel flow as shown in Figure 30. This also implies that combustion is not present at low air flow rates because the area at station 1a is too rich to effectively support combustion. As introduced air flow increases combustion begins to take place at this cavity location. Figure 33 shows the standard deviation at 75% fuel flow and low back pressure.

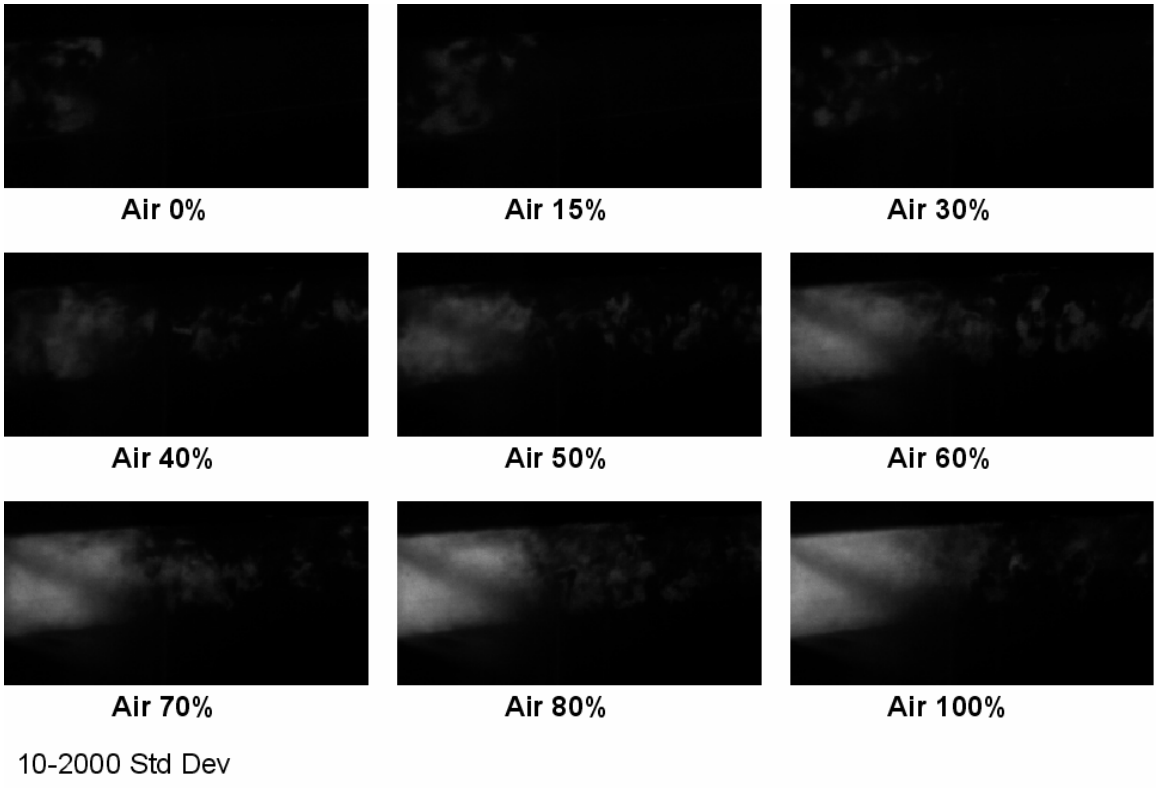


**Figure 33** LBP - 75% fuel flow (Station 1a; A1)

Standard deviation images also show improved combustion with increase in air flow. As expected 100% injected air flow provided the best combustion. This fuel loading was able to sustain combustion at high back pressure. As noted before, the fuel flow for lean blowout occurred at approximately 70 SLPM and therefore combustion should be expected at fuel flows above 70 SLPM. The results are presented below in both mean and standard deviation formats. Notice that the scale has not changed between the 75% fuel flow rate images taken at low and high backpressure. In other words, high backpressure, mean images can be directly compared to low backpressure mean images as they share the same scale. The same is true for standard deviation images.

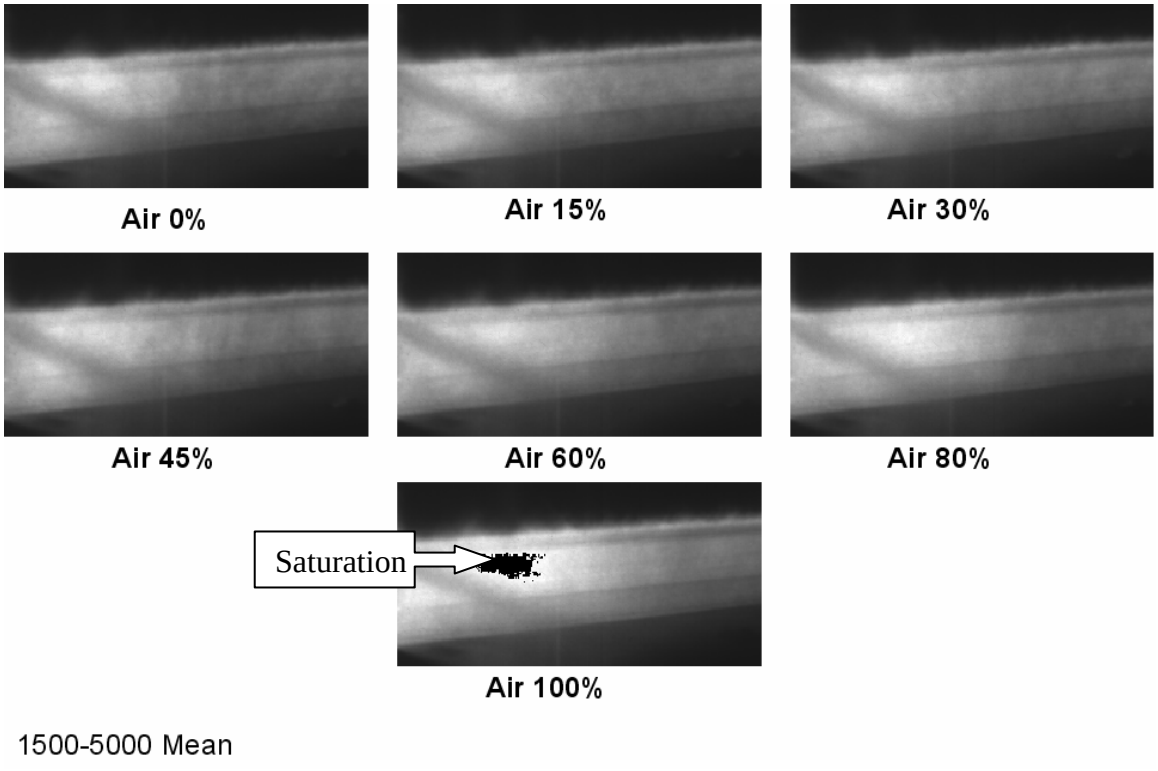


**Figure 34** HBP - 75% fuel flow (Station 1a; A1)

The most obvious feature of Figure 34 is the high intensity; in fact, part of the image take at 100% air flow is saturated at this scale. The saturated area appears as a dark region on the left hand side (LHS) of the image. At 75% fuel flow and low backpressure, it was noted that station 1a was relatively rich. Because air entrainment and turbulence (proportional to mixing) are significantly increased at the high backpressure (HBP) condition, a more suitable mixture of fuel and air is created and combustion was improved. Figure 35 shows the standard deviation of images obtained at 75% fuel flow, various air injection rates through A1 and high backpressure.

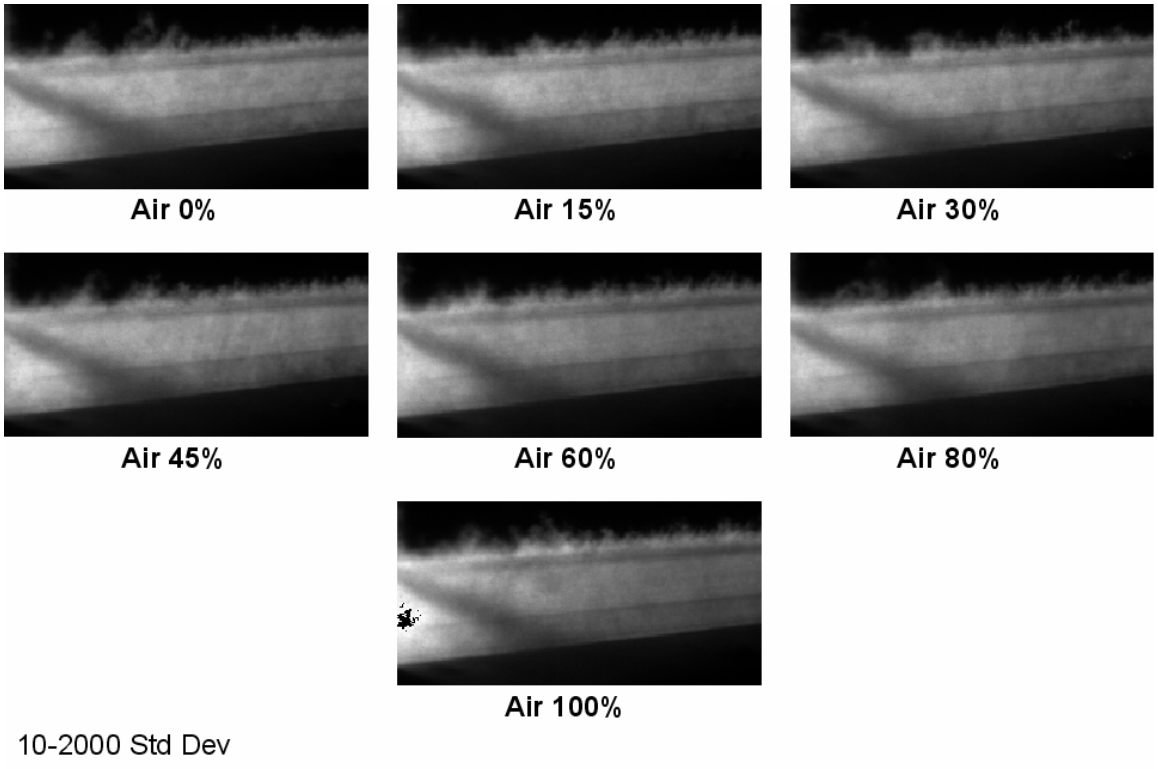


**Figure 35** HBP - 75% fuel flow (Station 1a; A1)

The images exhibit little difference between the fuel only case (0%) and the 100% air injection flow rate. However, at 100% air flow a small region was observed to be saturated at the extreme left hand side of the image. Due to the increased air entrainment, higher fuel flow rates are required for combustion. This explains why high backpressure images were not acquired for the 32% and 50% fuel flow rates. This trend was also observed in the lean blowout characterization. Combustion simply could not be sustained. The images shown below are for 90% (180 SLPM) fuel flow rates. The mean images acquired for the 75% fuel flow condition presented in figures 32 and 34 were scaled from 1500-5000. Notice that the scale was expanded to 2000-8000 for the higher fuel flow rate of 90% because, at the reduced scale, the images presented in Figure 36

would be saturated. Figure 36 shows the mean of images collected at 90% fuel flow, various air flow rates injected at A1 and high backpressure.

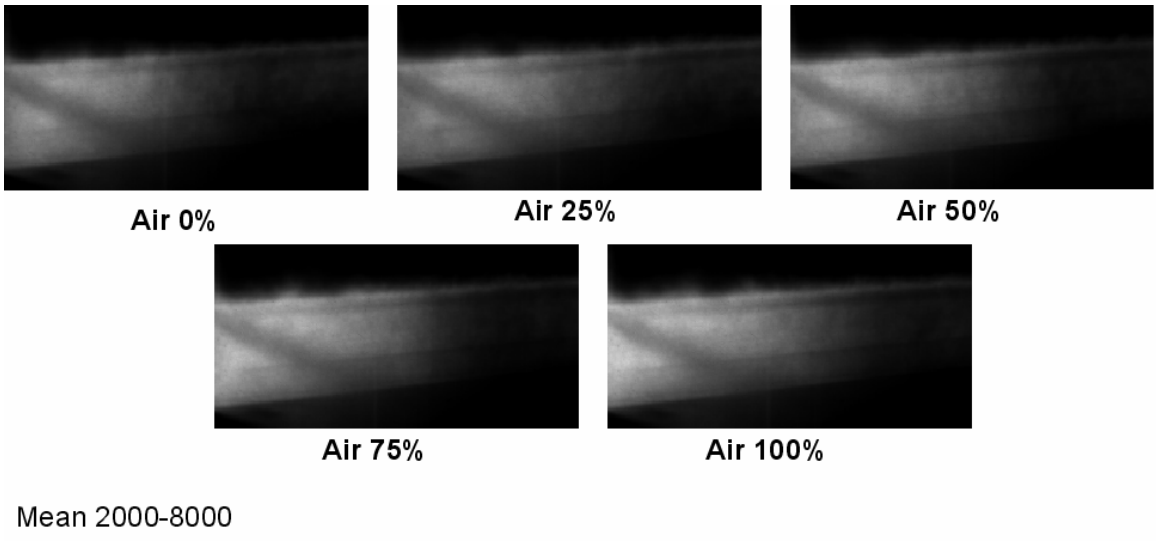


**Figure 36** HBP -90% fuel flow (Station 1a; A1)

Figure 36 shows that for increases in air flow rate an increase in combustion reaction rate at station 1a was observed. While evidence of combustion was only seen on the LHS of the cavity centerline given 0% air flow, evidence was seen on both sides of the centerline at 100% air flow. Figure 37 shows the standard deviation of images collected at 90% fuel flow, various air flow rates injected at A1 and high backpressure.

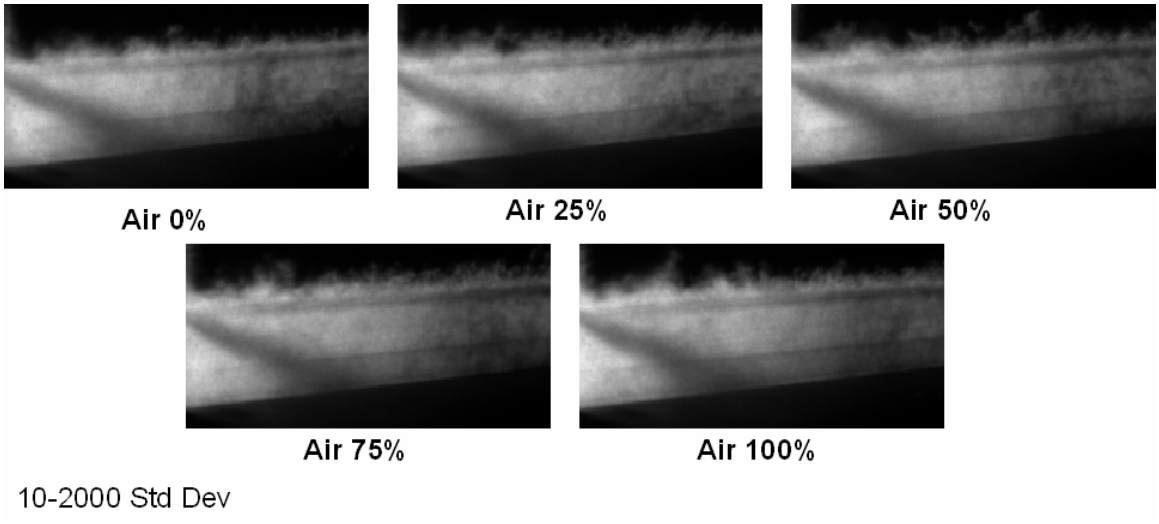


**Figure 37** HBP - 90% fuel flow (Station 1a; A1)

The increase in fuel flow from 75% to 90% at the high backpressure condition enhanced combustion at station 1a as the image intensity increased denoting a greater concentration of hydroxyl and therefore increased combustion reaction rate. However, at the high backpressure condition, air injection played a smaller role in optimizing combustion. In other words its contribution to combustion at station 1a was evident, but less significant than its contribution at the low back pressure condition.

Direct injection of both fuel and air provided additional capability to tune the cavity such that a more stable decentralized flame results. The most significant improvement over the baseline case (fuel only) was noted near the upstream portion of the cavity close to the cavity step. This injection scheme expanded the operational limits significantly for each selected fuel flow.

**Luminous Flame Emissions**

A high speed camera was positioned normal to the flow such that the entire cavity profile was visible. This method provided an overall view of combustion as evidenced by the presence of luminous parts of the flame within the cavity and was used to further extend the combustion information extracted from the PLIF diagnostics. No visible light emissions are shown in black while increases in flame emissions are reflected by increases in intensity (white). Data was taken at three fuel flows, various air flows and both high and low backpressure. A red reference line was added at the same location for each image. This line was intended to define the cavity boundaries, however it must not be taken as an exact representation of the cavity. The same nomenclature used previously to define specific images within a table was utilized. The image will be referenced by the following:

Location = (row of image, column of image)* (5)

*Array index begins at 1

The following series of images shown in figure 38 were derived from the mean of all images acquired at 32% fuel flow, low backpressure and increasing air flow through A1.

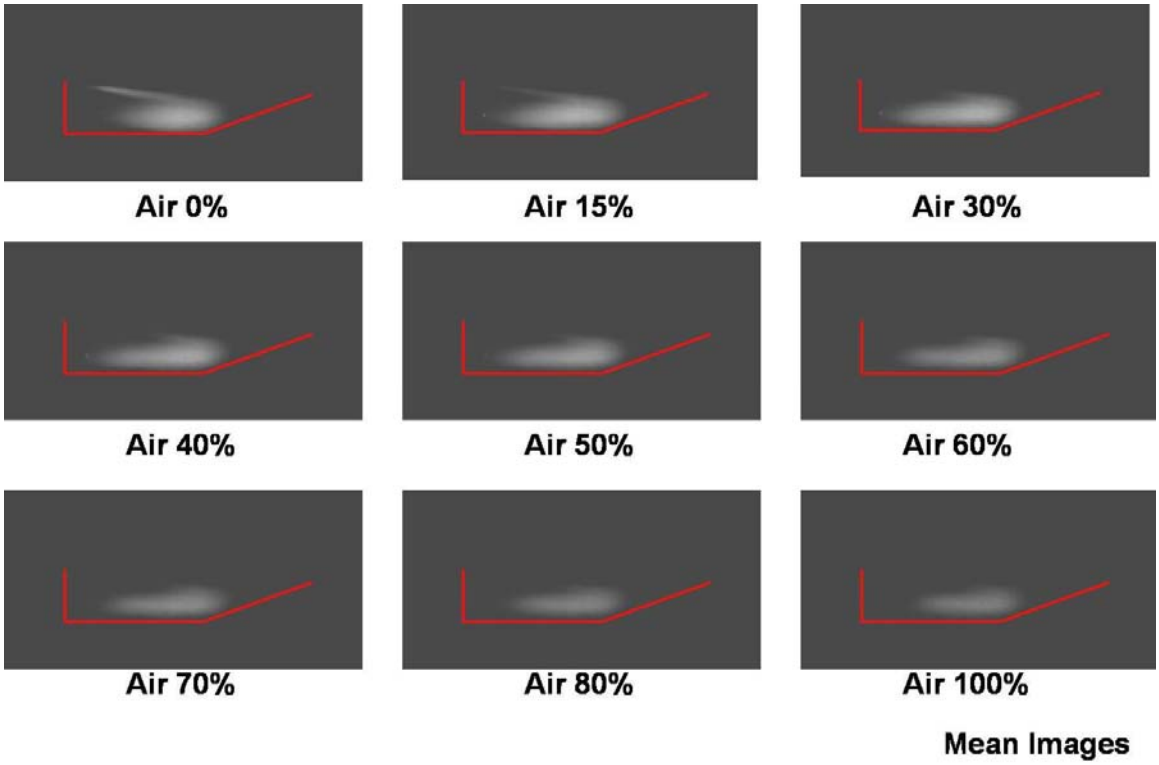


**Figure 38** 32% fuel flow (LBP)

Increased air flow decreases mean combustion throughout the cavity. The mean PLIF results for this fuel flow and low backpressure at station 1a (near the cavity step) are shown in Figure 28. The presence of a strong shear layer flame that extends almost the entire length of the cavity is shown at 0% air injection. As air flow increases the shear layer flame draws into the aft ramp combustion region and is no longer clearly evident at 70% air flow. Furthermore, as air flow increases the combustion region decreases in streamwise length toward the aft ramp. The presence of a strong shear layer flame on the fuel only case (image (1,1)) is an indicator of near optimum cavity combustion. Since this occurs with no air injection, the addition of more air should tend to lean out the global cavity mixture further reducing overall cavity combustion. Figure 39 shows the standard deviation images for 32% fuel flow.

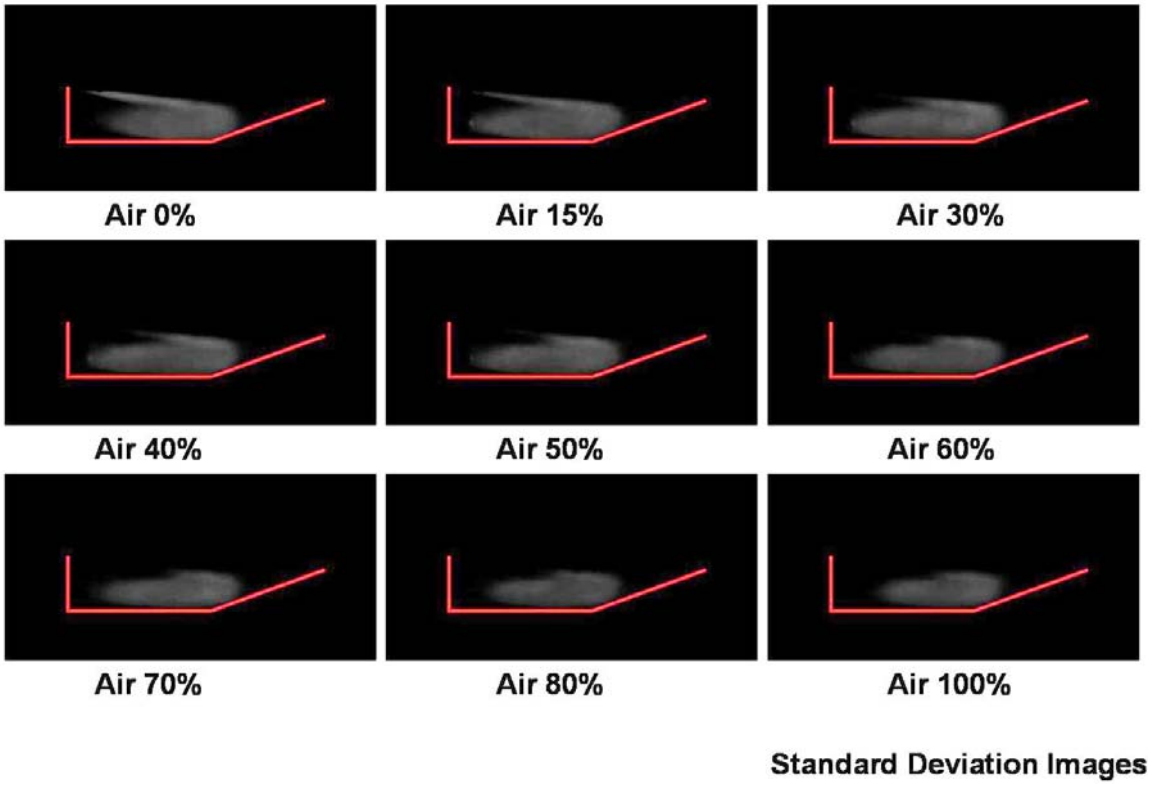


**Figure 39** - 32% fuel flow (standard deviation)

The standard deviation images show that between 0% and 80% introduced air flow, combustion does occur near the cavity step. However, as the cavity fuel to air mixture ratio decreases, fluctuations in the combustion region are known to occur. These fluctuations may have limited the effect combustion was represented at station 1 and 1a in the mean images. Most noteworthy was that the introduction of air to the cavity for this fuel loading did serve to effect combustion or "tune" the cavity. At which point it was optimally tuned should be the subject of additional research. When correlating PLIF and emissions images it is important to remember that, as noted previously, the concentration of OH (increased intensity) does not necessarily denote combustion at a specific location (plane) within the cavity. The mean PLIF images shown in Figure 28 show an increase and subsequent invariance in OH concentration with an increase in

injected air flow. However, the momentum of the injectant combined with the additive momentum of the cavity vortex may have increased the transfer of local hydroxyl radical from the region of combustion at the aft ramp toward the measurement location near the cavity step. This transport phenomenon, in general, could skew the PLIF images. Furthermore, PLIF and emissions data reveal different features owed to the combustion process.

The following figure was derived from the mean of all images acquired at 50% fuel flow, low back pressure and increasing air flow through A1.

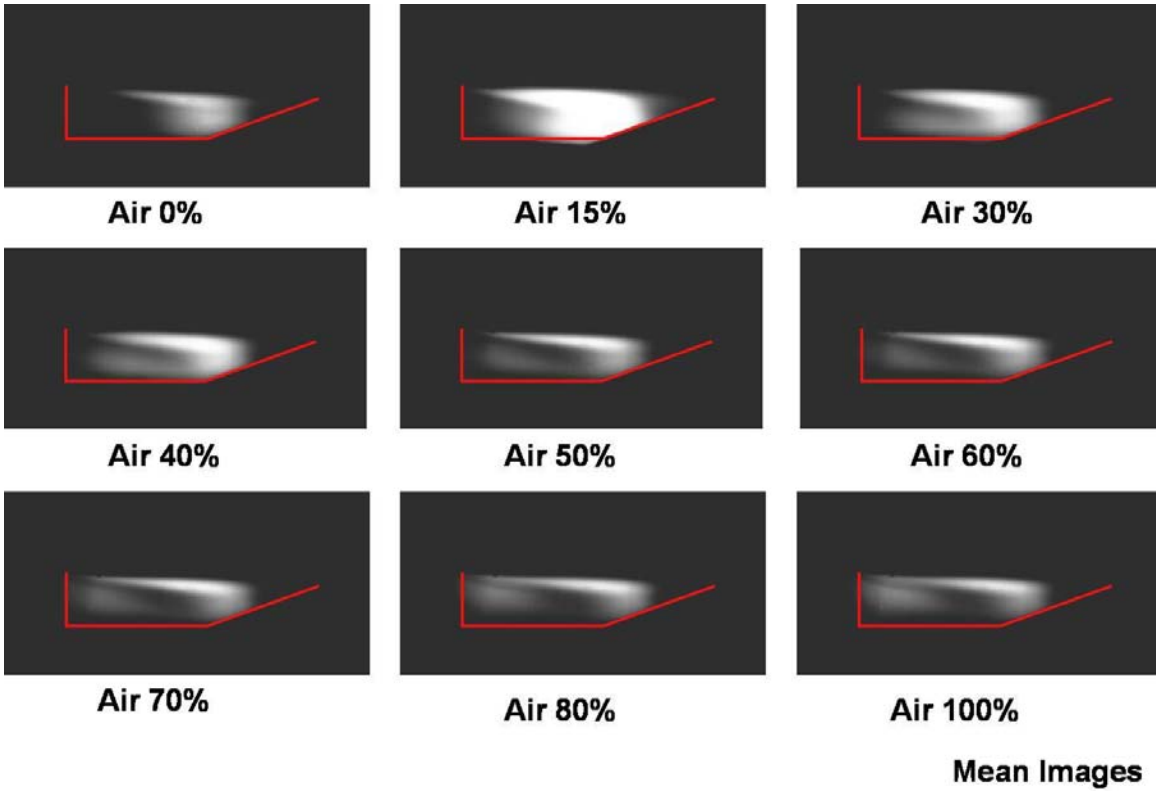


**Figure 40** - 50% fuel flow (mean)

Increased air flow increases combustion throughout the cavity. This compares well with the mean PLIF results shown in Figure 30. Note that at 0% air flow combustion is localized near the aft ramp, but the existence of a shear layer flame is evident. As air

flow is increased the shear layer flame extends farther from the aft ramp toward the forward step. Furthermore, at higher air loadings a non-reactive region is formed at the middle (streamwise) of the cavity.

Figure 42 shows the standard deviation images for 50% fuel flow, various air injection rates through A1 and low backpressure.

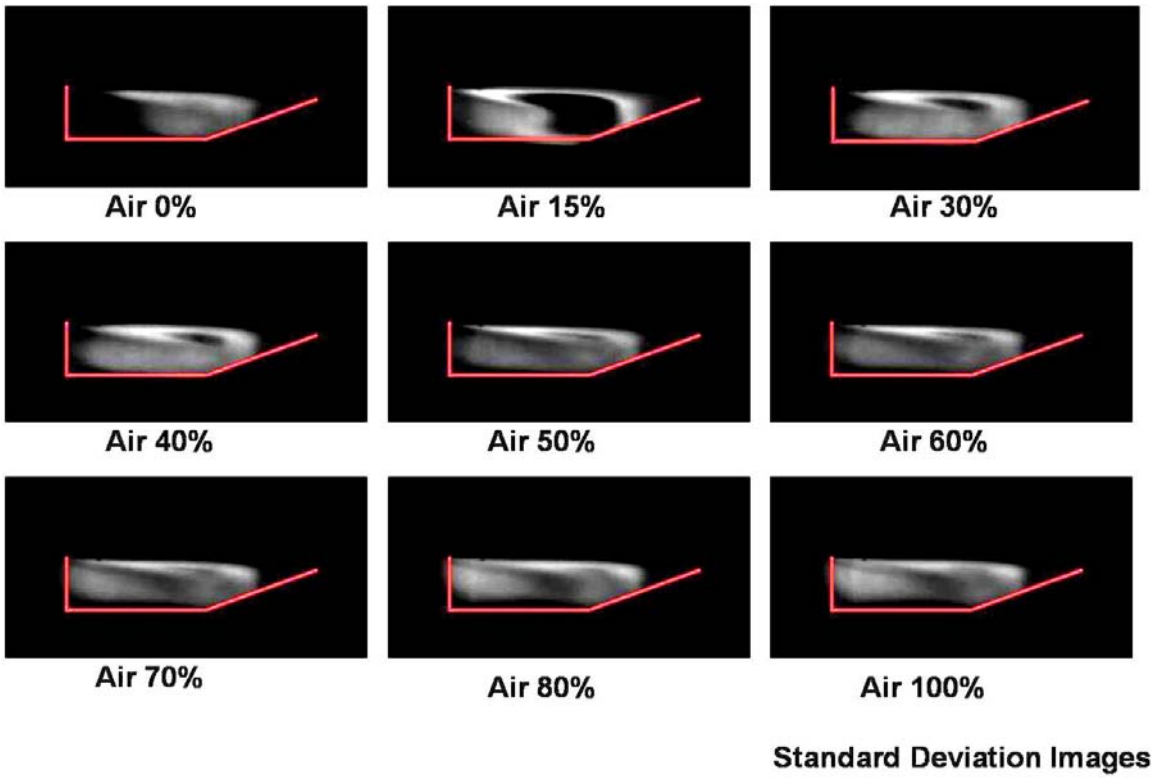


**Figure 41** 50% fuel flow (standard deviation)

It is obvious that the reference line does not exactly coincide with the cavity boundaries. However, it occupies a fixed location and served as a valid reference frame. All images, with the exception of (1,1) and (3,3), display a common attribute. They each exhibit a very consistent combustion region in the shear layer. This region is located by its low intensity. Figure 42 shows this area in more detail for a representative test point (50% fuel, 30% air).

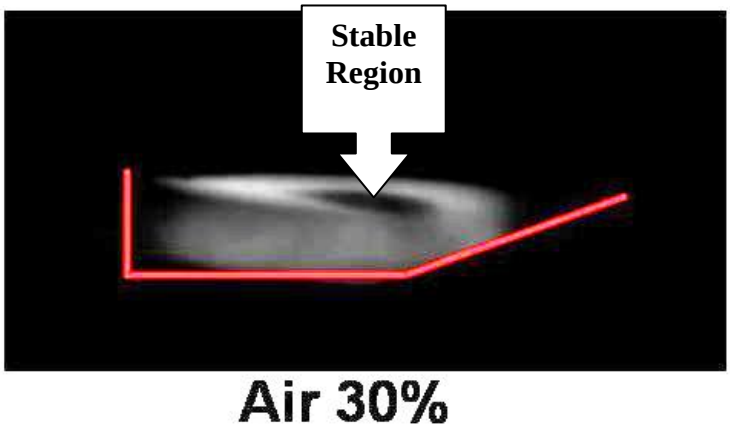


**Figure 42** Stable shear layer flame

A strong shear layer flame is considered to be a good indicator of an effective flameholding mechanism. Such a mechanism serves to sustain combustion within the cavity through the production of hot byproducts of combustion. These hot products are re-circulated by the cavity vortex structure and provide thermal energy to promote combustion. Additionally, a shear layer flame is well suited to transfer energy in the form of heat to the freestream flow furthering combustion reactions outside of the cavity. Air injection through A1 continues to have a beneficial effect on cavity combustion. Given 50% fuel flow, combustion filled the entire cavity volume at nearly every air flow rate resulting in effective use of cavity geometry.

The following figure was derived from the mean of 200 images acquired at 75% fuel flow, low back pressure and increasing air flow through A1.

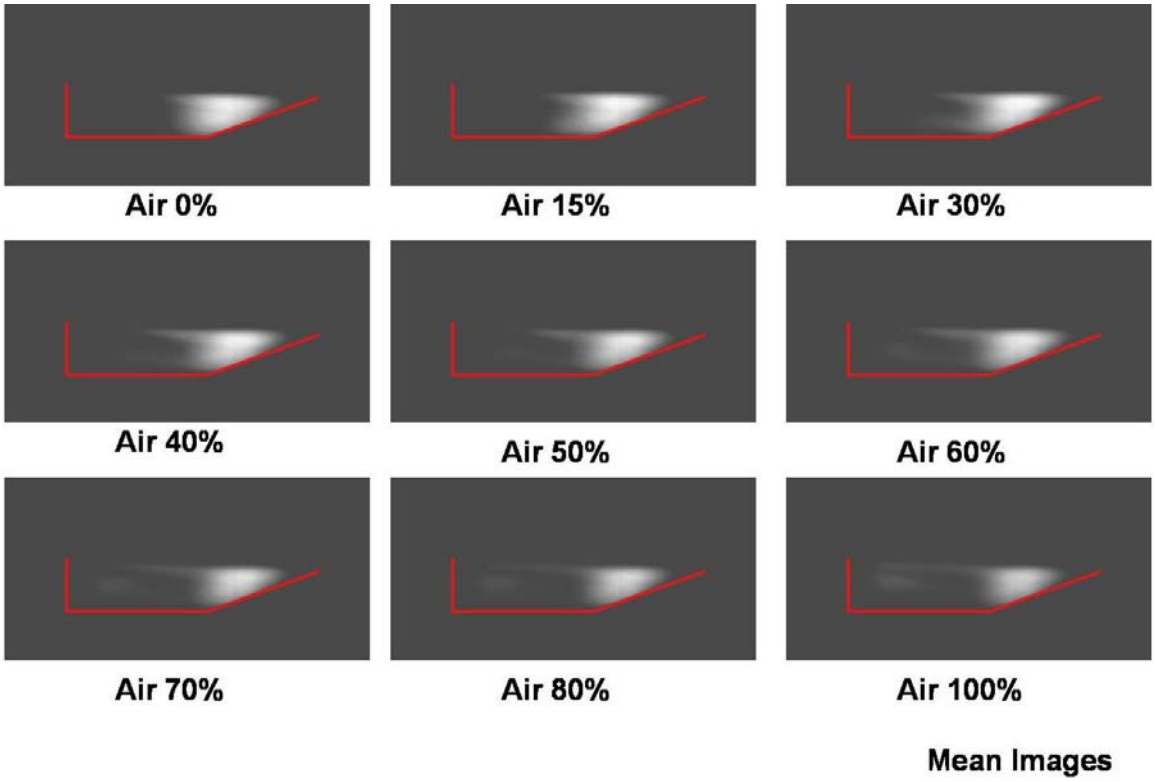


**Figure 43** 75% fuel flow (mean)

Combustion at the fuel only case is localized near the aft cavity ramp. The sequential addition of air produced the following structures: formation of shear layer flame, extension of the shear layer flame from the aft ramp to the cavity step, and the addition of a combustion zone near the cavity step. The formation of these structures based on controllable parameters (i.e. fuel and air flow rates) allows the cavity to be tuned to best serve as a flameholder throughout various operating conditions. Figure 44 shows the standard deviation for 75% fuel flow, increasing air flow through A1 and low backpressure.

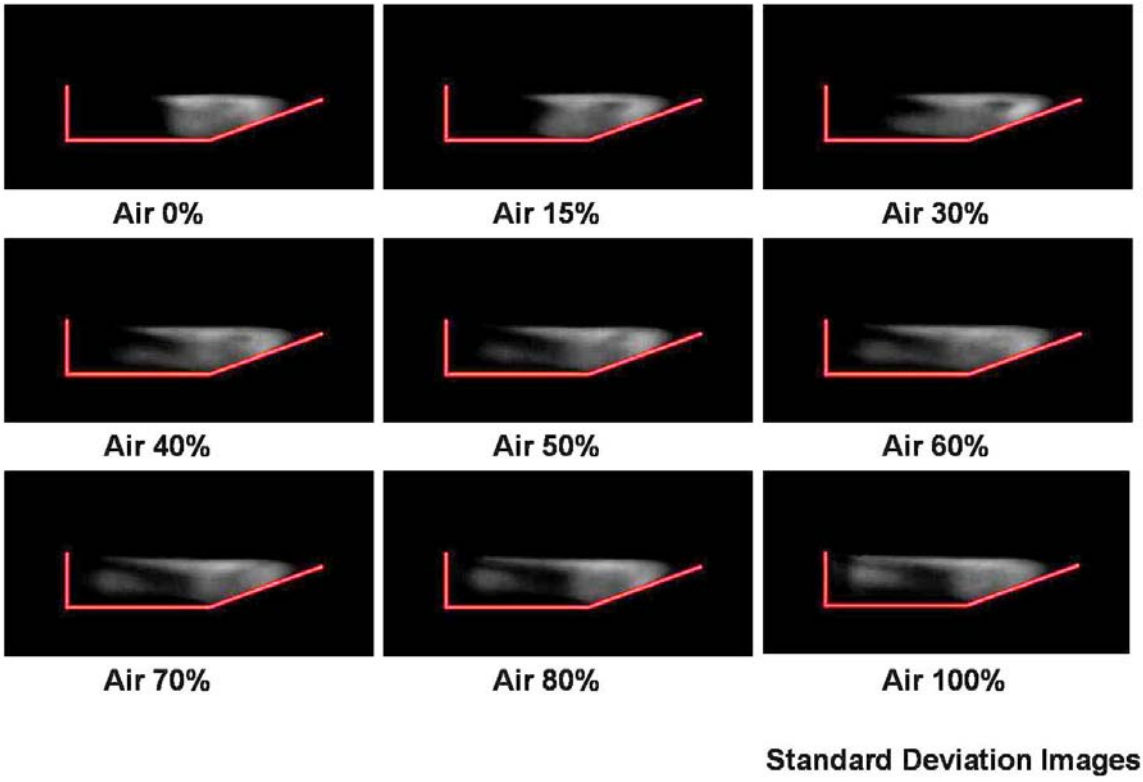


**Figure 44** 75% fuel flow (standard deviation)

Notice that a stable shear layer flame region was evidenced especially for the 15% through 40% air flows. At this point it is interesting to note the angle that the shear layer makes with the flow just above the cavity. A representative mean image was selected from each of the three fuel flow rates that exhibited a strong shear layer flame and global cavity combustion. A line was then drawn from the upper leftmost point of the reference line horizontally parallel to the freestream flow. Another line, representative of the shear layer flame, was drawn from the upper leftmost point of the reference line toward the aft cavity ramp bisecting the shear layer flame. Finally a line was drawn from the intersection of the cavity ramp and the representative shear layer line vertically to the intersection of the horizontal freestream line. This process is shown graphically in Figure 45 and is further explained in Table 4.

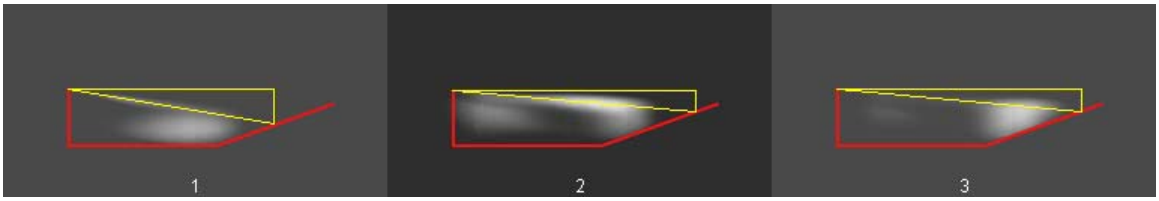


**Figure 45** Shear layer flame angle

Table 4 lists the geometry utilized to determine the flame angle. The angle is provided in degrees below horizontal.

**Table 4** Shear layer flame angle

| Figure 47 Designation | Fuel Flow (%) | Air Flow (%) | Horizontal Length (pixels) | Vertical Length (pixels) | Angle (deg) |
|---|---|---|---|---|---|
| 1 | 32 | 0 | 137 | 23 | 9.5 |
| 2 | 50 | 100 | 162 | 14 | 4.9 |
| 3 | 75 | 100 | 163 | 15 | 5.3 |

Figure 45 and Table 4 provide additional support to a previous assertion, namely that as cavity combustion increases, the shear layer is effectively lifted and therefore does not drop as far down prior to reattaching to the aft cavity ramp. This can significantly affect the drag produced by the aerodynamic interaction with the flameholding cavity. Drag is reduced as the shear layer angle, as defined above, approaches zero. This effect implies that combustion throughout the cavity is desirable due to a decrease in drag attributed to the lifting of the shear layer as well as the effective use of the cavity volume.

High backpressure data were not acquired for the 32% and 50% fuel flow conditions because combustion could not be sustained. However, sustained combustion was established given the 75% and 90% fuel flow injection. The images shown below

were acquired with a 75% fuel flow, high backpressure and various introduced air flows through A1.

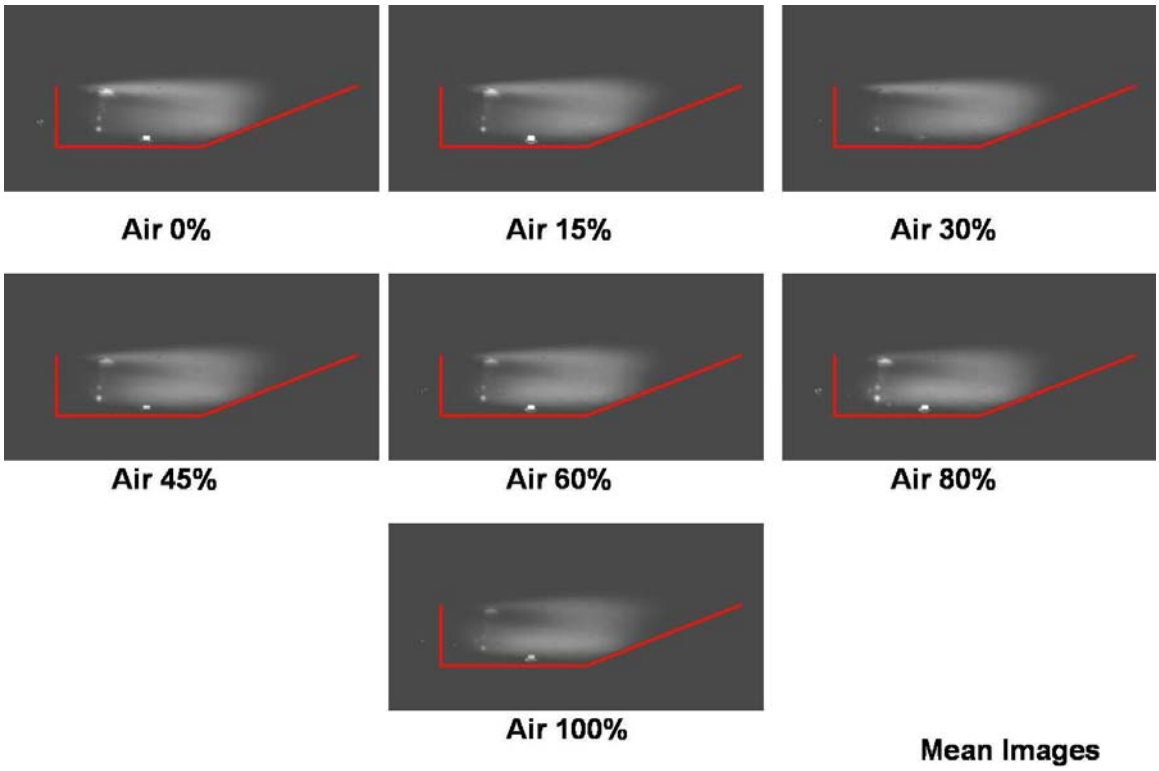


**Figure 46** 75% fuel flow (HBP)

Combustion, as indicated by mean images, fills the cavity volume throughout the range of injected air flow rates. The region near the cavity step appears to minimally contribute to the overall cavity combustion. Additionally, a less intense combustion region appears between upper and lower combustion regions for all air flows. The small area of high intensity on the cavity floor is the spark plug used to continue combustion. The spark plug was not visible in the low backpressure case because additional energy was not required. Combustion was self-sustaining for all low backpressure cases tested. Figure 47 is the mean image taken at high backpressure, 75% fuel flow and 60% air flow and shows a minimum reaction region characteristic of those seen in Figures 43 and 46.

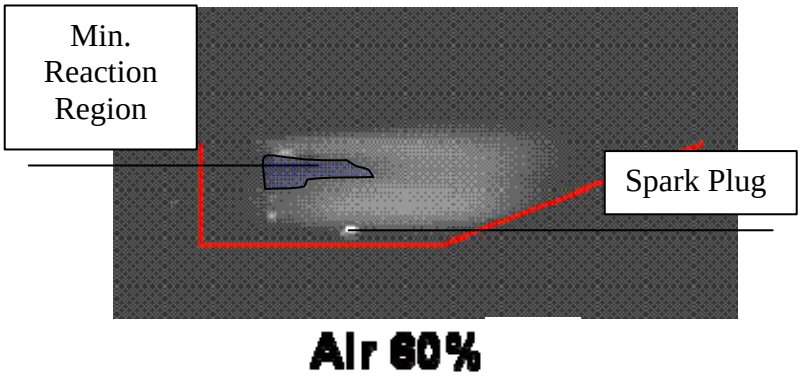


**Figure 47** Minimum reaction region

Figure 48 contains the standard deviation images taken with high backpressure, 75% fuel flow and various air injection rates through A1.

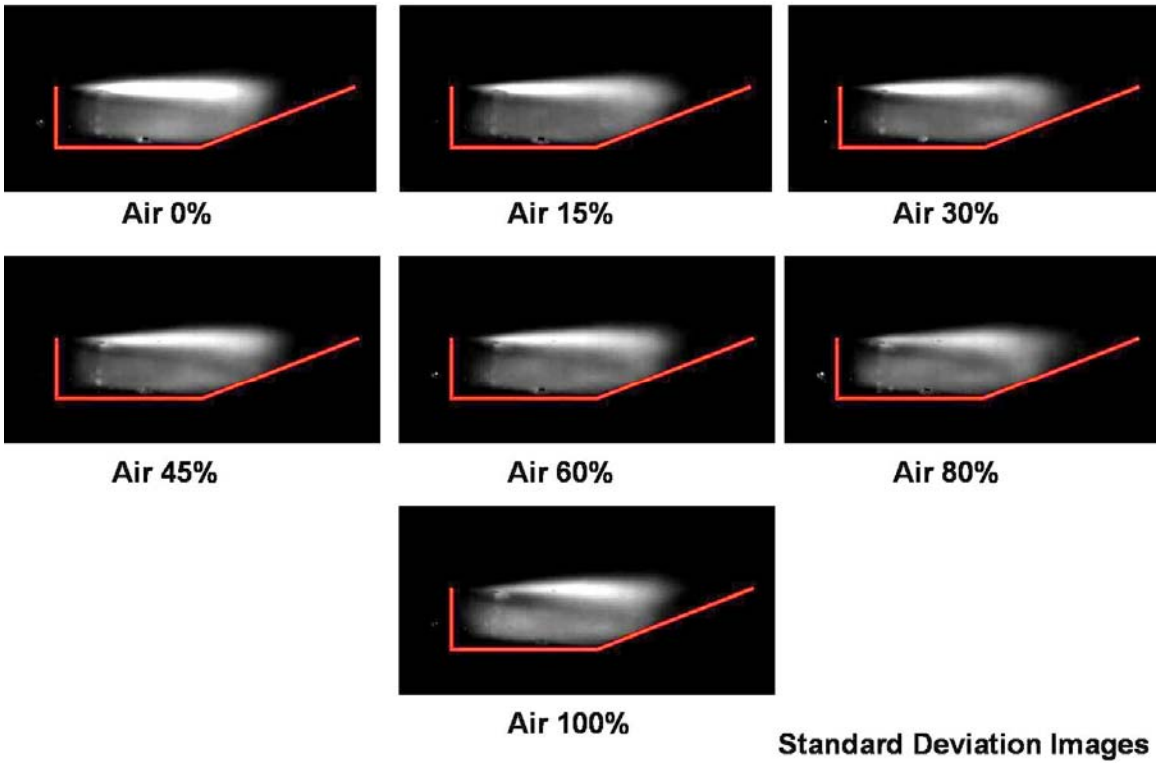


**Figure 48** 75% fuel flow (HBP)

The highest standard deviation (maximum image intensity) appears to be located in the shear layer for every air flow rate. As shown in both previous figures, an observed effect of high backpressure is to increase the area in the streamwise-transverse plane through

which combustion occurs. The combustion region extends farther in the transverse direction given higher backpressure. Figure 49 shows the standard deviation at 75% fuel flow and 60% air flow for both the low backpressure and high backpressure cases.

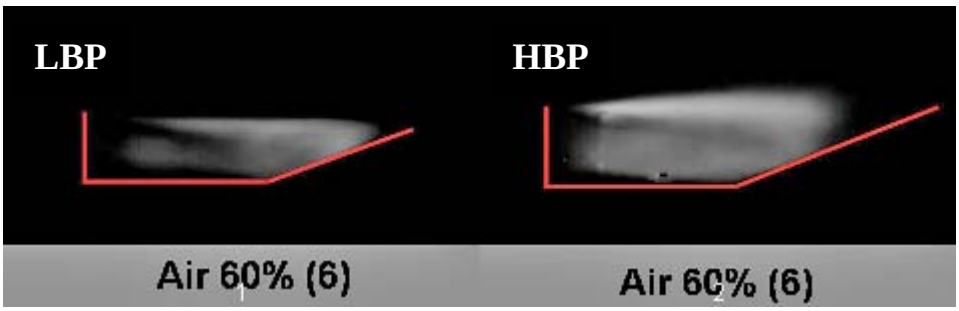


**Figure 49** Combustion area increase

The maximum vertical distance from the bottom of the combustion region to the top of the combustion region is 31 pixels for the low backpressure case and 48 pixels for the high backpressure case. The cavity step is approximately 0.65 inches and spans 40 pixels. This yields a vertical scale of roughly 61.5 pixels per inch. Based on these values the maximum height, measured in the transverse direction, of the low and high backpressure combustion regions are 0.50 inches and 0.78 inches respectively. Given that the cavity depth is 0.65 inches, the cavity combustion was noticed to protrude approximately 0.13 inches above the cavity. This was consistent with the previous assumption that increases in backpressure effectively results in increased cavity volume.

It has been noted that increases in backpressure cause increased freestream air entrainment and, in this study, combustion at high backpressure can be sustained only given higher fuel flow rates (75% and 90%). The following two figures represent the mean and standard deviation images acquired at high backpressure, 90% fuel flow and various air flows.

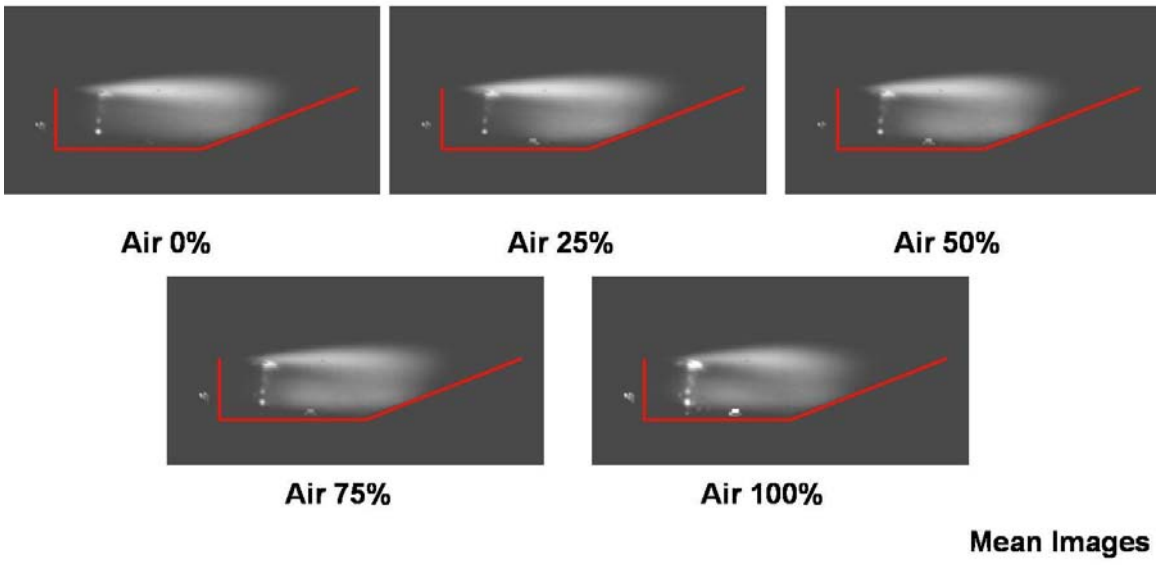


**Figure 50** 90% fuel flow (HBP)

The mean images acquired at 90% fuel flow were very similar to the mean images acquired at 75% fuel flow. Specifically, the luminous products of combustion were observed throughout the cavity volume and extend outside of the cavity in the transverse direction. Previous studies have concluded that the shock structure associated with the high backpressure condition benefits mixing within the cavity. The uniform combustion evidenced in figures 46 and 50 could be partially attributed to the increased mixing between the fuel and air. Figure 51 contains the standard deviation images acquired at 90% fuel flow and various air flow rates through A1.

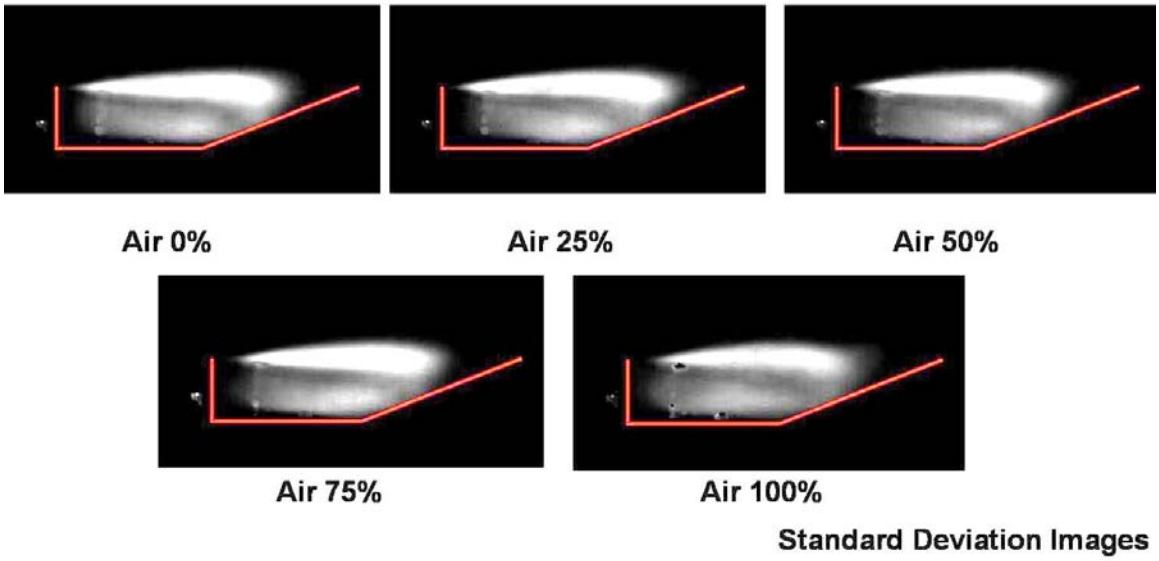


**Figure 51** 90% fuel flow (HBP)

Pressure data were collected along the top and bottom walls through the test section and were affected by the shock structure. The following analysis is based on mean pressures sampled along the top and bottom wall of the test section. The tunnel floor was superimposed on all charts to locate the flameholding cavity. The figures presented in this section are included to show the observed overall trends that static pressure exhibits as a function of both streamwise position and injected air flow rates. Duplicate figures of larger proportion are included in Appendix B. Figure 52 shows the static pressure on the bottom of the tunnel floor given low backpressure, 32% fuel flow and various air flows. Individual pressure series are denoted by percentage fuel flow followed by percentage air flow. For example, 32% fuel flow and 80% air flow is labeled F32A80 in the chart below.

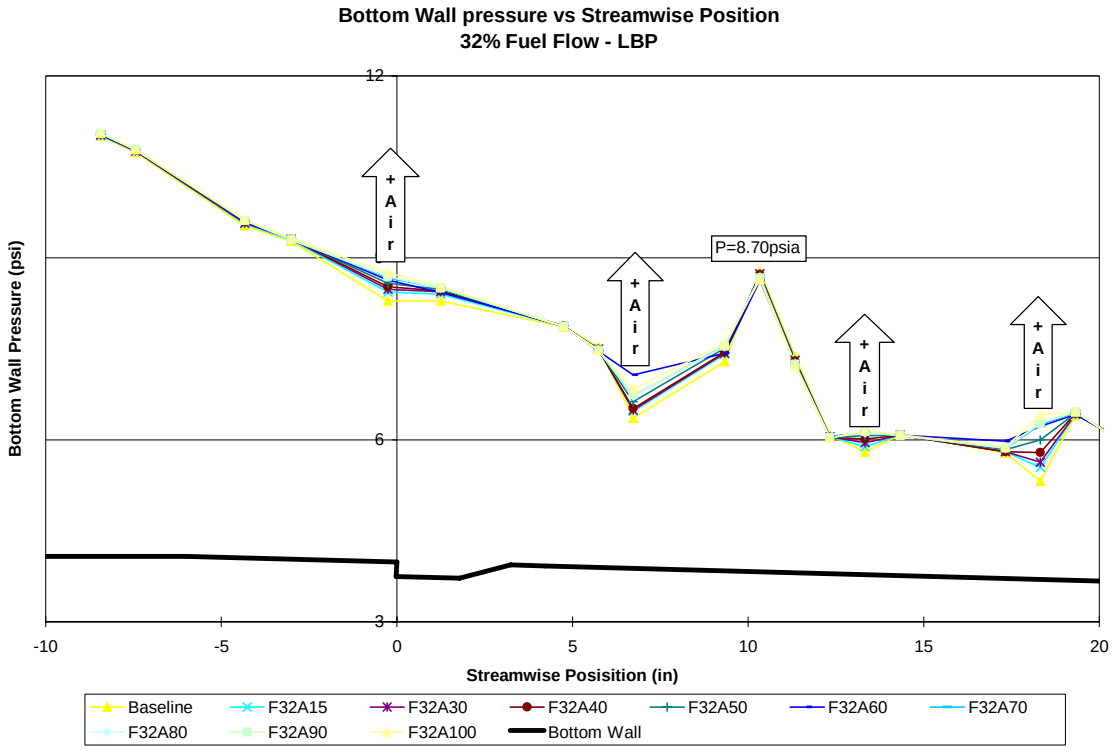


**Figure 52** 32% fuel flow (LBP; bottom)

Notice that the static pressures measured at various air flow rates are similar at some locations and different at others. This implies that air injection does not affect the static pressure throughout the measured region, but at discrete locations. The static pressures at four locations on the bottom wall were observed to be strong functions of air injection and the trend is shown in Figure 52 by the arrows. These trends were located at the following streamwise stations from the cavity step: -0.3, 6.7, 13.3 and 18.3 inches, and are repeated for all fuel flow conditions and occur at the same streamwise positions. Figure 53 shows the static pressure on the top wall at low backpressure given 32% fuel flow and various air flow rates through A1.

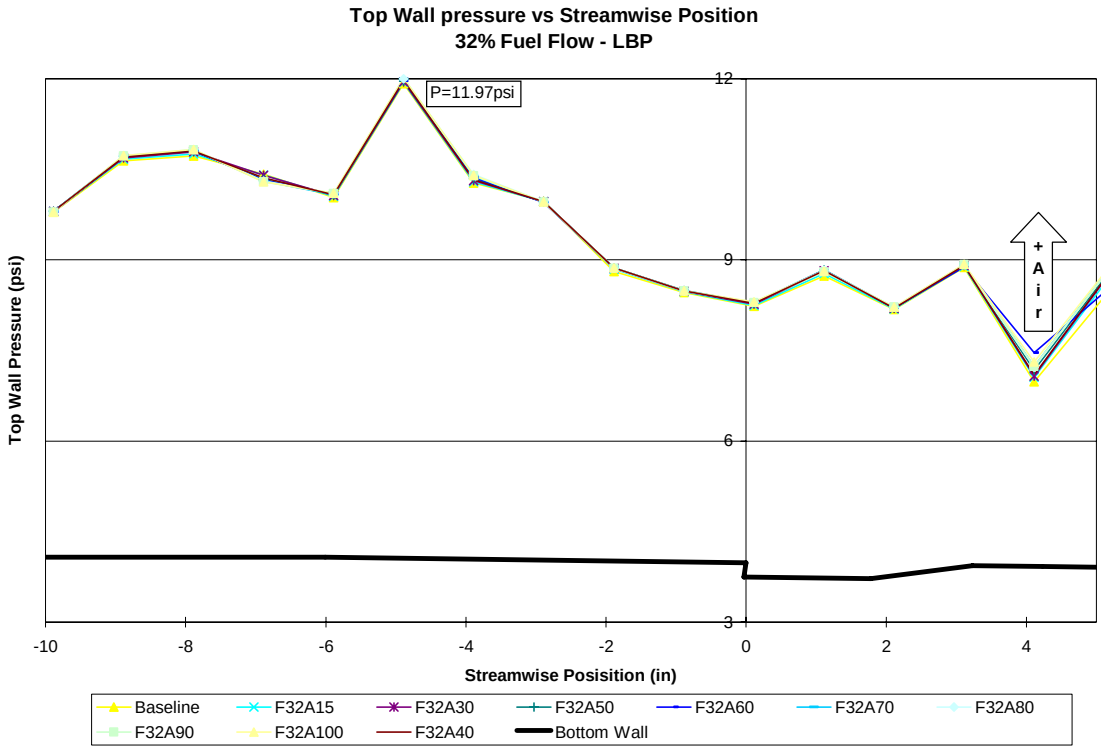


**Figure 53** 32% fuel flow (LBP; top)

The top wall pressure appears to be invariant with air flow rate upstream of the cavity. At approximately four inches aft of the cavity step, increasing air flow into the cavity causes an increase in pressure. Similar pressure traces can be found in Appendix B for the 50% and 75% fuel flow rates at low backpressure. The changes in pressure as functions of introduced air flow were most likely caused by changes in the shock structure through the cavity. As noted before, an increase in heat release due to combustion causes the shear layer to reattach farther up the aft ramp. The relocation of the shear layer causes a change in the aft recompression wave and therefore the shock system. The recompression wave will impinge on the top wall of the cavity and any change in wave angle will cause a streamwise shift in top wall impingement. This difference will cause increases or decreases in pressure measured on the top wall

depending on the direction of the shift. The shock structure which is influenced by cavity combustion is of significant importance to the overall performance of the engine. In general, total pressure losses increase as the shocks become more normal and decrease as shocks become more oblique. Stronger shocks cause greater decreases in total pressure which should be minimized throughout the engine and therefore the flameholder. The pressure distributions shown in figures 52 and 53 provide qualitative information regarding pressure losses. Figure 54 illustrates the compression wave shift as referenced by the top wall. Representative images of the location of an aft recompression wave can be found in Figures 5 and 6.

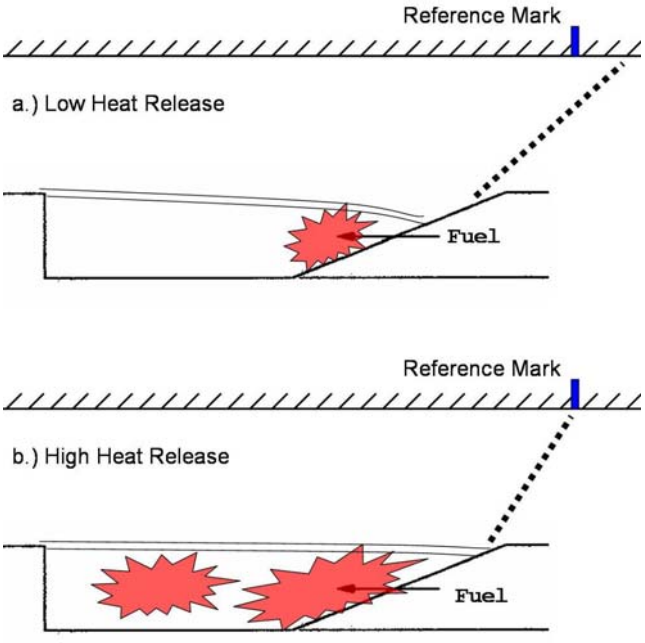


**Figure 54** Shock interaction

**Summary**

Cavity combustion was studied given three fuel flow rates and various air flow rates at both high (subsonic and supersonic test section flow) and low backpressure (pure

supersonic test section flow). PLIF, emissions and pressure data correlated well and served to characterize the effects of direct air and fuel injection.

# V. Conclusions and Recommendations

## Conclusions of Research

Air injection from the bottom injection site (A1) served to tune the cavity for optimum combustion for each fuel flow rate. That is, for a given fuel flow rate, air injection flow rates can be increased or decreased to produce a stable, uniform combustion region throughout the cavity. Cavity aerodynamics have shown that more freestream air is entrained by the cavity given high backpressure. Previous fuel only studies have been limited to lower fuel flow rates especially at low backpressure, due to this limited air entrainment. Therefore, this fueling scheme, where air and fuel are directly injected into the cavity, significantly increases the operating limits of the cavity flameholder.

The addition of air injection serves to lean out fuel rich lobes shown to exist near the cavity step allowing for combustion throughout the cavity thereby increasing its efficiency. Injection at A1 produced the greatest region of impact near the cavity step. Without air injection, the cavity step region contributes very little to the overall cavity combustion. Air injection through the top spanwise row of injectors (A2) minimally affected global cavity combustion. However, a localized region of influence was visually noted.

Lean blowout characteristics were shown to be a insensitive to air injection through either A1 or A2. In the low backpressure case, this is most likely due to the localized combustion structures that are formed on the aft wall. The air injectant does not have sufficient time to mix with the fuel injectant to affect the local fuel/air ratio.

Increases in cavity heat release were shown to lift the shear layer and drive its reattachment farther up the aft ramp. Furthermore, an increase in backpressure also caused an effective increase in cavity volume again to the lifting of the shear layer. Both increases in heat release and backpressure maximize the area (volume in three dimensions) that can be used for combustion and flameholding. Efficient combustion can be characterized by a strong, steady shear layer flame and global reaction, Increases in fuel flow, for the appropriate air flow, produced significant heat as evidenced by the increase in temperature within the cavity. The cavity step tended to retain the heat of combustion more so than the aft ramp, due to the cooling effects of the air and fuel flow through the ramp.

**Recommendations for Future Research**

Future research into the effects of cavity combustion and its application to flameholding in dual mode SCRAMJET engines could be accomplished in several different aspects. First, work should be done to characterize optimum combustion in a flameholder with special attention to physical properties that could be measured and input into a control system. The test facility has the capability to provide optical access from above the cavity. Future work should include optical flow visualization from that vantage point. Secondly, premixed fuels should be investigated. It would be possible to machine a ramp that had both premix and non-premixed injectors fed from the same fuel and air input. Additionally, other measurements could be accomplished to provide additional information on the combustion throughout the cavity. In particular temperature profiles could be evaluated as combustion is temperature dependent. Finally,

air and fuel injection could be studied at other injection ports within the cavity. Specifically, air injection at or near the cavity step could also serve to tune the cavity.

# Appendix A

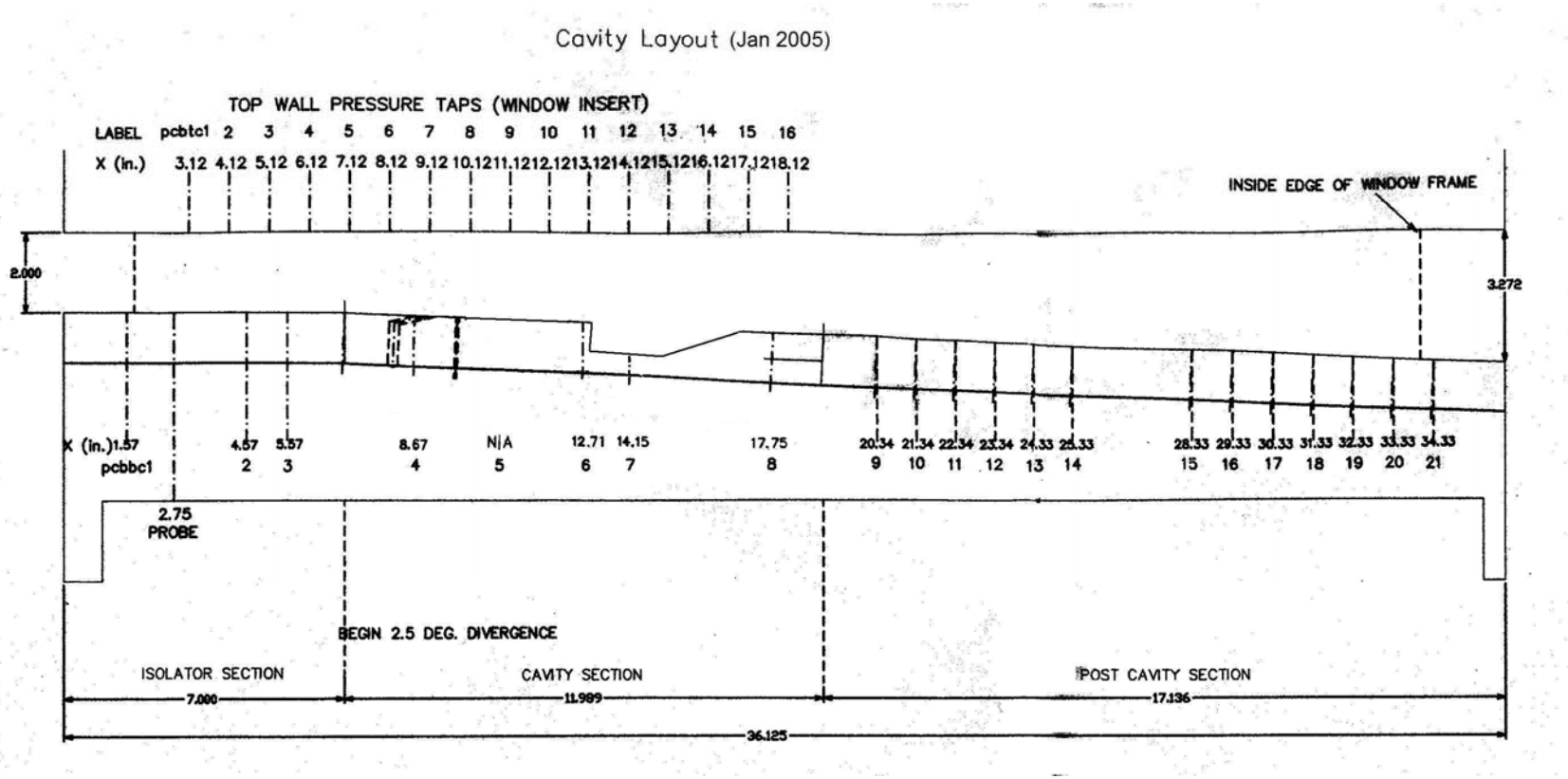


**Figure A 1** Pressure tap locations

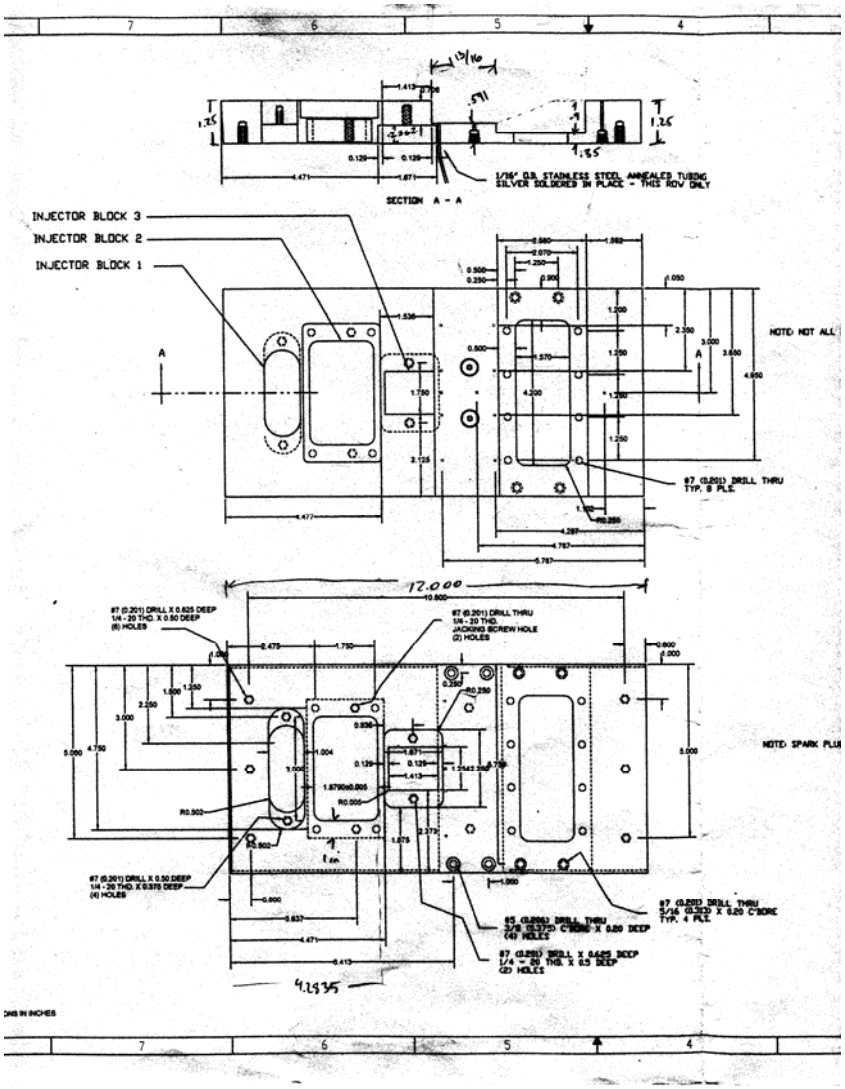


**Figure A 2** Base plate dimensions

# Appendix B

This appendix contains pressure as a function of airflow rates, backpressure and streamwise position.

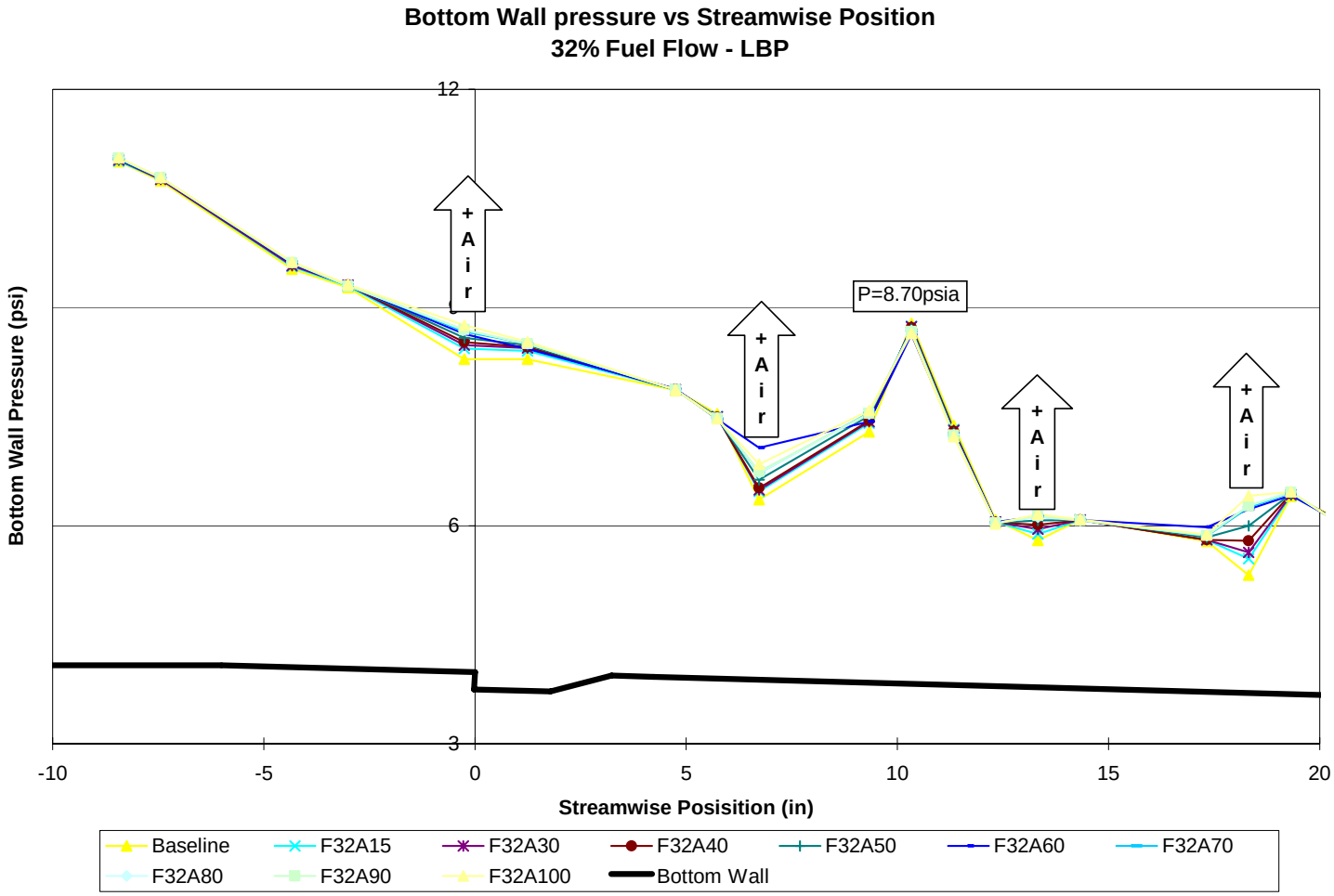


**Figure B 1** Bottom pressure (32% Fuel; LBP)

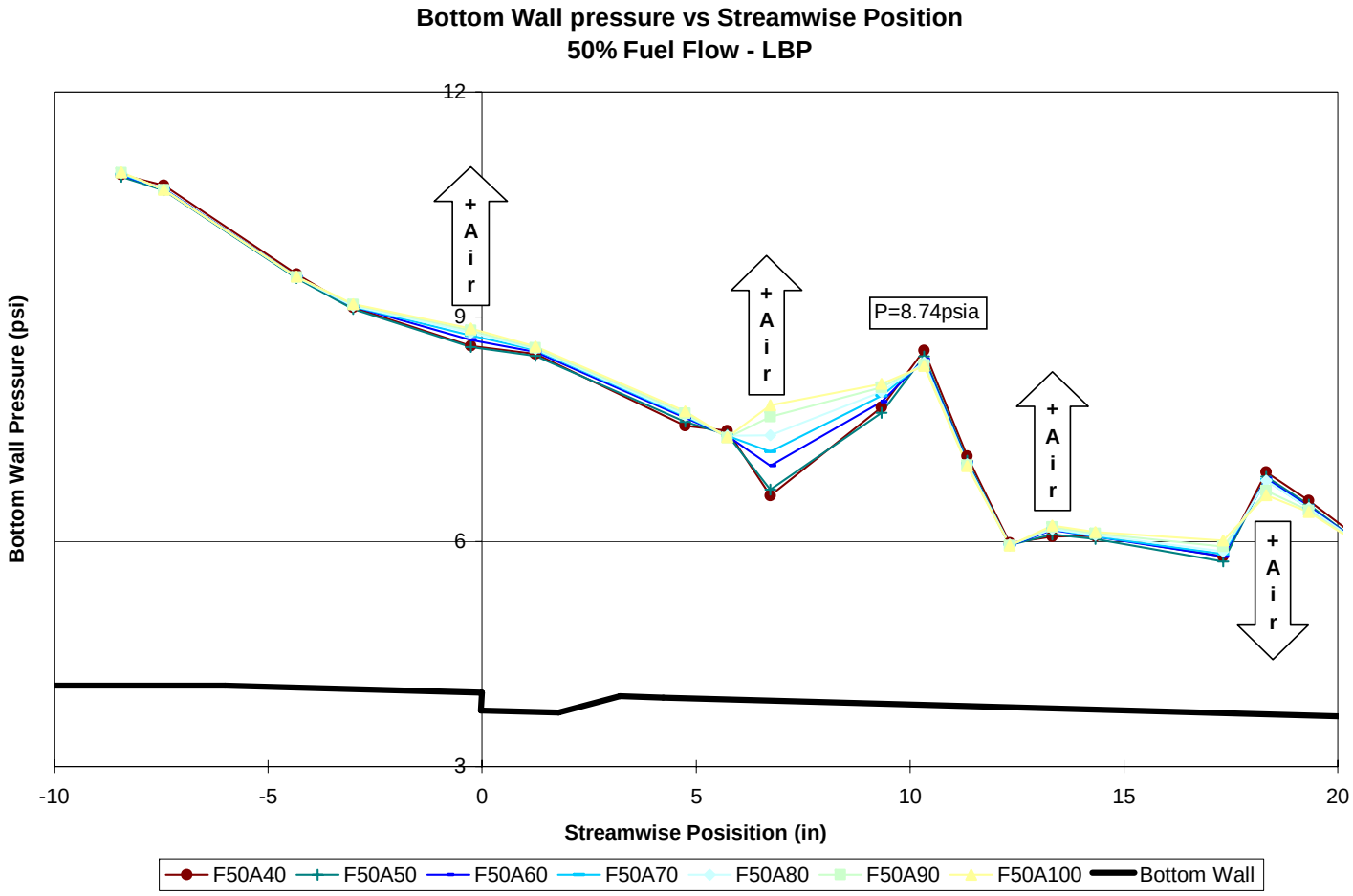


**Figure B 2** Bottom pressure (50% Fuel; LBP)

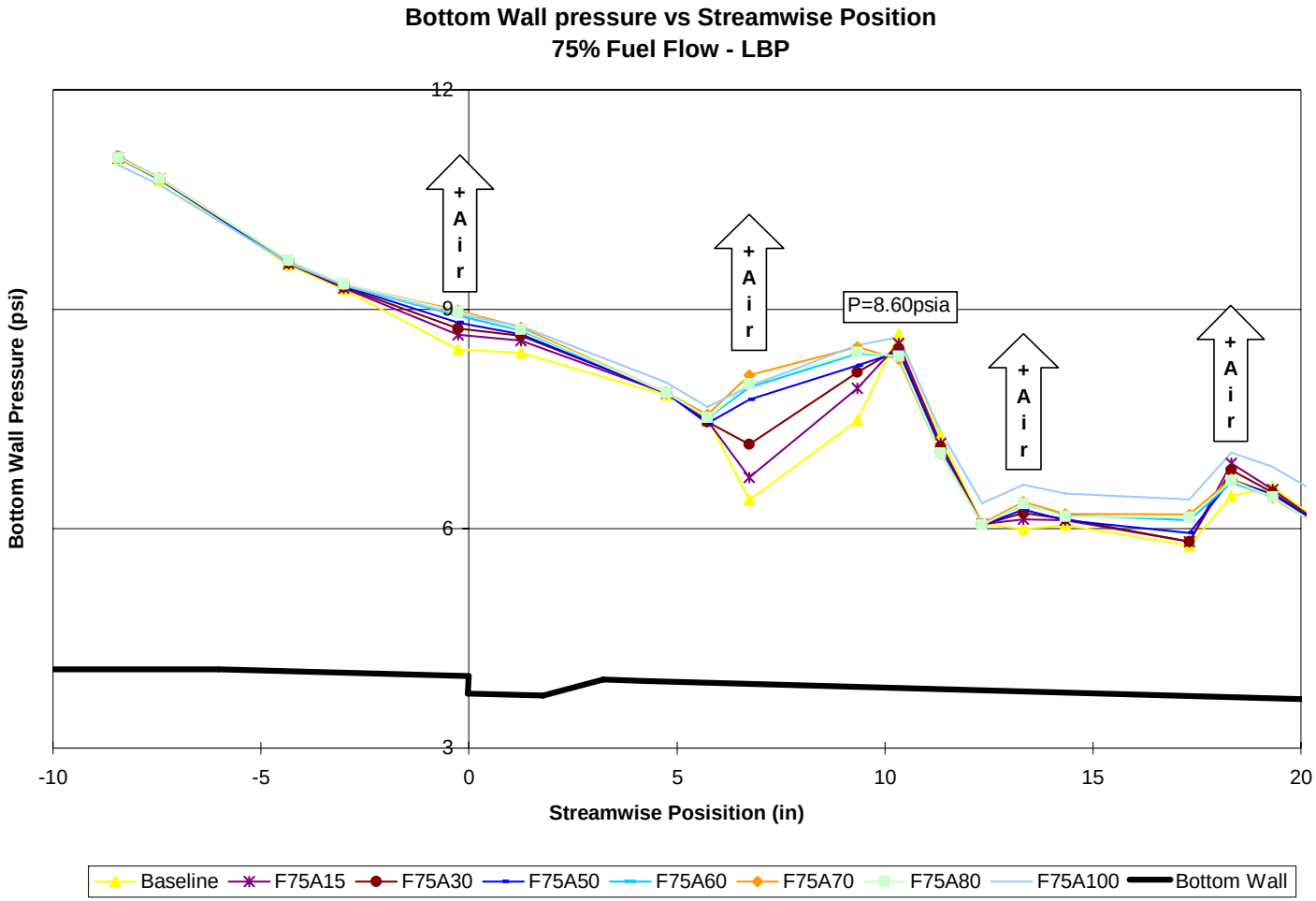


**Figure B 3** Bottom pressure (75% Fuel; LBP)

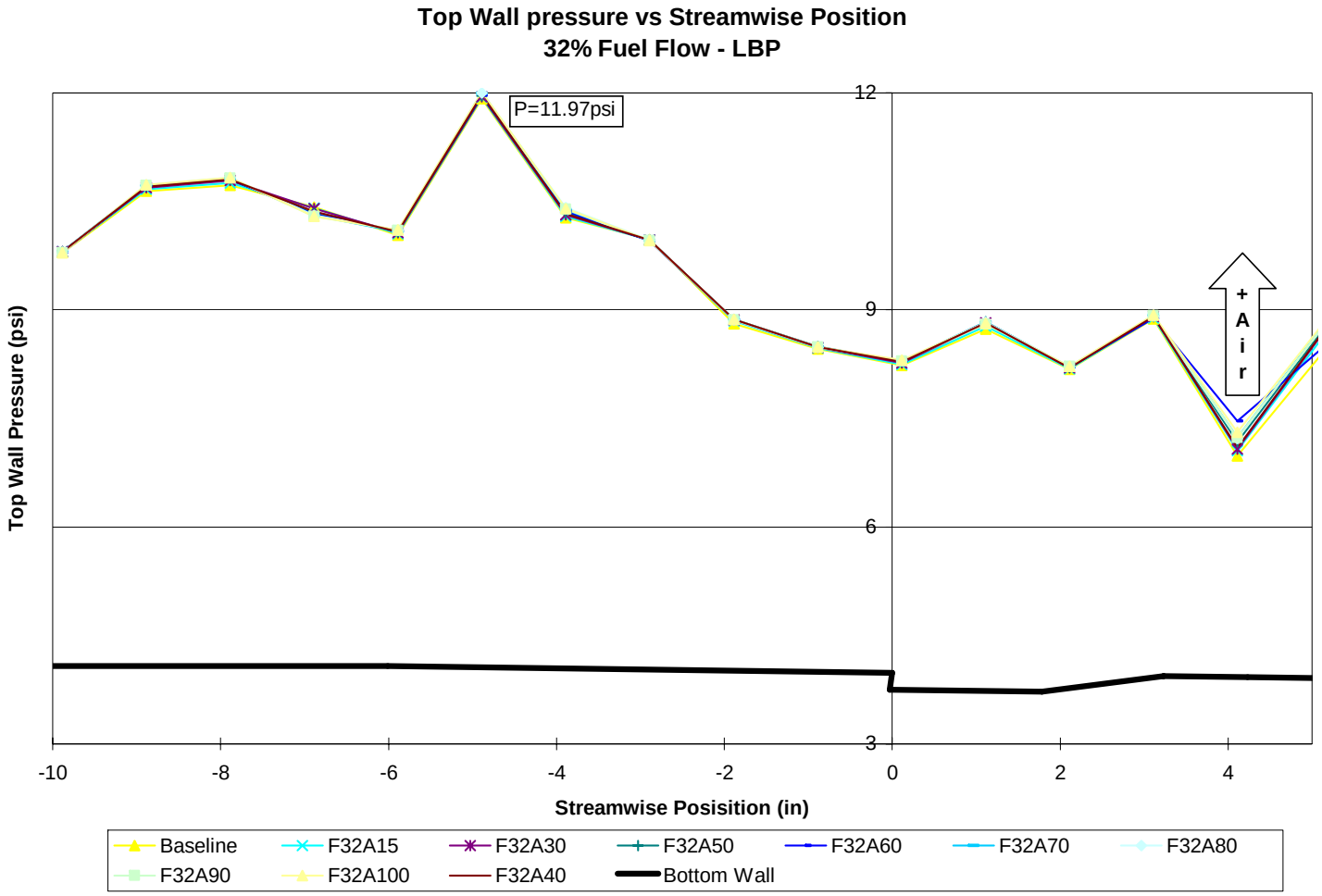


**Figure B 4** Top pressure (32% Fuel; LBP)

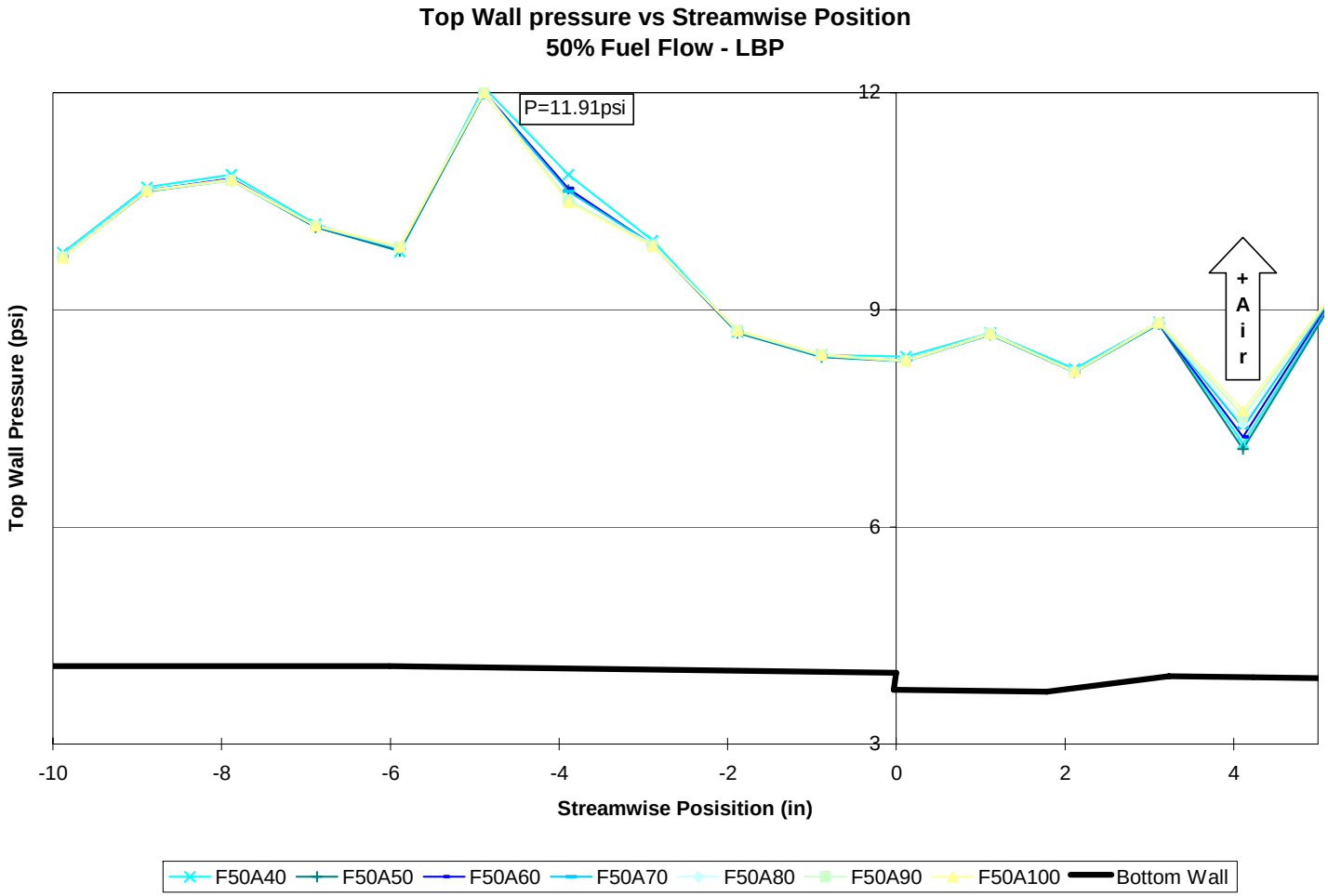


**Figure B 5** Top pressure (50% Fuel; LBP)

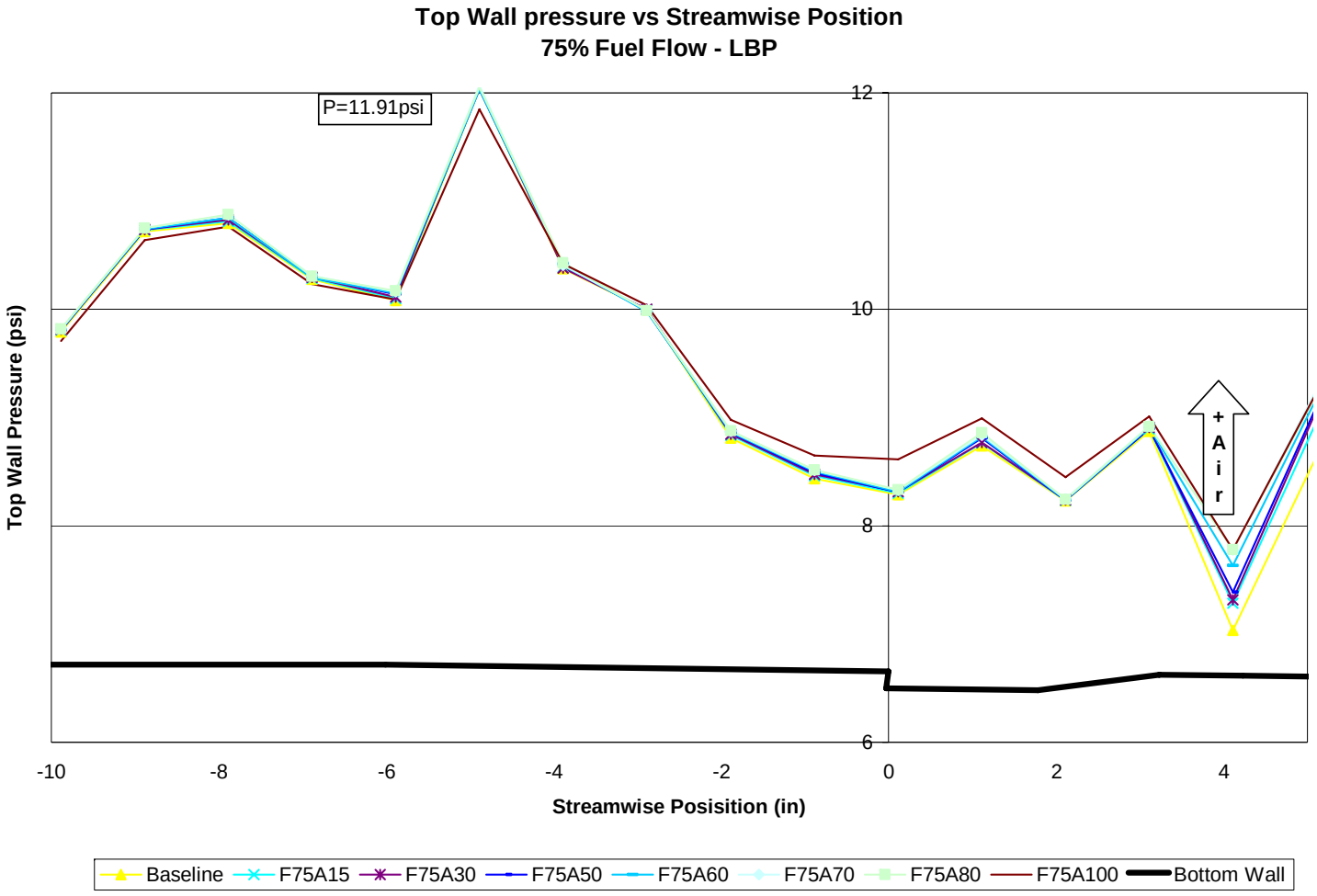


**Figure B 6** Top pressure (75% Fuel; LBP)

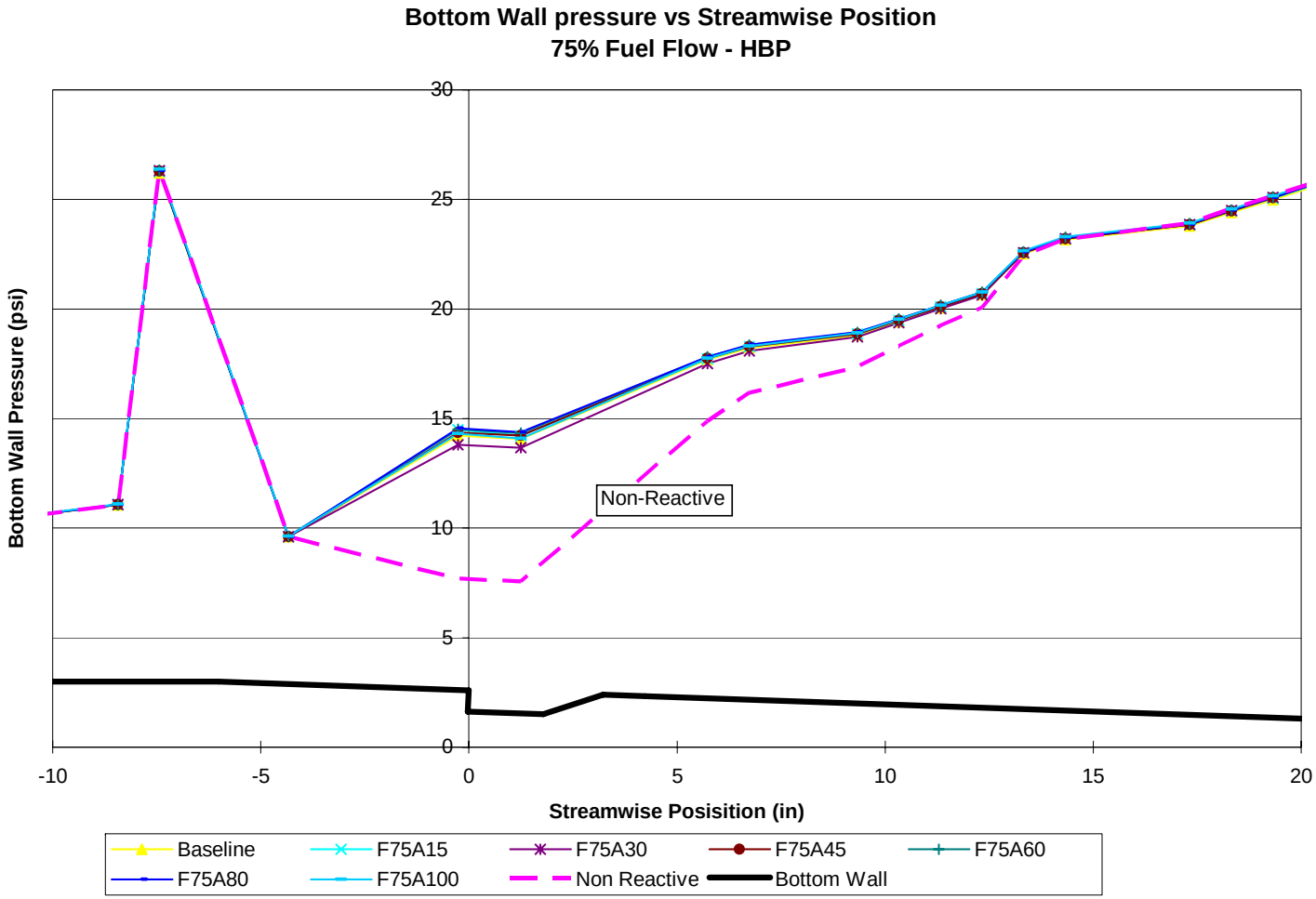


**Figure B 7** Bottom pressure (75% Fuel; HBP)

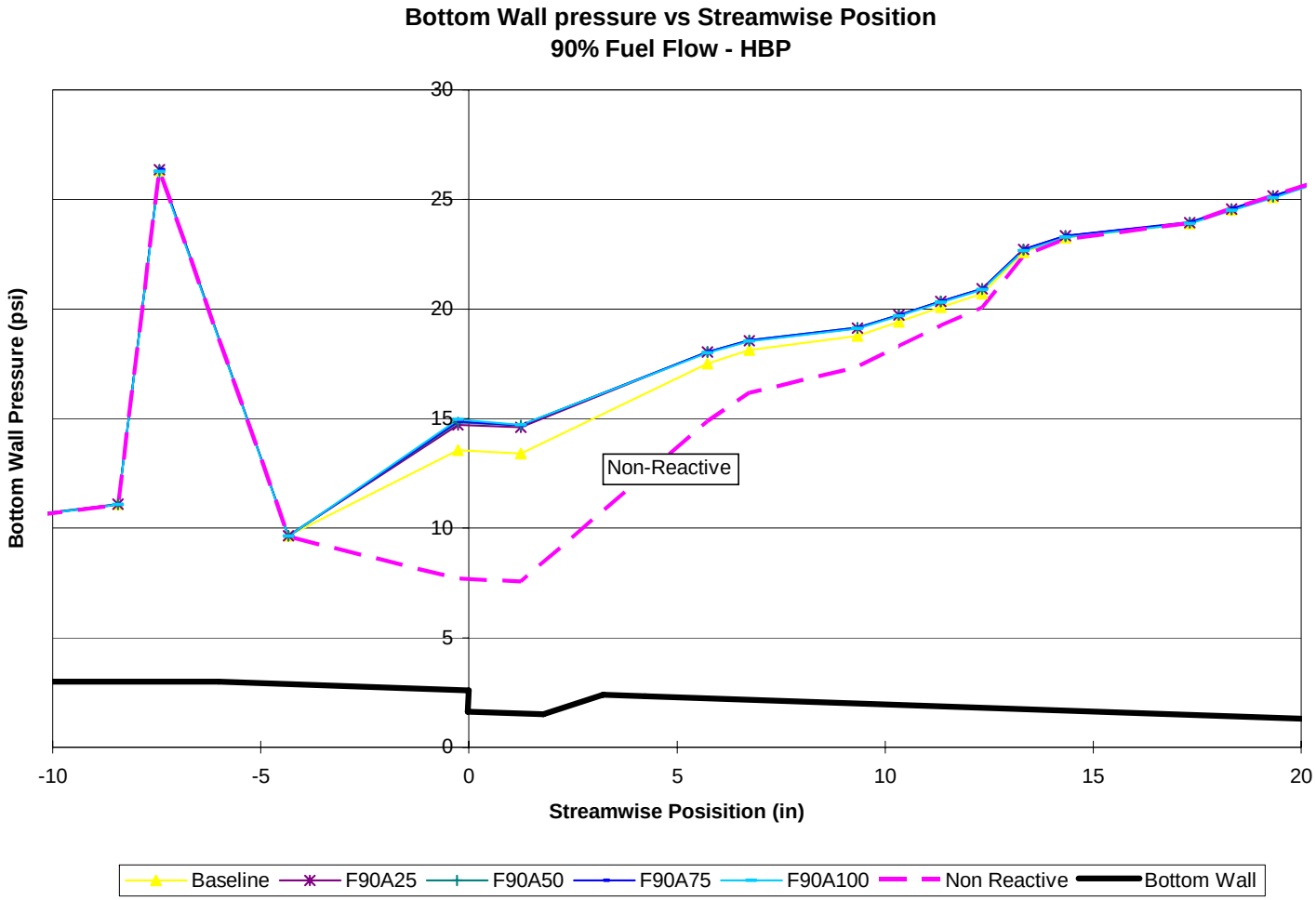


**Figure B 8** Bottom pressure (90% Fuel; HBP)

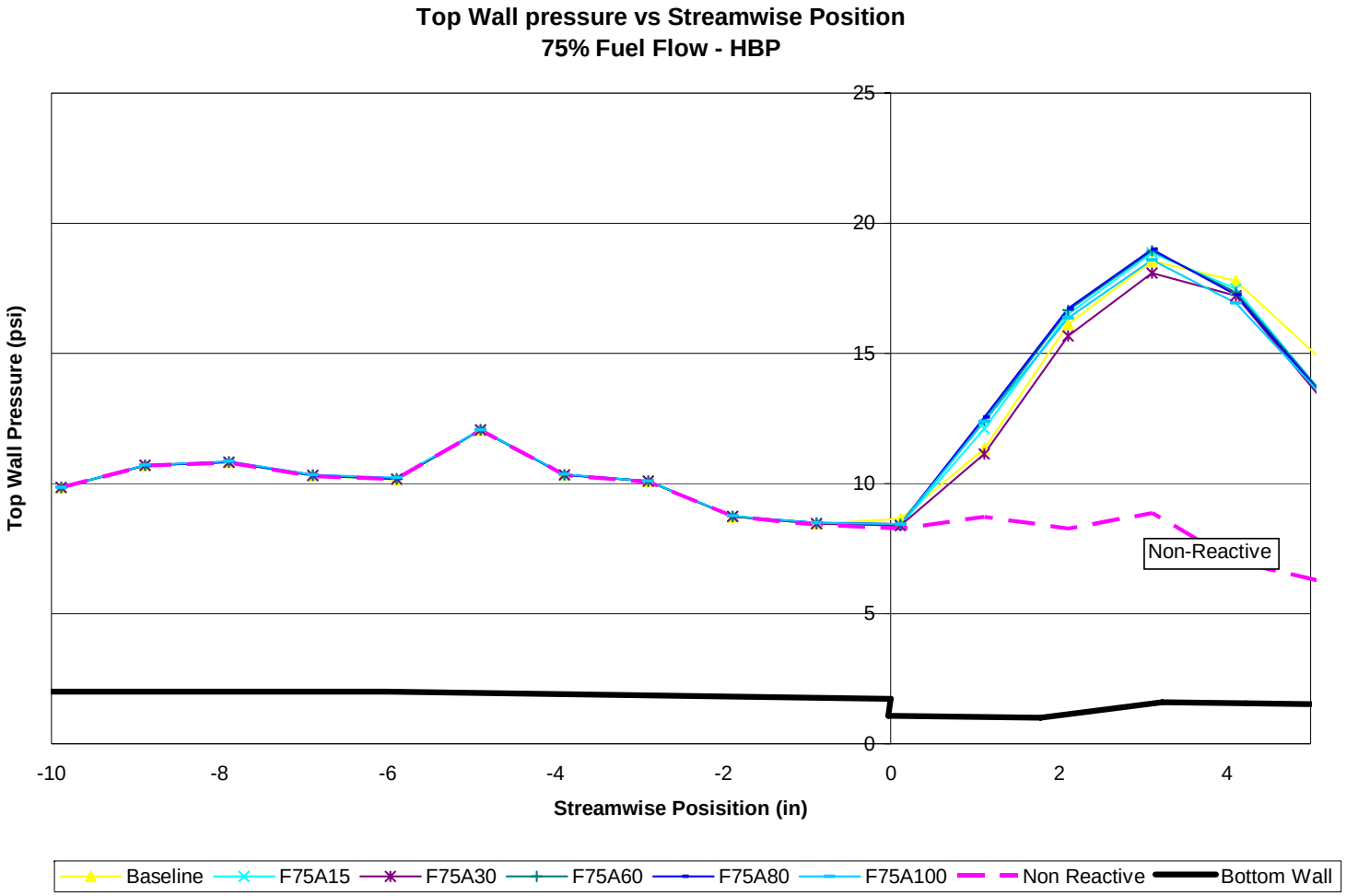


**Figure B 9** Top pressure (75% Fuel; HBP)

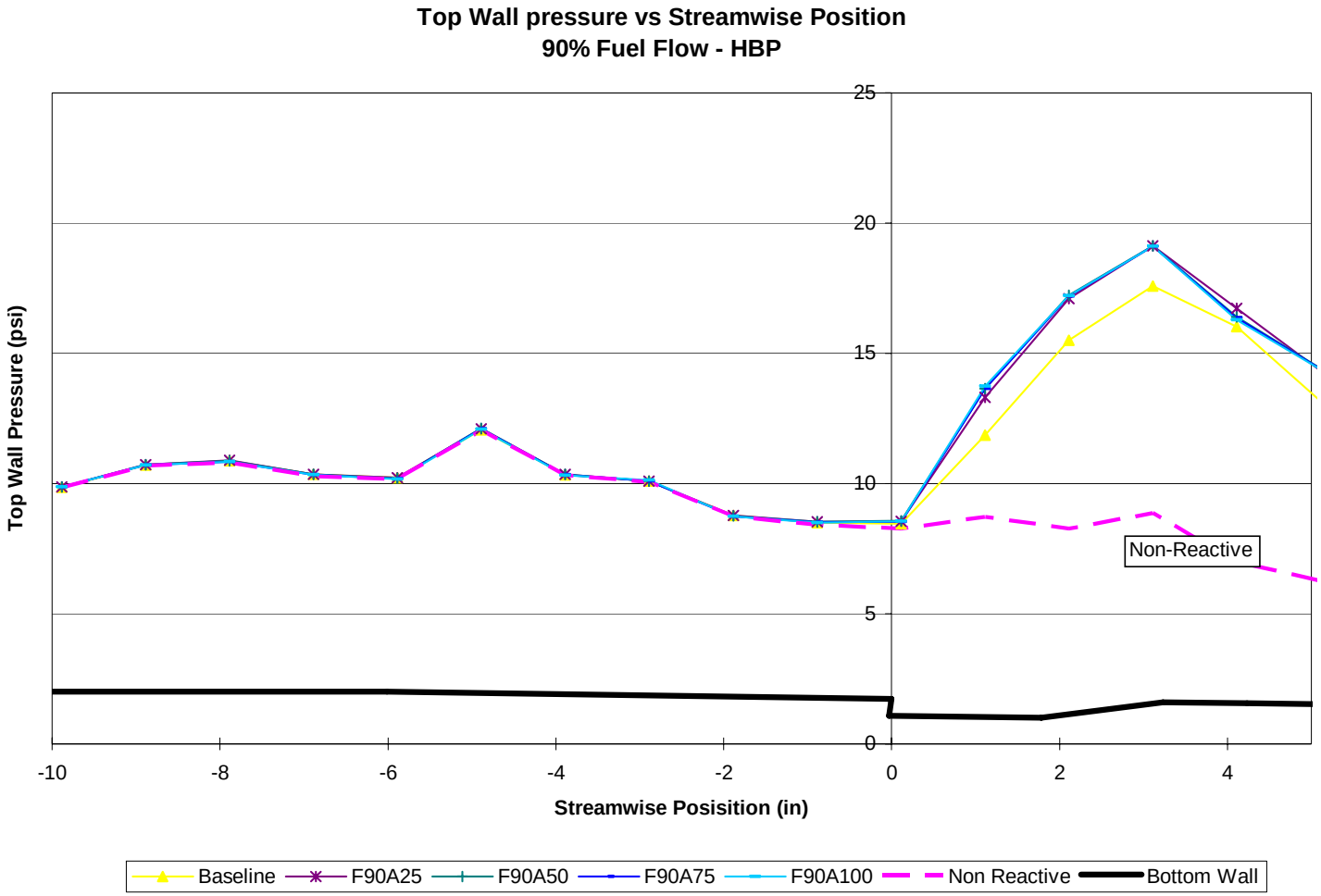


**Figure B 10** Top pressure (90% Fuel; HBP)

## Bibliography


[1] CNN, http://www.cnn.com Accessed July 2002.

[2] Youngbin, Yoon. "Blowout Stability Limits of a Hydrogen jet Flame In a Supersonic, Heated, Coflowing Air Stream." Combustion Science and Tecnology Vol 97 pp 137-156.

[3] Aviation History On Line Museum, http://www.aviation-history.com/engines/ramjet.html Accessed 20 Dec 2004.

[4] Gruber, M.R., Donbar, J.M., Carter, C.D. and Hsu, K-Y., "Mixing and Combustion Studies Using Cavity-Based Flameholders in Supersonic Flow," *ISABE-2003-1204*

5 Gruber, M., Baurle,R., Mathur,T., and Hsu, K., "Fundamental Studies of Cavity-Based Flameholder Concepts for Supersonic Combustors", *Journal of Propulsion and Power*, Vol. 17, No. 1, 2001, pp. 146-153.

[6] Mathur, T., Billig, F., "Supersonic Combustion Experiments with a Cavity-Based Fuel Injector," *Journal of Propulsion and Power*, Vol. 17, No. 6, 2001, pp. 1305-1312.

[7] Ben-Yakar, A., Hanson, R. K., "Cavity Flameholders For Ignition and Flame Stabilization in Scramjets: Review and Experimental Study," AIAA paper 98-3122, July 1998.

[8] Hsu, K.-Y., Goss, L.P., and Roquemore, W.M., "Study on Trapped-Vortex Combustor-Effect of Injection on Flow Dynamics," *Journal of Propulsion and Power*, Vol. 14, No. 1, 1998, pp. 57-65.

[9] Winterfeld, G., "On Processes of Turbulent Exchange Behind Flame Holders," *Tenth International Symposium on Combustion*, Combustion Inst., Pittsburgh, PA, 1965, pp.1265-1275.

[10] Gruber, M.R., Nejad, A.S., "Development of a Large-Scale Supersonic Combustion Research Facility," AIAA paper 94-0544, 32nd Aerospace Sciences Meeting and Exhibit, Reno, NV, 1994

[11] Lee, M.P., McMillin, B.K., "Planar Fluorescence Imaging of aTransverse Jet in a Supersonic Crossflow," *Journal of Propulsion and Power*, Vol. 8, No. 4, 1992, pp. 729-735.

[12] Mercier, R., McClinton C., "Hypersonic Propulsion – Transforming the Future of Flight," AIAA paper 2003-2732, AIAA/ICAS International Air and Space Symposium and Exposition, Dayton, OH 14-17 July 2003

[13] Boudreau, A., "Status of US Air Force HyTech Program," AIAA paper 2003-6947, 12th AIAA International Space Planes and Hypersonic Systems and Technologies, Norfolk, VA 15-19 December 2003

## Vita

Captain William H. Allen Jr. graduated from Christian Brothers High School in Memphis Tennessee. He entered undergraduate studies at Christian Brothers University in Memphis, Tennessee where he graduated with a Bachelor of Science degree in Mechanical Engineering in December 1999. He was commissioned through the Detachment 785 AFROTC at the University of Memphis into the United States Air Force.

After graduation from Christian Brothers University he was married and accepted his first assignment to Hill AFB as a munitions test engineer. There his primary job was to develop plan and execute the testing of Department of Defense munitions assets utilized in nearly every major Air Force weapon system. He also served as an aircraft battle damage repair (ABDR) engineer for both the F-16 and A-10 aircraft. In August 2003, he entered the Graduate School of Engineering and Management, Air Force Institute of Technology. Upon graduation, he will be assigned to the Air Force Research Labs, Propulsion Directorate (AFRL/PR) at Edwards AFB California.

# REPORT DOCUMENTATION PAGE

*Form Approved*
*OMB No. 074-0188*



| 1. REPORT DATE *(DD-MM-YYYY)* | 2. REPORT TYPE | 3. DATES COVERED *(From – To)* |
|---|---|---|
| 21-03-2005 | Master's Thesis | August 2003 – March 2005 |

**4. TITLE AND SUBTITLE**

FUEL-AIR INJECTION EFFECTS ON COMBUSTION IN CAVITY-BASED FLAMEHOLDERS IN A SUPERSONIC FLOW

**5a. CONTRACT NUMBER**

**5b. GRANT NUMBER**

**5c. PROGRAM ELEMENT NUMBER**

**6. AUTHOR(S)**

Allen Jr., William H., Captain, USAF

**5d. PROJECT NUMBER**

**5e. TASK NUMBER**

**5f. WORK UNIT NUMBER**

**7. PERFORMING ORGANIZATION NAMES(S) AND ADDRESS(S)**

Air Force Institute of Technology
Graduate School of Engineering and Management (AFIT/EN)
2950 Hobson Way, Building 640
WPAFB OH 45433-8865

**8. PERFORMING ORGANIZATION REPORT NUMBER**

AFIT/GAE/ENY/05-M02

**9. SPONSORING/MONITORING AGENCY NAME(S) AND ADDRESS(ES)**

Air Force Research Lab Propulsion Directorate (AFRL/PRAS)
1950 Fifth Street
WPAFB OH 45433-8865 DSN 785-7350

**10. SPONSOR/MONITOR'S ACRONYM(S)**

**11. SPONSOR/MONITOR'S REPORT NUMBER(S)**

**12. DISTRIBUTION/AVAILABILITY STATEMENT**

APPROVED FOR PUBLIC RELEASE; DISTRIBUTION UNLIMITED.

**13. SUPPLEMENTARY NOTES**

**14. ABSTRACT**

The Air Force Research Lab, Propulsion Directorate, Wright-Patterson Air Force Base, Ohio has studied several designs regarding cavity flameholding for supersonic RAMJET (SCRAMJET) applications. The most recent of these studies have concluded that direct injection of ethylene fuel into the aft cavity ramp produced an efficient, robust flameholder given specific freestream condition and fuel flow rate.

The main goals of this experiment are: 1) study the effect on combustion of direct fuel and air injection in the main flameholding cavity and 2) characterization of the operational limits (i.e., sustained combustion limits) over a variety of fuel and air flow rates. Direct injection of both fuel and air provided additional capability to tune the cavity such that a more stable decentralized flame results. The addition of air injection provided the most improvement over the baseline case (fuel only) near the upstream portion of the cavity close to the cavity step. Direct air injection provided a second source of oxygen to be consumed during the combustion process thereby expanding the operational limits drastically for each selected fuel flow. This experimental investigation was limited by the size of the flow controllers available and by the maximum allowable material temperature given cavity flow parameters. Lean blowout was not observed to be a function of injected air flow.

**15. SUBJECT TERMS**

Supersonic Combustion, Flameholding, Direct Injection, Cavity

| 16. SECURITY CLASSIFICATION OF: | | | 17. LIMITATION OF ABSTRACT | 18. NUMBER OF PAGES | 19a. NAME OF RESPONSIBLE PERSON |
|---|---|---|---|---|---|
| a. REPORT | b. ABSTRACT | c. THIS PAGE | | | Paul King, AFIT |
| U | U | U | UU | 104 | 19b. TELEPHONE NUMBER *(Include area code)* (937) 255-6565, x4628 (pking@afit.edu) |